EXPERIMENTAL CHARACTERIZATION OF CANOLA OIL EMULSION COMBUSTION IN A MODIFIED FURNACE

A Thesis

by

SHREYAS MAHESH BHIMANI

Submitted to the Office of Graduate Studies of
Texas A&M University
in partial fulfillment of the requirements for the degree of

MASTER OF SCIENCE

May 2011

Major Subject: Mechanical Engineering

Experimental Characterization of Canola Oil Emulsion Combustion in a Modified Furnace

EXPERIMENTAL CHARACTERIZATION OF CANOLA OIL EMULSION COMBUSTION IN A MODIFIED FURNACE

A Thesis

by

SHREYAS MAHESH BHIMANI

Submitted to the Office of Graduate Studies of
Texas A&M University
in partial fulfillment of the requirements for the degree of

MASTER OF SCIENCE

Approved by:

Chair of Committee,	Jorge Alvarado
Committee Members,	Kalyan Annamalai
	Sergio Capareda
Head of Department,	Dennis L. O'Neal

May 2011

Major Subject: Mechanical Engineering

ABSTRACT

Experimental Characterization of Canola Oil Emulsion Combustion in a Modified Furnace. (May 2011)

Shreyas Mahesh Bhimani, B.E., Charotar Institute of Technology

Chair of Advisory Committee: Dr. Jorge Alvarado

Vegetable oils have been researched as alternative source of energy for many years because they have proven themselves as efficient fuel sources for diesel engines when used in the form of biodiesel, vegetable oil–diesel blends, vegetable oil-water-diesel blends and mixtures thereof. However, very few studies involving the use of emulsified low grade alcohols in straight vegetable oils, as fuels for combustion have been published. Even, the published literature involves the use of emulsified fuels only for compression ignition diesel engines. Through this project, an attempt has been made to suggest the use of alcohol-in-vegetable oil emulsions (AVOE) as an alternate fuel in stationary burners like electric utility boiler producing steam for electricity generation and more dynamic systems like diesel engines. The main goal of this study is to understand the effect of the combustion of different methanol-in-canola oil emulsions, swirl angle and equivalence ratio on the emission levels of NO_x, unburned hydrocarbons (UHC), CO and CO_2.

The 30 kW furnace facility available at Coal and Biomass Energy Laboratory at Texas A&M University was modified using a twin fluid atomizer, a swirler and a new

liquid fuel injection system. The swirler blades were positioned at 60° and 51° angles (with respect to vertical axis) in order to achieve swirl numbers of 1.40 and 1.0, respectively. The three different fuels studied were, pure canola oil, 89-9 emulsion [9% methanol – in – 89% canola oil emulsion with 2% surfactant (w/w)] and 85-12.5 emulsion [12.5% methanol – in – 85% canola oil (w/w) emulsion with 2.5% surfactant].

All the combustion experiments were conducted for a constant heat output of 72,750 kJ/hr. One of the major findings of this research work was the influence of fuel type and swirl number on emission levels. Both the emulsions produced lower NO_x, unburned (UHC) hydrocarbon and CO emissions than pure canola oil at both swirl numbers and all equivalence ratios. The emulsions also showed higher burned fraction values than pure oil and produced more CO_2. Comparing the performance of only the two emulsions, it was seen that the percentage amount of methanol added to the blend had a definite positive impact on the combustion products of the fuel. The higher the percentage of methanol in the emulsions, the lesser the NO_x, UHC and CO emissions. Of all the three fuels, 85-12.5 emulsion produced the least emissions. The vorticity imparted to the secondary air by the swirler also affected the emission levels. Increased vorticity at higher swirl number led to proper mixing of air and fuel which minimized emission levels at SN = 1.4. The effect of equivalence ratio on NO_x formation requires a more detailed analysis especially with regards to the mechanism which produces nitrogen oxides during the combustion of the studied fuels.

DEDICATION

This thesis is dedicated to my parents, Mr. Mahesh Bhimani and Mrs. Shobhana Bhimani, for their love, guidance, encouragement and continuous support throughout my vital educational years. This work would not have been possible without their blessings.

ACKNOWLEDGEMENTS

I would like to express my sincere gratitude to several people who made this thesis possible. Of all, I would first like to thank my committee chair, Dr. Jorge Alvarado, for his mentorship, guidance and continuous support. I am grateful for having the opportunity to conduct this research under his supervision and to learn from all the discussions we had during the course of this research work. I would like to thank Dr. Kalyan Annamalai for opening the doors to his Coal and Biomass Energy Laboratory and making this facility available to us for liquid fuel combustion. I would also like to thank my other committee member, Dr. Sergio Capareda for his cooperation and advice. Additionally, I would like to thank Mr. Michael Golla for all his valuable inputs.

I would like to thank all the graduate students working under Dr. Alvarado for their minutest help and encouragement in difficult times. I would personally like to thank Ben Lawrence for all the help he gave me for conducting the combustion experiments. I want to thank my research team members: Hyunseok Nam, Gautam Savant and Ulysses Franca for all their cooperation and assistance in this experimental work. Very special thanks to Udaya Bhanu Sunku for his help with SolidWorks. I would like to specifically recognize and thank Layne Wylie in the mechanical engineering department's machine shop for teaching me how to use the different metal fabrication machines, not to forget the innumerable, though minor but extremely important tips, which can come only from a skilled and an experienced machinist.

Before closing, I want to extend my gratitude to Shri Shilchandrasuri swarji maharajsaheb, my guru, for always reminding me the importance of hard work and

persistence in whatever endeavors I take in life. This work would not have been possible without his blessings.

In closing, I want to thank my parents and all the family members for their unconditional love, inspiration and the values they have instilled in me right from the time when I was a little child.

TABLE OF CONTENTS

Page

Page

LIST OF FIGURES

FIGURE Page

FIGURE Page

FIGURE Page

LIST OF TABLES

TABLE Page

1. INTRODUCTION

We are all aware about the depletion of fossil fuels, rapid increase in their cost and the harmful emissions produced during their combustion. The ever increasing difficulty being faced to find and extract more of these fuels from miles below the earth crust is very evident these days. Fossil fuels include gases like natural gas, solids like coal and liquids like petroleum. Different fuels are used for different applications. For example, coal is used in boilers to produce steam, for smelting in industrial furnaces, electricity generation in thermal power plants; coal can be gasified to produce syngas and liquefied into gasoline and diesel. Natural gas is also used for electricity generation, for cooking in homes, heating applications, manufacturing plants and as a CNG fuel in automobiles. Diesel fuel is widely used in road, rail and air transportation.

The three main sources for electricity generation in the United States are coal, natural gas and nuclear energy. To date, majority number of utility boilers used for generating electricity in the United States are coal fired [1]. Figure 1 shows that coal forms more than 48% of the source for producing electricity amongst all the other available sources.

This thesis follows the style of Applied Thermal Engineering.

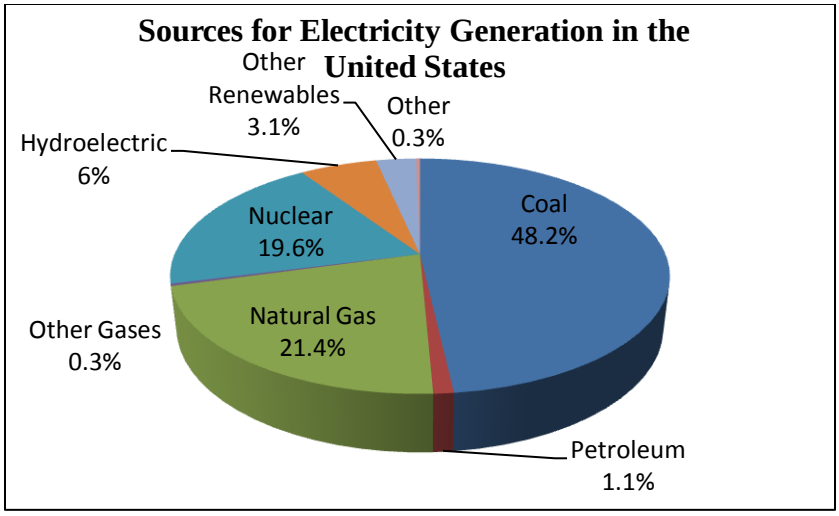

Figure 1: US electric power industry net generation (2008) [1]

One of the main disadvantages of combusting coal and any other fossil fuel is the production of the harmful gases which have a negative impact on both, human health and the environment surrounding us. The exhaust gases include nitrogen oxides (NO_x), sulfur oxides (SO_x), carbon monoxide (CO), carbon dioxide (CO_2), soot and unburnt hydrocarbons. Amongst all these exhaust gases, a major concern today is the production of NO_x. NO_x is a generic term for a group of highly reactive gases, containing nitrogen and oxygen in varying molecular formations. This group of gases includes NO, NO_2, NO_3, N_2O, N_2O_3, N_2O_4, N_3O_4 and mixtures thereof. Amongst this group, the two primary gases which are represented as NO_x are NO and NO_2 [2].

In order to reduce harmful emissions, many researchers have tried to use vegetable oil as an alternative to fossil fuels. Vegetable oils are basically sulfur free fuels and have very less nitrogen content. The different methods of using vegetable oil (VO) as a fuel are:

- Preheating the oil to high temperatures before injection
- Making water-in-oil emulsions
- Making alcohol-in-oil emulsions
- Blends of VO with diesel
- Blends of VO with diesel, water and other additives
- Making biodiesel from vegetable oil

The most common and widely adopted form of using VO from the ones mentioned above is biodiesel, a product of transesterification of VO with simple alcohols like ethanol. However, biodiesel has a number of disadvantages. First and foremost being the formation of glycerol as a by-product during the process of making biodiesel. Even though glycerol has found its application in the pharmaceutical, cosmetics and food industry, it needs extensive washing and purification from trace compounds, diminishing its usefulness [3]. Much of glycerol is discarded off due to this reason causing environmental pollution and a disposal issue. Performance of biodiesel is debatable and researchers have also concluded that biodiesel does not greatly reduce NO_x emissions when compared to crude-oil based diesel. Researchers have also found and reported on bio-diesel related problems such as fuel injector clogging and lubrication problems inside engines[4-7].

Alcohol in vegetable oil emulsions (AVOE) is another method of replacing fossil fuel while still producing sufficient heat energy in a relatively more environmentally friendly way. The advantage of using such emulsions is manifold. Firstly, it can be used to offset the time and energy typically needed to produce biodiesel. Economically,

making vegetable oil based emulsions is cheaper than making biodiesel because biodiesel production involves additional chemical processes after VO has been extracted from the crop. Secondly, emulsions containing highly volatile alcohol droplet trapped inside a less volatile vegetable oil should exhibit a micro explosion effect during combustion. It has been reported that micro explosion results in lower fuel emission [8]. When an emulsion is sprayed inside a combustion chamber, the alcohol droplet in the interior of oil is subjected to high temperatures. This causes the high volatile liquid to immediately superheat and change to gas phase. The sudden expansion of this gas results in a localized micro-explosion phenomenon. The oil explodes into numerous minute droplet particles which should auto-ignite providing optimal conditions for a more complete combustion, lesser exhaust emissions and better combustion efficiency. Additionally, vegetable oil has negligible ash content indicating that it is nearly 100% volatile, combustible fuel. Lastly, vegetable oil is a renewable source of energy. There are crops like Jatropa whose seeds have up to 40% oil content. Since this oil is not edible, it can be specially harvested to extract oil for combustion purpose. The crop has a capacity to grow on any terrain, from waste lands to desserts. So, economical feasibility can definitely be seen for such cultivations and oil extraction.

The current research focused on the design and modification of a small scale 30kW (100,000 BTU/hr) furnace facility located at CBEL (Coal and Biomass Energy Laboratory) at TAMU. The furnace, originally coal fired, was modified with a liquid fuel injection system, a twin fluid atomizer and a swirler to combust liquid fuels. Considering the benefits offered by AVOE fuels, methanol-in-canola oil emulsions

(MCOE) were chosen as the alternate liquid fuel for this liquid fuel fired facility. The different emulsions studied were 89-9 emulsion [9% methanol – in – 89% canola oil with 2% surfactant (w/w)] and 85-12.5 emulsion [12.5% methanol – in – 85% canola oil with 2.5% surfactant (w/w)]. Both the emulsions were stabilized by using a mixture of two surfactants, Span 80 and Tween 80. The 89-9 and 85-12.5 emulsions were stable for 7 hours and 4 hours, respectively. Pure canola oil was chosen as the alternate fuel for this project because of many reasons. Firstly, canola oil has low nitrogen content and is easily available in the US market at a relatively cheaper cost. Secondly, canola cultivar yields 40% - 45% oil which is the highest amongst other oils such as soybean, palm, corn and peanut oil. Lastly, majority of researchers in the past have used soybean oil and rapeseed oil as the alternate fuel in their experiments. So, in this project we decided to explore the combustion characteristics of a different energy source, canola oil. Pure canola oil was used as the baseline fuel to compare the performance of all the emulsions.

The main goal of this project was to illustrate the effect of different canola oil emulsions, swirl blade angle and equivalence ratio on the exhaust emissions and combustion efficiency of the modified furnace. The swirler was used with two different set of blades. The blades were positioned at 60° and 51° angles, giving swirl numbers of 1.4 and 1.0 respectively. All the experiments were conducted for a constant heat output of 72,750 kJ/hr. The combustion was done under fuel lean, stoichiometric conditions and fuel rich conditions. The different equivalence ratios during combustion experiments were 0.83, 0.91, 1.0, 1.05 and 1.11. Different equivalence ratios were obtained by varying the amount of secondary air only. During all the experiments, emissions levels

of CO, NO_x, unburned hydrocarbons (C_xH_y) and CO_2 was recorded. Data for O_2 in the exhaust was also collected in order to calculate the burned fraction of all the fuels. Through this project, an attempt has been made to suggest the use of AVOE as an alternate fuel in stationary burners like electric utility boilers, producing steam for electricity generation and more dynamic systems like diesel engines in the future.

One of the major findings of this research work was the influence of fuel type and swirl number on emission levels. Both the emulsions produced lower NOx, unburned (UHC) hydrocarbon and CO emissions than pure canola oil at both swirl numbers and all equivalence ratios. The emulsions also showed higher burned fraction values than pure oil. Comparing the performance of only the two emulsions, it was seen that the percentage amount of methanol added to the blend had a definite impact on the combustion products of the fuel. Higher the percentage of methanol in the emulsion, lesser the NOx, UHC and CO emissions. 85-12.5 emulsion produced the least emissions of all the three fuels. The vorticity imparted to the secondary air by the swirler also affected the emission levels. Increased vorticity at higher swirl number lead to minimal emission levels at SN = 1.4. The effect of equivalence ratio on NOx formation requires a more detailed analysis especially with regards to the mechanism which produces nitrogen oxides during the combustion of the studied fuels.

2. LITERATURE REVIEW

In this section, a short description of canola oil and its properties is presented. The section also discusses emulsions, surfactants, swirl effects, micro-explosion phenomena and past research done in the field of vegetable oil emulsions.

2.1 Canola Oil

A general definition of canola cultivar is referred to as a rapeseed cultivar that contains less than 2% erucic acid in its oil and less than 30µmol/g of one or any combination of the four known glucosinolates, namely, gluconapin, progoitrin, glucobrassicanapin and napoleiferin [9]. Glucosinolates are plant products that contain nitrogen and sulfur. They are secondary metabolites which are derived from glucose and amino acid. They are indirectly involved in the growth and development of the plant. Since the canola crop contains very less amount of these glucosinolates, it can be a promising alternative fuel. Lesser content of glucosinolate in the oil means lesser nitrogen and sulfur in the fuel which should result in lower emissions of NO_x and SO_x during combustion.

2.2 Canola Oil History

The traditional rapeseed oil has about 22% - 60% erucic acid, and a high amount goitrogenic glucosinolates. Oils with high erucic content are harmful for heart tissues. Glucosinolates on the other hand, impart a pungent taste to the oil. So, in order to produce a less bitter tasting multi-purpose oil that would appeal to larger markets, the

Canadian Rapeseed Industry genetically modified the rapeseed cultivar to produce a low erucic acid rapeseed known today as canola oil.

The first, low erucic acid rapeseed (LEAR) oil with less than 5% erucic acid was produced in Canada in 1968. The LEAR oils were then called "single low" variety. The crop was modified more to give both, low erucic acid as well as low glucosinolate content which is referred to as "double low" variety. By 1974, many of these cultivars were licensed. The name "canola" was adopted in Canada in the year 1979, referring to all "double low" cultivars. In 1985, the US Food and Drug Administration (FDA) recognized that rapeseed and canola were two different species of crop and thus granted GRAS (generally recognized as safe) status to canola [9].

Table 1: Generic properties of rapeseed and canola oil [9]

Oil composition	**Traditional Rapeseed Oil**	**Canola Oil**
Erucic acid (%)	45.0	<1.0
Linolenic acid (%)	8-9	8-12
Linoleic acid (%)	14-18	19-23
Oleic acid (%)	18-27	53-60
Palmitic acid (%)	3-5	3-5
Stearic acid (%)	1-3	1-3
Sulfur (ppm)	25-40	<17
Glucosinolates (µmol/g)	70-120	<26.5

As seen in Table 1 above, the glucosinolate content in canola oil is almost 4 times lesser as that in traditional rape seed oil. This is the main reason for canola oil having

such a less percentage of both, nitrogen and sulfur. Also, the extremely less amount of erucic acid content in canola oil makes it more hygienic for human consumption.

2.3 Emulsions

An emulsion is a fine dispersion of two or more mutually insoluble liquids that exhibit homogeneous physical properties [10]. The liquid component which is present in the form of finely distributed spherical droplets is called the "dispersed phase" and the liquid in which these droplets are dispersed is called the "continuous phase". The size of an emulsion can be nano, micro or macro, depending upon the use of surfactants and the amount of energy imparted to form the emulsion. There are two main ways to categorize emulsions:

1. Emulsion type
    i. Water in Oil (W/O) emulsion – Water dispersed in oil (hydrocarbon) phase
    ii. Oil in water (O/W) emulsion – Oil dispersed in water phase
    iii. Double emulsions – Water in oil in water emulsion (W/O/W)
    – Oil in water in oil emulsion (O/W/O)
2. Emulsion size [11]
    i. Micro emulsion – 10 to 100 nm
    ii. Nano emulsions – Less than 1000 nm
    iii. Macro emulsion – 0.5 to 100 µm

2.4 Emulsion Formation

There are many different ways to produce an emulsion from liquid phases which are not mutually or very slightly soluble. The basic procedure is to break the dispersed phase into droplets by the application of mechanical energy. These droplets are then surrounded by the continuous phase forming a stable emulsion. Some of the common methods used to impart the required mechanical energy are ultrasonication, high pressure homogenizer, stirring and blending, laminar and turbulent pipe flow, injection of dispersed into continuous phase and the phase inversion technique.

2.4.1 Surfactants

The word surfactant is an acronym for Surface Active Agent which is needed to produce an emulsion. It is also referred to as an emulsifier. Surfactants are amphiphilic organic compounds. The surfactant molecule has a hydrophilic head and hydrophobic tail. It is this molecular structure which helps the surfactant to reduce the interfacial tension between two immiscible liquids. For example, in case of oil in water emulsion, the hydrophilic head will dissolve in water as it is a polar solvent, and the hydrophobic tail will dissolve in the oil phase, keeping the oil droplets finely suspended in the continuous water phase. Figure 2 shows an oil-in-water emulsion.

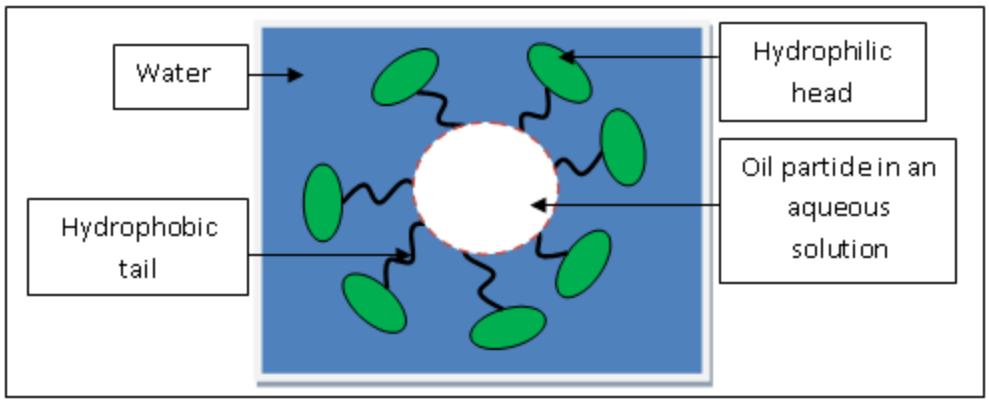

Figure 2: Oil in water emulsion

As mentioned afore, at the beginning of emulsion formation, the dispersed phase is in the form of macro droplets. In order to get a more stable emulsion, these droplets should be broken into smaller size so that the probability to coalesce and separate through Stokes flow is reduced. This deformation is opposed by the Laplace pressure. The pressure at the concave side of the curved interface with interfacial tension γ (gamma) is higher than at the convex side [12], which is given by

$$\Delta p = 2\gamma / R \quad (1)$$

where,

R is the radius of curvature for the spherical droplet

Δp is the difference in pressure

A surfactant lowers this Laplace pressure by decreasing the interfacial tension, thereby facilitating the disruption of droplets into smaller size and ensuring that there is a sufficient layer of emulsifier surrounding these dispersed smaller droplets. Using surfactants reduces the amount of agitation energy required for achieving a particular

droplet size within the emulsion. An emulsifier increases the kinetic stability of emulsions greatly so that emulsions do not change much over time, sometimes, even over months of storage.

Surfactants are broadly classified into 2 main types:

1. Ionic surfactants – The head of an ionic surfactant carries a net electrical charge in it. If the net charge is negative, the surfactant is called an anionic surfactant and if the charge is positive, it is called a cationic surfactant. There are surfactants whose heads have two oppositely charged groups. They are referred to as zwitterionic/amphoteric surfactants.
2. Nonionic surfactants – These are the surfactants whose heads do not have any charged groups in them.

2.4.2 HLB Concept and Its Relation to Emulsion Stability

In the year 1949, Griffin devised a semi-empirical scale for selecting the appropriate surfactant or a blend of surfactants to maintain a stable emulsion[12]. This scale is called the Hydrophile - Lipophile Balance (HLB). This scale takes into account the percentage of hydrophilic and hydrophobic groups present in a surfactant molecule(s) and assigns a HLB number to that molecule(s). Generally, surfactants with a low HLB number form W/O emulsions where as those with a high HLB number are used to form O/W emulsions. Table 2 summarizes the range of HLB numbers that the surfactant molecule(s) possess and the purpose they would serve [12].

Table 2: HLB range of surfactants and suitable applications

HLB range of surfactant molecule(s)	Application
3 to 6	W/O emulsifier
7 to 9	Wetting Agent
8 to 18	O/W emulsifier
13 to 15	Detergent
15 to 18	Solubilizer

2.5 Past Research on the Use of Alcohol-In-Oil Emulsions

One of the first works that considered the use of vegetable oils as alternative fuels was for a diesel engine. It was done in the early 1980's by Strayer et. al. [13]. After collecting data from different countries around the world, the authors did several calculations and came to a conclusion that the ratio of output energy (in terms of heating value) to input energy (with regards to the cultivation of crop and producing canola oil) is in the range of 3:1 to 5:1. The same energy ratio for ethanol production from biomass fermentation is between the range of 1:1 to 1.6:1. These statistics indicate that bio-diesel production is less energy favorable as it involves trans-esterification of vegetable oil with low grade alcohols like ethanol. This work was also first of its kind to suggest that, up to 13% (vol.) anhydrous alcohol can be blended with canola oil in order to reduce the viscosity and get better flow properties from the oil. The tests conducted on small diesel engine showed that 90% canola oil – 10% ethanol blend gave reduced power and higher fuel consumption.

In 1986, Ziejewski et. al.[14] performed tests on a 75 kW, four cylinder diesel engine. They used a blend of non-ionic sunflower oil and aqueous ethanol micro emulsion as an alternate to diesel. This study revealed that adding alcohol reduced the combustion temperature causing ignition delay and leading to better brake specific energy consumption (BSEC). Due to the high viscosity of sunflower oil, there was less internal leakage in the fuel injection system, giving higher flow rates in case of the alcohol-oil blend when compared to diesel. The higher fuel flow rate resulted in the blend giving more power outputs than diesel. The alcohol-oil blend gave lower exhaust smoke levels and better combustion efficiency.

Yoshimoto et. al. [15] used blends of rapeseed oil with four other alcohols, namely, methanol, ethanol, 1-propanol and 1-butanol to study the performance and emissions from a single cylinder diesel engine. The authors found that low grade alcohols like 1-propanol and 1-butanol had very good dissolving capabilities in rapeseed oil. Completely dissolved mixtures were obtained with up to 40% (vol.) addition of these two alcohols. The authors also found that methanol did not mix with the oil but some mixing was observed when only 10% (vol.) ethanol was added. From their experiments, the authors concluded that, 1-propanol and 1-butanol blends with oil gave good stable combustion results almost similar to those of diesel fuel. As compared to diesel, these two blends showed lower smoke emissions, unchanged NO_x and slightly higher BSEC.

In the subsequent year, Yoshimoto et. al. [16] did the same experiments with four new oxygenates namely, 1-pentanol, 2-methoxyethanol, 2-ethoxyethanol and 2-butoxyethanol, along with the previous fuels as listed in [15]. Completely dissolved

mixtures were obtained by addition of 29% (vol.) of lower alcohols and 33% (vol.) of the oxygenates in rapeseed oil. The authors observed that the alcohol blended fuel showed 0% to 41% lower smoke emissions, 3% to 5% higher BSEC and unchanged NO_x. Only, the ethanol blend had lower NO_x emissions as compared to diesel. The performance of the oxygenate blends was influenced by the engine load. Overall, the blends yielded stable combustion and considerable improvement in smoke emissions.

Kerihuel et. al. [17] tried to use animal fat as an alternate fuel for diesel engines. They made emulsions from duck fat, water, ethanol and Span 83. The optimum emulsion with more than one week of stability was formulated by having a blend of 50% duck fat, 36.4% ethanol, 10% water and 3.6% Span 83 on a (v/v) basis. Ethanol was the co-surfactant and was added to reduce the viscosity of animal fat and to improve the migration of the primary surfactant, Span 83 towards the fat/water interface. The emulsion was then tested for its combustion characteristics in a 2.8 KW single cylinder diesel engine [18]. The experimental results showed that, as compared to diesel fuel the smoke number and CO emissions for the emulsion were less only at higher power outputs of 2 KW and beyond. The hydro-carbon emissions were more than that observed for diesel, irrespective of the output load. However, the NO_x levels for emulsion combustion was always lower than the diesel fuel.

A large number of experiments have been initiated since 1980 on rape seed oil as fuel for diesel engines but very few studies have been published or mentioned in literature on its use as fuel for commercial boilers.

In 1998, Vaitilingom et. al. [19] carried out experiments in a C22.2 CUENOD burner fixed on a 260 KW GUILLOT boiler. In this work, they used both, crude and refined rapeseed oil as fuel in place of domestic fuel. The experimental results showed that the use of crude oil lead to clogging of the inlet filter in less than 30 minutes of operation. Refined and degummed rape seed oil when preheated to 80°C gave a reliable starting and combustion efficiency similar to that of domestic fuel. Even though the fuel consumption rate is slightly more in case of pure rape seed oil, the emission levels are lower than that for domestic fuel and within the European norms. The authors [19] believe that the use of vegetable oils in commercial burners is far easier than in diesel vehicles in terms of technical or legislative constraints.

Krumdieck et. al. [20] sprayed a blend of 90% (vol.) pyrolysis oil from poplar wood and 10% (vol.) ethanol in a laboratory scale boiler. They observed fewer visible burning droplets when 10% ethanol was added to the oil as compared to the case of pure oil combustion. This indicated that ethanol addition improved the performance of the combustor and flame stability. During the tests, no caking was observed on the ignition electrode which suggests that ethanol addition gave better atomization quality and that ethanol is easily solubilized in the pyrolysis oil used. The authors concluded that steady flame conditions with recirculating flow gave the minimum emissions including 0.02% (vol.) carbon monoxide (CO) and 65 ppm hydro-carbon (HC) particulates.

Emulsified fuels have not only been thought as alternate fuels for boilers and diesel engines but also for turbines. Asea Brown Boveri (ABB) was the first company to test emulsified fuels in turbines in 1985. The paper published by Chellini [21] illustrates

experimental work done on a GEC Alstom, MS9001B 100 MW gas turbine with water-in-diesel emulsion as the fuel. The authors monitored the performance of the turbine for different output levels of 20, 40, 60, 80 and 92.4 MW. The results of the experiments showed that NO_x emissions reduced constantly with increasing amount of water in the emulsion at all the power output levels. No changes in the turbine group vibrations were detected. The combustion efficiency was same as in case of diesel fuel combustion. Smoke opacity remained within the tolerance margin and CO emissions were within the permitted limit. The authors suggest that fuel emulsification has proved itself as a new method for reducing emissions as compared to water/steam injection. The effect of both methods is almost the same but the authors prefer emulsion in order to avoid the cost and time involved with installing and maintaining the water/steam injection systems in the turbine.

2.6 Swirl Effects

Swirl refers to the rotational motion imparted to the primary, secondary or tertiary air needed for combustion. The rotary motion imparted to a fluid upstream of an orifice leads to the development of tangential velocity component within the fluid emerging out of the orifice, along with the radial and axial components. So, a swirler creates a vortex once the air passes through it, ensuring better mixing of the fuel and air during combustion. Swirl number is the ratio of the angular momentum to the axial momentum of the air flow inside the combustion chamber [22] . The swirl number of an annular swirler with a hub and constant vane angle is given by the following formula [22],

$$SN = \frac{2}{3} * \left[\frac{1-\left(\frac{R_h}{R}\right)^3}{1-\left(\frac{R_h}{R}\right)^2}\right] * \text{Tan}\,(\alpha) \quad (2)$$

where,

SN = Swirl number

R_h = Outer radius of the hub

R = Inner radius of the tube

α = Vane angle/Blade angle

The presence of a swirl leads to the generation of radial and axial pressure gradients. For example, in case of strong swirl (S > 0.6) [22], there is an adverse pressure gradient in the core of the vortex which results in reverse flow along the combustion chamber axis setting up an internal recirculation zone (IRZ). The IRZ has a form of torroidal vortex. This recirculation zone plays an important part in flame stabilization as it contains a mixture of chemically active combustion products and acts as storage of heat facilitating easy burning of the newly sprayed fuel.

Following paragraphs illustrate the use of swirler in burners which help combust liquid fuels like LPG, diesel and heavy fuel oil by providing proper mixing and heat transfer properties. Researchers have found out that in order achieve fast evaporation of fuel in the torroidal vortex (induced by the use of swirler), obtain uniform heat intensity and to minimize emissions from liquid fuel combustion, strong swirl intensity or Swirl number (S > 0.6) [22] should be used. Weak swirl intensity (S < 0.6) [22] always leads to an insufficient fuel-mixture vortex giving poor mixing of air and fuel and thus an increase in emission levels.

Mafra et. al. [23] tested liquefied petroleum gas in a burner with 0.47 m diameter which was equipped with an adjustable swirler. From the experiments, the authors concluded that for the same equivalence ratio, when the swirl number was increased from 0.48 to 1.315, the NO formation decreased from 70 ppmv to 55 ppmv. For the same swirl number, if the fuel equivalence ratio was decreased from 0.84 to 0.61, NO formation decreases from 120 ppmv to 70 ppmv. This shows that the highest swirl number of 1.315 and the lowest fuel equivalence ratio of 0.61 gave the minimal NO formation.

Ishak et. al. [24] ran combustion experiments with diesel fuel in a liquid fuel burner system having a radial swirler. The swirler vane angle was increased in increments of 10 degrees starting from 10° (S = 0.046) to 70° (S = 1.911). A vast reduction in NO_x, CO and CO_2 emissions was observed as the swirl number was increased from 10° to 70°. Equivalence ratio was 0.83 in all cases. A 26% reduction in NOx emissions was achieved at 60° vane angle (S = 1.427) compared to the base case. The CO emissions were reduced by 48% and CO_2 emissions decreased by 15.5% for the vane angle of 70°.

Villasenor et. al. [25] tested four swirl numbers 0.1, 0.4, 0.75 and 1.0 for the movable block type swirler fitted in a horizontal cylindrical burner. Mexican heavy fuel oil was combusted in the burner with a Swirl number of 0.75 giving the fastest droplet evaporation and maximum radiation intensity, leading to optimal combustion efficiency.

2.7 Micro-Explosions

Microexplosion is caused when a fuel blend consisting of fuels with different vapor pressures is emulsified and combusted. For example, in case of water-in-oil emulsions, water has a higher vapor pressure. When the water phase reaches superheated conditions, water droplets surrounded by the oil phase explode resulting in the dispersion of the big oil globule into very fine particles. Figures 3 and 4 show the difference between pure fuel and emulsified fuel combustion.

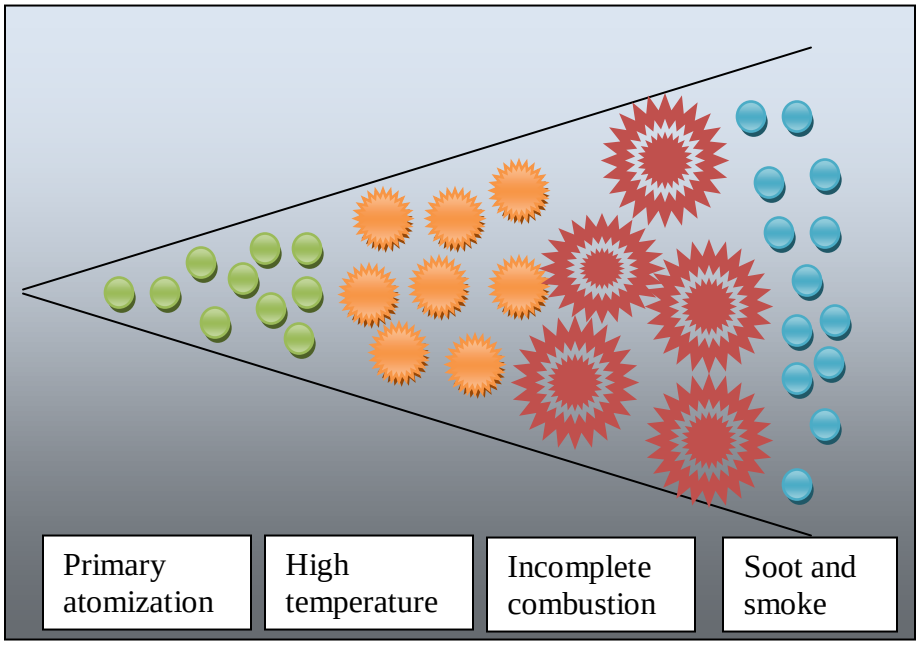

Figure 3: Regular fuel oil combustion [8]

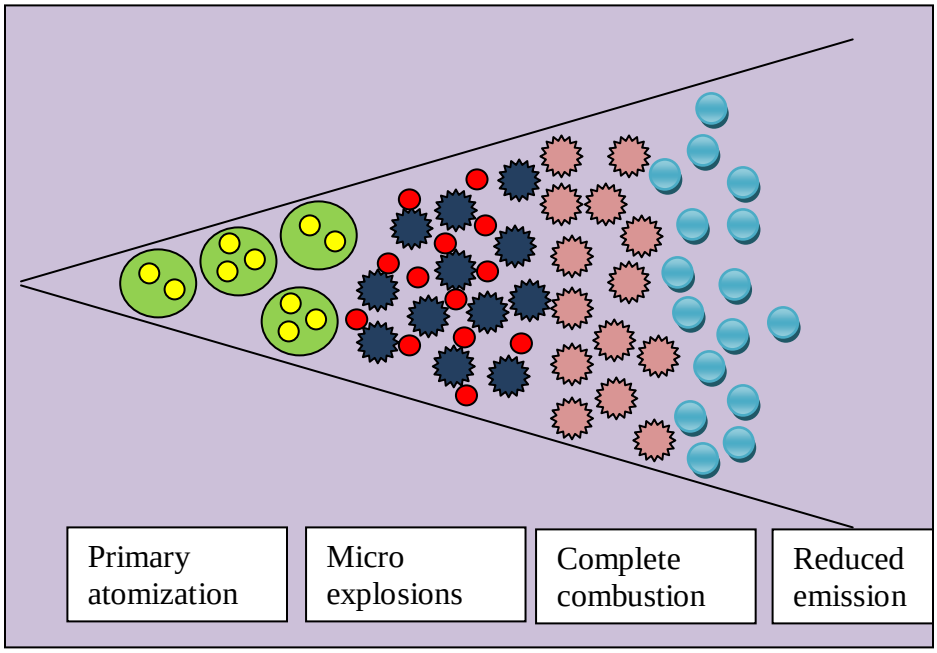

Figure 4: Emulsified fuel combustion [8]

Kadota et. al. [26] suggested that in case of combustion of water-in-fuel emulsions, micro-explosion causes secondary atomization of the emulsion by breaking it up into still finer droplets. These droplets can evaporate really fast owing to their small size. Faster evaporation reduces the time for pyrolytic reactions suppressing the formation of carbonaceous residue. The violent disintegration of the primary emulsion into finer secondary droplets enhances the fuel-air mixing which should result in better combustion efficiency and reduction in soot and unburned hydrocarbon formation as illustrated in Figure 4. Since micro-explosions can provide secondary atomization of the primary droplet, it gives more design flexibility for selection of fuel atomizing devices. Water vapor helps reduce the rate of heat release in the flame also. This is beneficial

because, the major source of thermal NO_x is high flame temperature. By using water, a cooling effect can suppress the chemical NOx forming reaction ultimately leading to significant reduction in NO_x production. Addition of water also helps to increase ignition delay, giving more residence time and cleaner combustion [26]. The water addition to fuel has one more advantage. Evaporation of water increases the number of OH radicals in the combustion field which can oxidize the soot precursors, again helping to decrease the soot level. The authors [26] believe that the above mentioned advantages of emulsified fuels and the expected micro-explosion phenomena during their combustion can help us extend the range of fuel resources, including the use of less volatile fuels like vegetable oil. Furthermore, use of less volatile liquids decrease the risk of fire hazards when compared to petroleum based fuels.

Houlihan [8] has given a theoretical illustration about how emulsified fuel technology (EFT) can deliver "triple-crown" benefits including a reduction in NO_x and particulate matter, better fuel efficiency and decrease in greenhouse gases (GHG), unlike most fossil fuels. All the three benefits are due to the micro-explosion phenomena. The author suggests that the addition of water vapor decreases the combustion zone temperature. This helps in less energetic oxidation of nitrogen in the fuel and air resulting in an overall reduction in NO_x production. The more complete combustion achieved due to secondary atomization means that the emulsified fuel can give higher power output per fuel input. Thus, if the same amount of a hydrocarbon fuel (base fuel forming the continuous phase of the emulsion) is burnt in both, pure form and emulsified form to attain a specific power output, the fuel consumption will be lesser for the

emulsified fuel indicating higher fuel efficiency. Lesser fuel consumption gives a direct reduction in the formation of oxides of carbon and hence decreased GHG. Soot (PM) is also reduced because of a more complete combustion.

In 1990, Kitamura et. al. [27] studied micro-explosion of various emulsified fuels. The base fuels used were kerosene, diesel and tetradecane. The dispersed liquids were water, aqueous methanol and ethanol solutions. Span 80, in the amount of 10 wt% of dispersed phase was used as the surfactant. During the experiments, 0.1 ml of emulsion sample was taken in a Pyrex tube, immersed inside an oil bath, and heated at a rate of 2K/min till explosive evaporation occurred. The authors observed that the flashing temperature of the water-in-kerosene emulsions had a broad range and it decreases with increasing fraction of dispersed phase. The reason for this broad range was the presence of surfactants at the water-oil interface. Bubble nucleation at the water-oil interface was the most probable cause for the violent vaporization of the dispersed phase at the interface.

Ferrante et. al. [28] studied micro-explosion of biodiesel fuel in a fluidized bed. A part of their work involved the use of pressure transducers to characterize the bed fluid dynamics and a Matlab program to simulate its behavior. Experiments were conducted at low bed temperatures, between 600° C and 800° C, to induce micro-explosions in a zone where it could be characterized. A sequence of pictures was captured with a high speed camera to correlate the events occurring inside the combustion chamber and the readings of the pressure transducer. The authors observed that when the biodiesel was injected at a temperature of 650 °C, a light yellow flash extended throughout the area of the

fluidized bed, and rapidly disappeared. The transducer revealed high pressure peaks during the same time interval as the existence of the light flash. The pressure peaks (acoustic signal) smoothened out after a short duration of time. The authors suggest that, these sudden pressure peaks were an indication of multiple micro-explosions occurring across the entire bed area inside the combustion chamber. Pressure readings were also taken with and without fuel injection inside the chamber. Similar pressure peaks were observed when biodiesel was injected and underwent combustion. The authors found that when the bed temperature was at 650 °C, the location of the micro-explosions was just at the bed surface. Above 650°C, the location went inside the bed surface and moved further deep inside the bed as the temperature was increased to 800°C.

3. RECENT RESEARCH ON STRAIGHT VEGETABLE OIL AS A FUEL AT TEXAS A&M UNIVERSITY

During Fall 2008 and Spring 2009, a study was done to form nano-emulsions of methanol-in-canola oil. The project was funded by Leonardo Technologies, Inc., Ohio and the US Army Corps of Engineers. The aim of the project was to determine the impact of shear induced micro-emulsions on the viscosity and stability of straight vegetable oil (SVO). The whole purpose of the project was to make nano-emulsions as fuel for a modified diesel engine.

3.1 Equipment

The equipment used for forming nano-emulsions was a microfluidizer, as shown in Figure 5. A microfluidizer is an ultra-high shear force generator. The main components of the fluidizer are intensifier pump, interaction chamber, auxiliary processing module and cooling coil reservoir. The high pressure, pneumatically actuated pump is capable of increasing the working pressure to 160 MPA and generating shear rates of the order of 6,000,000 sec^{-1}. The interaction chambers have Z-shaped or Y-shaped micro-channels in them which help to create highly-controlled shear on the entire fluid volume passing through them. The ultra-high shear force produces extremely small and uniformly sized particles in the entire product stream resulting in stable emulsions. In the case of Z-shape chamber, the fluid experiences sudden change in the flow direction. In the Y-shape chamber, two fluid streams collide at high velocities and merge into a single channel. The auxiliary chamber reduces the pressure of the fluid before it reaches the outlet pipe.

Figure 5: Microfluidizer [29]

To measure the viscosity of the pure oil and emulsions, a Brookfield's DV-I Prime viscometer was used. The viscometer calculated the torque on its rotating spindle and converted it into viscosity value of the fluid. The spindle could rotate at a minimum speed of 1.5 RPM and maximum speed of 60 RPM.

3.2 Sample Preparation

Pure canola oil of Crisco brand (purchased from the local HEB grocery store) and 99.99% concentrated methanol from EMD biosciences was used for making the emulsions. Span 20 and Tween 20 surfactants were purchased from Sigma-Aldrich, USA.

Two emulsion samples were made:

1. 90/10 emulsion – 10% methanol in 90% canola oil (v/v), without any surfactant.

2. 79/20 emulsion – 20% methanol in 79% canola oil with a 2% mixture of Span 20 and Tween 20 surfactants (v/v).

500 ml of each emulsion was made. First, the canola oil and methanol were mixed with a mechanical blender for 7 minutes (a minimum of 5 minutes of blending was necessary for the sample to pre-mix uniformly before it is emulsified in the fluidizer) in a glass beaker. This blended mixture was then poured into the inlet reservoir of the microfluidizer. The compressed air was supplied to the fluidizer at a pressure of about 690 kPa – 830 kPa (100 psi – 120 psi) to get the desired fluid pressure of about 103MPa – 138 MPa (15,000 psi – 20,000 psi), necessary for forming emulsions. The F-20Y interaction chamber and G30Z auxiliary module were used to make emulsions in this project.

The temperature of the sample increased by almost 2° C after every pass due to high friction in the micro channels. To reduce the temperature of the emulsion coming out of the microchannels, the cooling coil reservoir was filled with ice and water. Once all the fluid in the inlet reservoir passed through the microfluidizer, “one pass” was complete. The collected sample was again poured back into the reservoir, for running the “second pass”. The procedure was repeated for about 10-20 passes depending upon the stability of the sample. After every two passes, some amount of sample was collected in a vial to measure the viscosity and stability of the emulsion over time.

The preparation method for 79/20 emulsion was the same as explained above except, the oil-alcohol mixture along with the surfactant was blended for 10 minutes. Amount of surfactant used was 1% weight of the plain 79/20 mixture of canola oil and methanol. Of

this 1%, 60% (weight basis) Span 20 and 40% (weight basis) Tween 20 were used to make the emulsion.

3.3 Results and Discussions

The viscosity of pure canola oil as measured in the viscometer at 25°C was 57.5 cp. Figure 6 shows the variation in viscosity for the 90/10 emulsion with the number of passes in the microfluidizer. The plot has four different curves for four different spindle speeds. The operating pressure for the microfluidizer was 965 MPa (14,000 psi). A total of 18 passes were done and the viscosity was measured after every two passes. The maximum value of viscosity after the 18th pass was 41.2 cP.

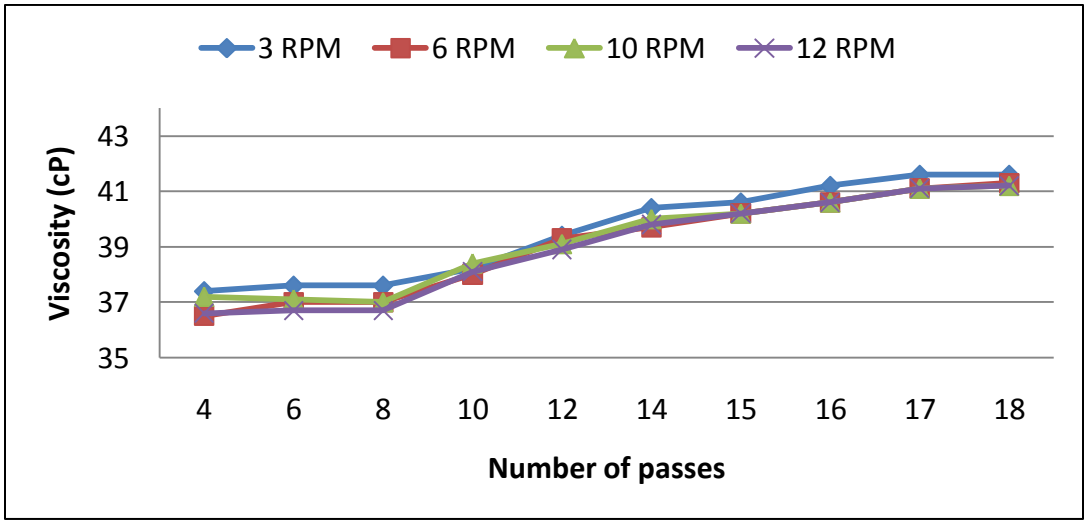

Figure 6: Variation in viscosity of nano-emulsified SVO at a concentration of 90/10 at 25 °C

Figure 7 shows the variation in viscosity for a 79/20 emulsion with the number of passes in the micro-fluidiser emulsion. Since the amount of alcohol to be emulsified was double as that in the 90/10 concentration, higher pressure was needed to form the emulsion. The operating pressure for the microfluidizer was 124 MPa (18000 psi). A total of 18 passes were done. Due to the higher amount of methanol, the fluid was passed multiple times through the fluidizer without stopping after every two pass in order to prevent methanol evaporation. The viscosity was measured at the 8th and 18th passes. The maximum value of viscosity after the 18th pass was 45.5 cP.

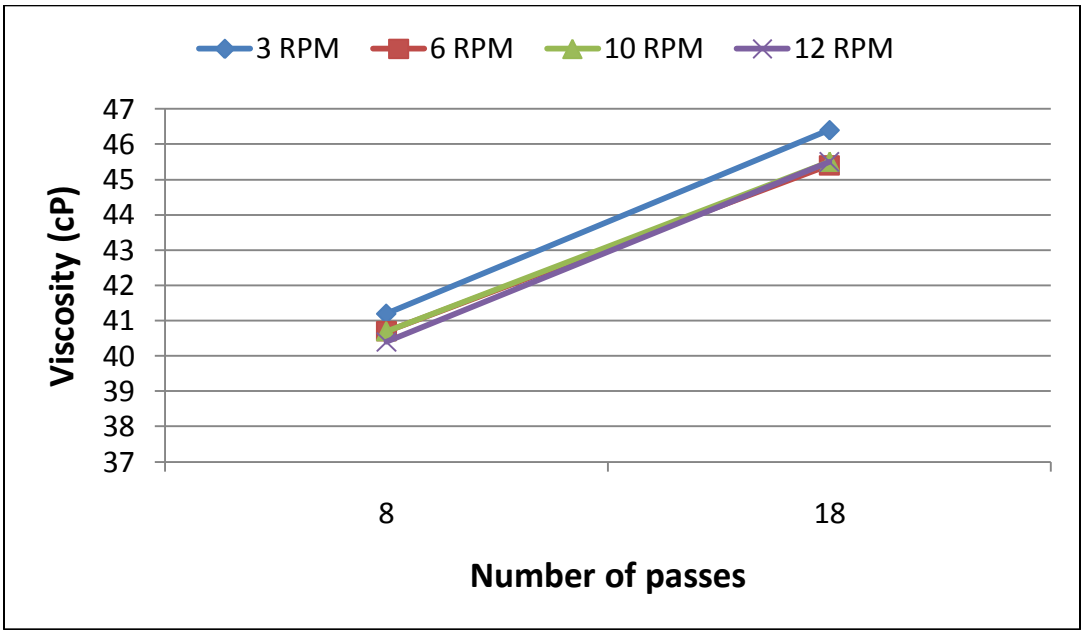

Figure 7: Variation in viscosity of nano-emulsified SVO at a concentration of 79/20 at 25 °C

Both figures show a gradual increase in the viscosity of the emulsion with an increase in the number of passes in the microfluidizer. As the fluid makes more number

of passes in the fluidizer, it is subject to more and more shear decreasing the droplet size of the dispersed phase. Due to a decrease in droplet size, the surface-to-volume ratio of the dispersed droplets in the continuous phase increases. Since the surface-to-volume ratio increases, the hydrodynamic forces between the suspended droplets are higher resulting in higher viscous resistance [30]. The same was observed by Pal [30] where he concluded that, in case of dilute and concentrated dispersions of monodispersed soft spheres, there is an increase in viscosity with a decrease in particle size. Table 3 summarizes the results from both the plots.

Table 3: Property of nano-emulsions produced by microfluidization

	Emulsion Type	
	90% canola oil + 10% methanol	79% canola oil + 20% methanol + 1% surfactant
Temperature	25 ℃	25 ℃
Dynamic Viscosity	41.2 cP	45.5 cP
% Reduction in Viscosity	28.35 %	20.87 %
Stability Period	7 days	2 days

The table shows that the viscosity of 90/10 emulsion and 79/20 emulsion after 18 passes in the fluidizer were 41.2 cP. and 45.5 cP. respectively. The reduction in viscosity for 90/10 emulsion was higher due to the absence of any surfactant. Also, 90/10 emulsion was stable for a longer time because it had lesser amount of alcohol as compared to 79/20 emulsion. Overall, stable emulsions were obtained from the microfluidizer.

Even though the results of the afore mentioned work was good, further work in the area was not completely justifiable due to the high amount of energy required for complete microemulsification. Other reasons for discontinuing the microfluidizer method for making emulsion were quite a few including the inability of form stable emulsion without using surfactants. Greater stability needed more passes and thus more energy. Secondly, stability issues were also encountered when higher percentage of alcohol was used. Higher percentage of alcohol dictated more usage of non-ionic surfactants like Span 80 and Tween 20. Furthermore, the emulsifying properties of non-ionic surfactants are highly temperature dependent. Since there was an increase in temperature of the fluid inside the micro-channels, it was very difficult to achieve good repeatability of results. Additionally, the microfluidizer needed compressed air at a minimum flow rate of 1416 l/min (50 scfm) and a minimum pressure of 827 kPa 120 psi. These requirements increased as the percentage of alcohol to be emulsified increased. In general, the microfluidizer needs a separate dedicated air compressor for efficient operation. The microfluidizer was very noisy when under operation.

Given all the challenges associated with the microemulsification of SVO, a change of research strategy was undertaken. Instead of forming micro-emulsions using a microfluidizer, the research team decided to purchase and test an air-operated fuel nozzle capable of mixing and dispersing SVO with viscosity values as high as 100 cP. The following sections describe the efforts undertaken in this direction.

4. OBJECTIVES AND TASKS

The overall objective of this research work was to understand the effect of combustion of pure canola oil and methanol-in-canola oil emulsions, swirl angle and equivalence ratio on the emission levels of nitrogen oxides, carbon monoxide and unburnt hydrocarbons. In order to achieve the overall objective, following tasks were performed:

1. Obtain the chemical composition and higher heating value of canola oil by conducting ultimate analysis and bomb calorimeter tests.

2. Make stable methanol-in-canola oil emulsions having 2 different compositions,

    i. 9% methanol-in-89% canola oil emulsion with 2% (w/w) surfactant
    ii. 12.5% methanol-in-85% canola oil emulsion with 2.5% (w/w) surfactant

3. Obtain the viscosity values of pure canola oil and its corresponding emulsions. Determine the change in the viscosity of pure oil due to the addition of methanol and surfactants.

4. Derive the chemical formula and estimate higher heating value of the emulsions by knowing the percentage mass of each component in the blend.

5. Conduct adiabatic flame temperature calculations in Engineering Equation Solver (EES) for all the fuels at equivalence ratios of 0.83, 0.91, 1.0, 1.05 and 1.11.

6. Design and build a radial vane swirler.

7. Complete the modification of the existing coal fired boiler by fitting a new swirler and an entirely new fuel injection system.

8. Perform combustion experiments of canola oil and methanol-in-canola oil emulsions under constant heat output. Obtain combustion and emission characteristics of the fuels.

The objectives were undertaken to characterize the effects of combusting canola oil and its blends under different operating conditions. The conditions imposed on the combustion process had a significant effect on emission levels as discussed in the Results and Discussion section.

5. EXPERIMENTAL SET UP

This section gives a detailed description of the experimental facility, instrumentation and experimental procedures followed during this project.

5.1 Introduction

All the experiments were done in a small scale 30 kW (100,000 BTU/hr) furnace built at Coal and Biomass Energy Laboratory (CBEL) at Texas A&M University (TAMU). The initial design and construction work of the furnace was performed by Dr. Annamalai's research group. The furnace was primarily built to combust solid fuels like coal and biomass. The furnace has been under operation for more than 10 years. The modifications required for combusting liquid fuels were carried out during this research project.

5.2 Furnace Modification

The furnace (combustion chamber) had to be modified to be able to combust liquid fuels. Modification of the furnace was completed by designing and building:

1. A swirler
2. A liquid fuel injection system

5.2.1 Swirler

The swirler used in this research work was a vane type swirler. It was made from two concentric steel cylinders and, and steel vanes of 0.5 mm thickness. Dimensions of the hub are D_i = 53.9 mm (2.124 in), D_o= 59.4 mm (2.340 in), H = 25.4 mm (1 in). Dimensions of the outer cylinder are D_i = 100.4 mm (4.10 in), D_o= 113.6 mm (4.475 in),

H = 25.4 mm (1 in). Two sets of vanes were made. Each set had a total of 8 vanes. The first set of vanes was positioned at an angle of 60 degrees with respect to the vertical axis (swirl number = 1.4) and the second set at 51 degrees (swirl number = 1.0), with respect to the vertical axis. Tungsten wire, steel nut and bolts were used to hold the blades in-between the hub and the outer cylinder. Figure 8 shows the swirler with vanes at 60 degrees.

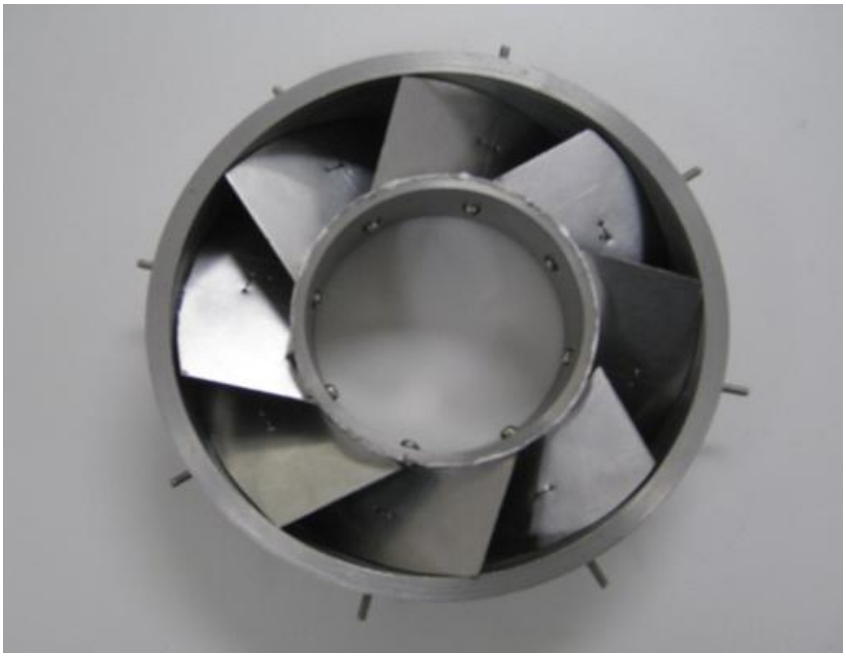

Figure 8: Swirler with a vane angle of 60 degrees

5.2.2 The Liquid Fuel Injection System

The injection system used for spraying liquid fuel in the furnace consisted of the following equipments:

1. A twin fluid atomizer/nozzle

Twin fluid atomizers are basically used to spray viscous liquids. They are supplied with two fluids. One is a liquid and the other is a low, medium or high pressure gas, most commonly, air or steam. The nozzle has a mixing chamber within it where the gas stream impinges on the liquid jet and forms a good quality liquid-gas mixture which is then sprayed as a very fine mist. The volume of each fluid coming out of the nozzle is directly proportional to the pressure at which it is supplied to the nozzle. I.e., higher the pumping pressure of a fluid, higher is its dispersed volume from the nozzle. The nozzle design is such that, the increase in the pressure of one fluid can result in the reduction of flow of the other. So, as a general rule, the gas stream is supplied at a higher pressure than the liquid to obtain a fine mist.

A twin fluid nozzle was purchased from Bete Spray Nozzles Company, USA. The nozzle was made from Hastelloy C276 (Nickel-Molybdenum-Chromium alloy with some percent tungsten). This alloy was specially selected as it had a high melting temperature of 1100° C (rated by the manufacturer). The nozzle had two 6.35 mm (1/4 in) inlet ports for liquid and air and a 0.5 mm (0.020 in) diameter orifice at its centre, from which the fuel-air mixture was sprayed in the furnace. Figure 9 shows the twin fluid atomizer used in this project.

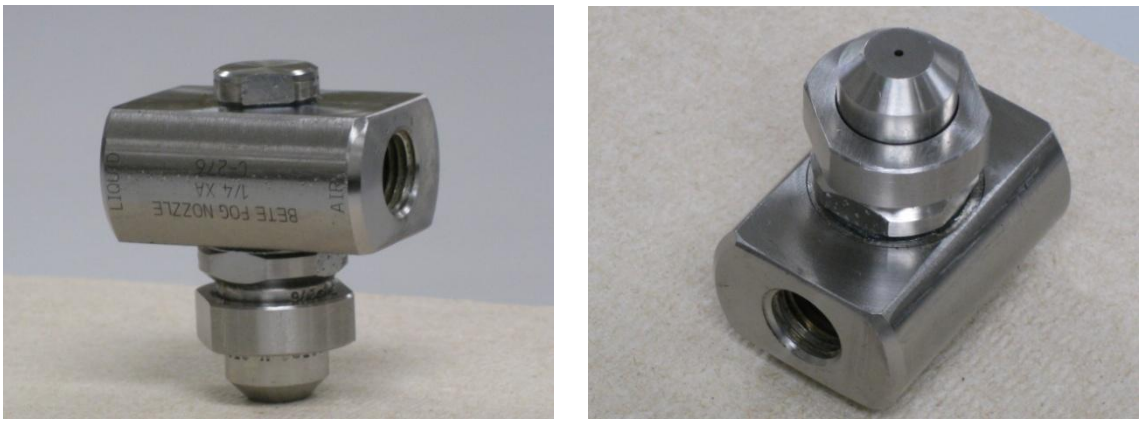

Figure 9: Twin fluid atomizer

2. A digital oil flow meter

An oval gear, digital flow meter was purchased from McMaster-Carr Supply Company, USA. The flow meter was compatible with liquids possessing viscosity as low as 5 cP. up to 1000 cP. It could read a minimum flow of 0.5 l/hr (LPH) to a maximum of 50 l/hr (LPH) with an accuracy of ± 1%. In this project, the flow meter was used to read the flow rate of pure canola oil and its emulsions. The oil flow meter is shown in Figure 10.

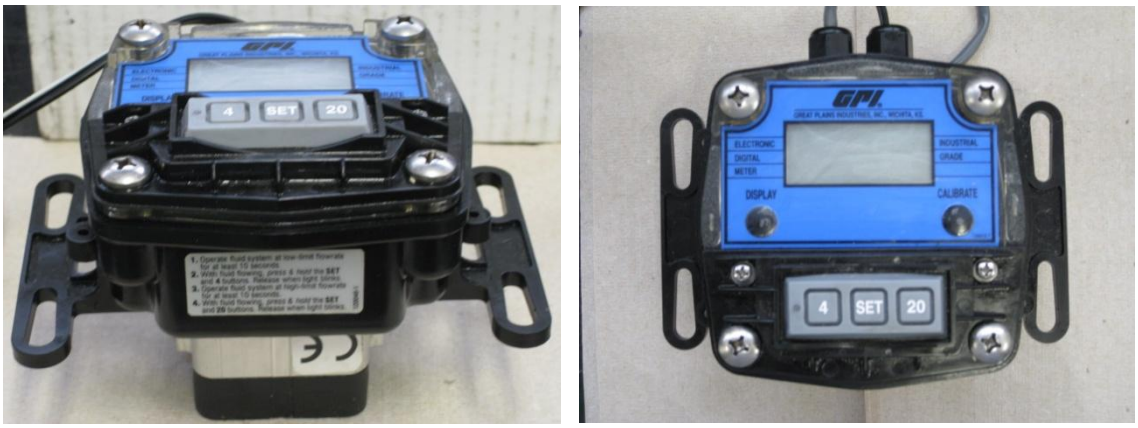

Figure 10: Digital flow meter

3. Gear Pump

A low flow gear pump was purchased from Suntec Industries Incorporated, USA. The pump had a factory setting of 690 kPa (100 psi) fluid pressure at its outlet and pumping capacity of 3.8 l/hr (1 GPH) to 11.4 l/hr (3 GPH). The pump supplied the canola oil and its emulsions to the nozzle. The fuel pump is shown in Figure 11.

Figure 11: Fuel pump

4. Primary Air Compressor

A high capacity air compressor was purchased from Cole-Parmer Instrument Company, USA. The air compressor was rated at a free air capacity of 31.2 l/min and maximum air pressure of 413.6 kPa (60 psi). The compressor was used to supply primary air to the nozzle. The air flow rate was regulated by regulating the valve on the compressor. Figure 12 shows the air compressor.

Figure 12: Air compressor for supplying primary air

5. Air Flow Meter

The flow rate of primary air supplied to the nozzle was measured using a digital air flow meter purchased from Omega Engineering Inc., USA. The flow meter had a display screen and could measure flows from 4.0 l/min to 20 l/min. Figure 13 shows the air flow meter used in this project.

Figure 13: Air flow meter for primary air

6. Ball Valve and Pressure Gauge

A 3.175 mm (1/8 in) ball valve was attached between the fuel pump and the oil flow meter to regulate the flow of the fuel going to the nozzle. A Pressure gauge was also used in the liquid line. Figure 14 shows the valve and the gauge.

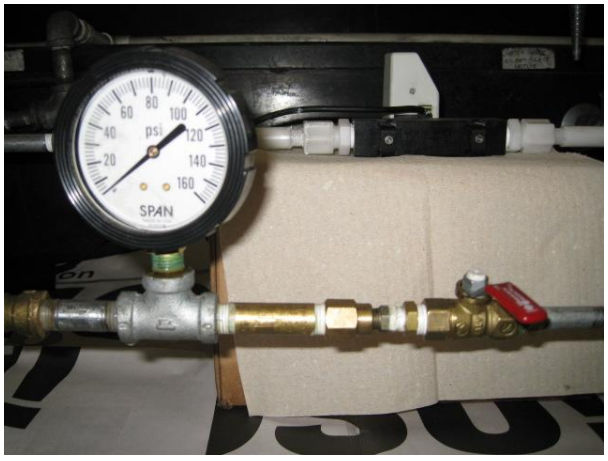

Figure 14: Pressure gauge and ball valve

Next part of section 5 describes some other instruments used in the research project. These instruments were already available at Coal and Biomass Energy Laboratory at TAMU.

5.3 Instrumentation

1. Secondary Air Compressor

A Gardner Denver, Inc. made, rotary positive displacement air compressor was used to supply the secondary air, which formed the major part of air needed for combustion. The compressor was powered by a 1730 RPM OPTIM built electric motor. The compressor could provide a maximum air flow rate of 650 l/min at a pressure of 117.2 kPa (17 psia). A digital air flow meter measured the flow rate of the secondary air. Figure 15 shows the air compressor.

Figure 15: Air compressor for supplying secondary air

2. Exhaust Gas Analyzer

A Greenline 8000 Gas Analyzer purchased from Eurotron Instruments was used to study the exhaust gas composition from the furnace. The gas analyzer provided a digital and printed summary for the amount of O_2, CO, CO_2, NO, NO_2, NO_x, SO_2, and C_xH_y present in the exhaust gases. Figure 16 shows the gas analyzer.

The analyzer used electrochemical (EC) cells for measuring the concentration of O_2, CO, NO, NO_2 and SO_2 in the exhaust gas. NO_x was measured by adding the concentrations of NO and NO_2. Electrochemical cells are basically composed of two electrodes and an electrolyte solution, depending on which gas needs to be detected. The gas sample goes through a selective diffusion membrane. The oxidation process produces an electrical signal proportional to the gas concentration. This electrical signal is evaluated by the electronics, converted into digital, processed by the microprocessor and displayed on the screen. Each electrochemical sensor has a different response time; O_2 – 20 sec, CO – 50 sec, NO_2 – 50 sec and NO – 40 sec. The gas analyzer also used gas sensors based on infrared (IR sensors) spectroscopy to measure the concentration of CO_2 and unburned hydrocarbon groups in the exhaust. The principle of operation of IR sensors is based on the absorption of a specific wavelength by a particular gas. The IR system of the analyzer consisted of an IR light source, a chamber containing the gas sample and a photo-detector with optical filter. The light passes through the chamber and the gas sample absorbs at a specific wavelength. The photo-detector identifies the gas on the basis of the absorption spectrum. The signal collected by the photo-detector is processed by electronics to obtain the concentration of the particular gas.

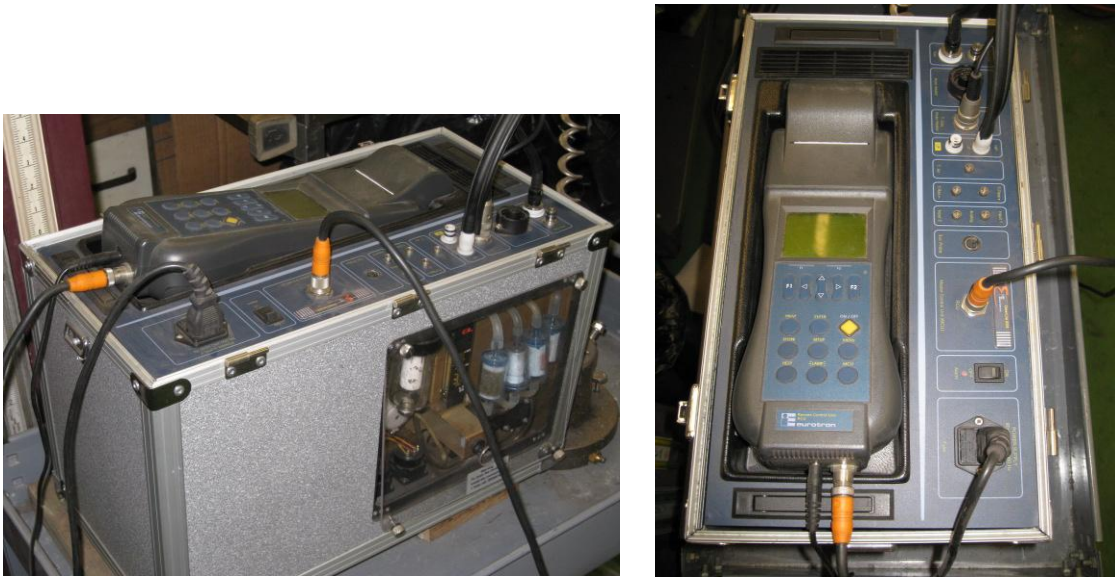

Figure 16: Exhaust gas analyzer

A suction pump, (see Figure 17) was used to transfer the flue gases from the combustion chamber to the gas analyzer. The flue gases were supplied to the gas analyzer at a constant flow rate of 200 l/hr.

Figure 17: Suction pump

A filter was used was to trap the solid carbon particles (soot) from the flue gases before they entered suction pump. The filter was changed after each experiment and new one was fitted in-line. This was done to ensure that the soot particles did not act as adsorbents for the gases and to avoid any obstruction in the path of exhaust gases being supplied to the analyzer.

3. Gas Flow controller

The volumetric flow rate of natural gas used for preheating the furnace was regulated by a digital gas flow controller purchased from Cole-Parmer Instrument Company, USA. Figure 18 shows the gas flow controller.

Figure 18: Natural gas flow controller

4. Data Acquisition System

All the thermocouples were connected to a data acquisition (DAQ) system purchased from Agilent Technologies, USA. The DAQ was connected to a computer where the temperature was logged at an interval of every 20 seconds. Figure 19 shows the DAQ.

Figure 19: Agilent data acquisition system

5.4 Experimental Facility - The Modified Furnace Description

The 30 kW furnace at CBEL was given the ability to combust liquid fuels by using a radial vane swirler, twin fluid atomizer, fuel and air pumps, oil and air flow meters. Figure 20 shows the furnace after the modification was complete.

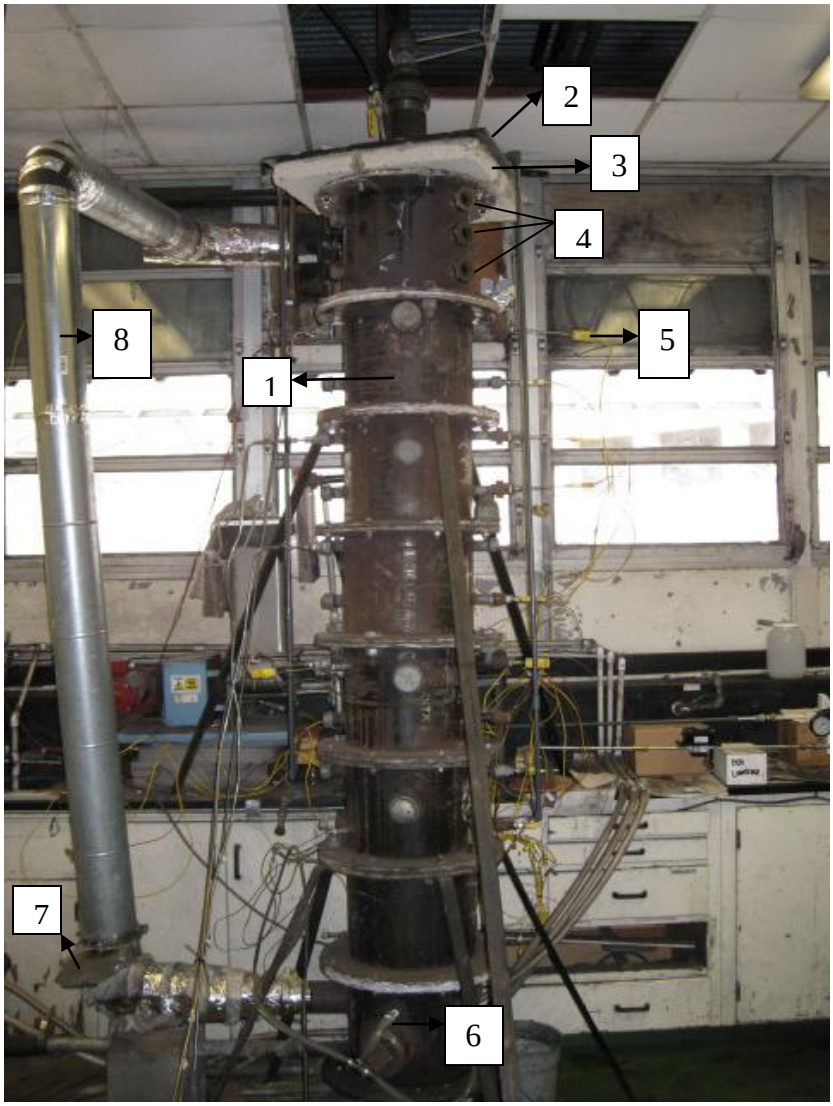

Figure 20: 30 kW furnace at Coal and Biomass Energy Laboratory, TAMU

The numbered components in the Figure 20 are,

1 – Furnace, 2 – Boiler top plate, 3 – Furnace cement insulation, 4 – Eye hole, 5 – Thermocouple, 6 – Water spray, 7 – Exhaust vent port, 8- Exhaust duct

The modified furnace had a total height of 2.4 m (8 ft and 2.5 in). The inner wall of the furnace has a refractory lining made from Greencast 94 Ceramic. The net hollow diameter of the furnace was 152.4 mm (6 in) all throughout its height. Figure 21 shows a cross section of one cylindrical element of the furnace. The furnace was built with a total of 8 such pieces.

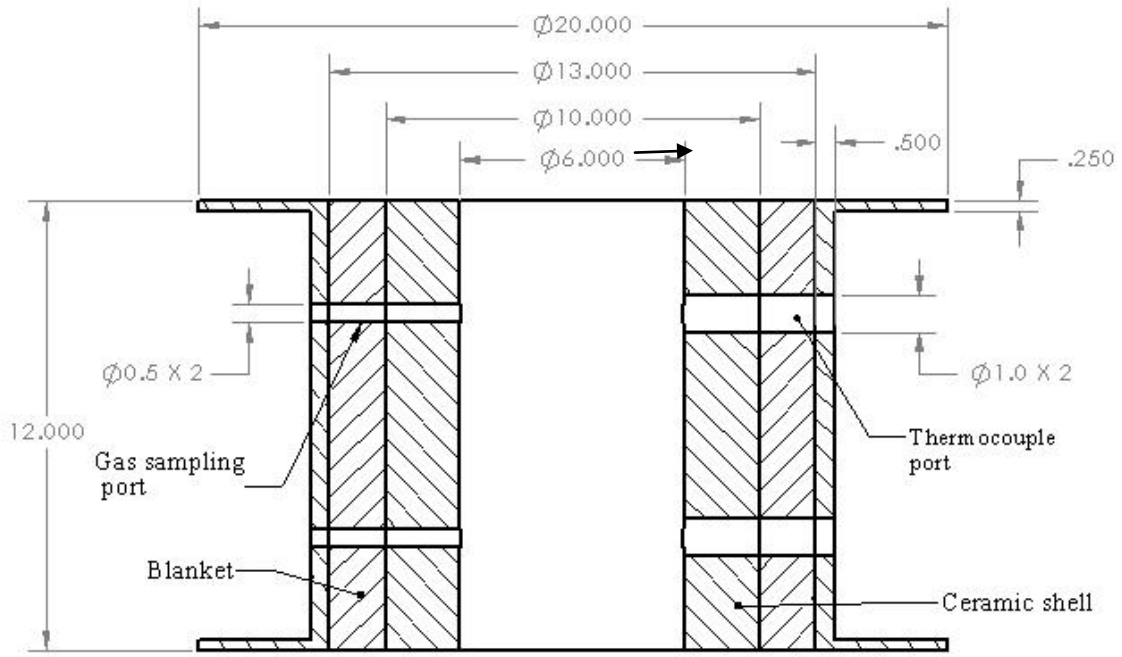

Figure 21: Cross section of the furnace (all dimensions are in inches)

The top of the furnace was enclosed with a 0.55 m x 0.55 m x 0.05 m (22 in x 22 in x 2.125 in) furnace cement insulation block as shown in Figure 20. This insulation could withstand high temperatures up-to 2700 °C. The cement block had a152.4 mm (6 in) diameter hole at its centre. On top of this insulation was placed a0.6 m x 0.6 m x 0.006

m (24 in x 24 in x 0.25 in) iron plate with a 104.1 mm (4.10 in) diameter hole at its centre. The swirler was fixed on top of this plate with screws and nuts, covering the hole at the centre. A 12.7 mm (1/2") diameter hole was drilled in the furnace top plate to place the natural gas pipeline inside the furnace. As seen in Figure 22, a 101.6 mm (4") steel pipe connected to 101.6 mm (4)" to 50.8 mm (2)" reduced coupling marked the end of the secondary air line at the top of furnace. The 101.6 mm (4") pipe was fused with the swirler wall and sealed with silicone to ensure uniform turbulent conditions.

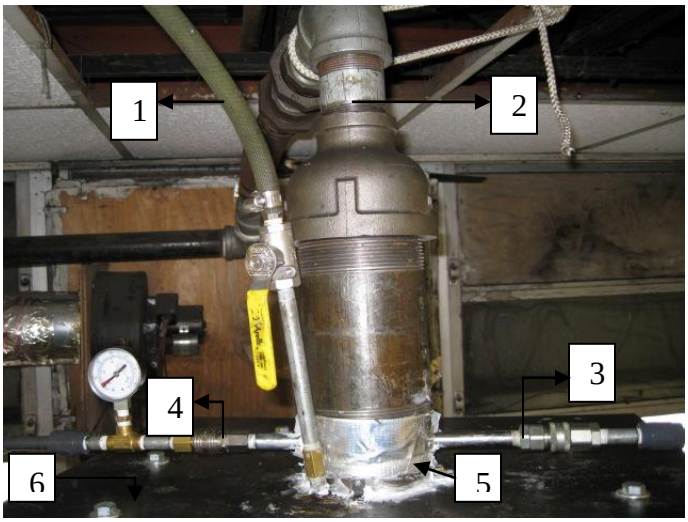

Figure 22: Component assembly above the boiler plate

The numbered components in Figure 22 are,

1 – Natural gas pipeline, 2 – secondary air pipeline, 3 – liquid line to the nozzle, 4 – primary air line to the nozzle, 5 – swirler, 6 – Boiler top plate

The furnace was preheated to temperatures of about 800° C by burning natural gas with a help of a gas (propane) torch. The propane torch was inserted in the furnace through the second eye hole from the top. Type K thermocouples were used to obtain the temperature profile of the combustion zone. The first thermocouple was at a distance of 44.45 cm (17.5 inches) below the nozzle tip. The furnace had three sight holes to view the flame, each separated by a distance of 90 cm (3.5 inches). The first sight hole is located 14cm (5.5 inches) below the nozzle tip.

The pipe lines for carrying the fuel and primary air from their respective sources to the nozzle were basically constructed from 6.35 mm (1/4 in) and 3.175 mm (1/8 in) PVC and steel pipes. Several pipe fittings like couplings, adapters and quick disconnects were also used for constructing the entire fuel and primary air transport lines. Figure 23 shows the assembly of components in the transport lines.

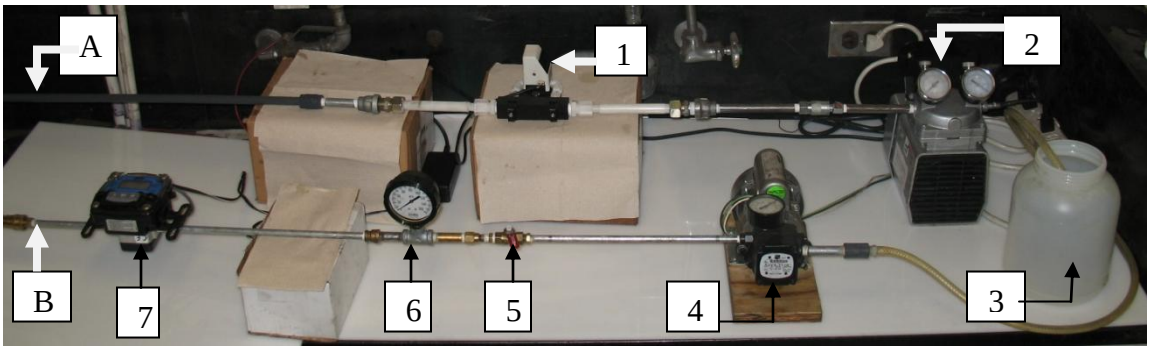

Figure 23: Assembly of components in the primary air and fuel pipelines

The marked components in Figure 23 are,

A – Primary air line to the nozzle B – Liquid line to the nozzle

1-Primary air flow meter, 2 – Primary air compressor, 3 – Fuel tank, 4 – Fuel pump, 5 – Ball valve, 6 - Pressure gauge, 7 – Oil flow meter

The twin fluid nozzle was positioned inside an aluminum cone which in-turn was placed inside the inner cylinder of the swirler. The system was designed such to ensure that all the secondary air passed through the swirler blades and attained maximum rotary motion downstream. The nozzle was placed such that the tip of the nozzle was positioned approximately 5 mm above the edge of the swirler. Figures 24 shows the positioning of the nozzle and the aluminum cone inside the swirler.

Figure 24: Position of the nozzle and aluminum cone inside the swirler

The gas analyzer was connected to the combustion chamber at a sample port located 1.85 m (71 inches) below the nozzle tip. Before entering the analyzer, the exhaust gases were first passed through a condenser to condensate and remove the water vapor coming out of the combustion chamber. After the condenser, the gases passed through a filter as described above. This was done in order to collect solid carbon particles. The

temperature of the exhaust gases released to the atmosphere was lowered for safety purposes with a water cooling spray located at the base of the furnace.

5.5 Experimental Procedure

Combustion experiments of pure canola oil, 89-9 emulsion and 85-12.5 emulsion were done after completing the modification of the furnace. Even though the flash point of pure canola oil is around 275° C – 290 °C [31], it was necessary to preheat the furnace until it reached about 800 °C in order to produce a self igniting flame of the liquid fuels. At this temperature, the thermal energy contained within the combustion zone was sufficient to produce a stable flame. Each experiment took around 3 to 4 hrs including 1 hour and 15 minutes of preheating time. The procedure followed to conduct the experiments has been discussed below:

1. The furnace was inspected to ensure that it was completely sealed and that, air was not able to enter the furnace from anywhere other than primary and secondary air inlets.
2. The secondary air compressor was started and the secondary air flow was set to about 400 l/min (LPM).
3. The exhaust fan was turned on. The exhaust port of the furnace was also opened to ensure negative pressure (approximately 39 kPa) inside the furnace and to remove any combustible gases left behind from the previous experiments.
4. The water pump and water spray located near the exhaust vent port were switched on to ensure that exhaust gases were cooled prior to exiting the furnace.
5. The primary air compressor was started. Primary air flow was set to 5 l/min (LPM). This was done to keep the nozzle cool during the preheating phase.

6. The gas torch was started and inserted in the second sight hole from the top.
7. Natural gas flow was turned on and allowed to flow inside the furnace at a flow rate of 40 SLPM . The flame from the gas torch ignited the natural gas. It was mandatory to first insert the gas torch inside the furnace and only then start the natural gas flow. Interchanging the sequence of these two steps entailed high chances of a major explosion.
8. The gas torch was shut off and removed from the furnace when the 1st thermocouple showed a temperature of 650 °C. The second sight hole was closed with the lid.
9. The preheating of the furnace from 650 °C to 800 °C (as indicated by 1st thermocouple) was done exclusively by the burning of natural gas.
10. The fuel pump was started after the temperature of the 1st thermocouple reached to about 800 °C. The flow of natural gas was gradually decreased from 40 l/min (LPM) to 10 l/min (LPM) in decrements of 10 l/min (LPM). By doing this, the natural gas and liquid fuel were burned simultaneously for about 5 minutes. After that the natural gas was shut off completely.
11. The natural gas pipeline was removed from the furnace top plate. The 12.7 mm hole was closed with a12.7 mm (1/2 in) NPT screw. This was done to prevent any air leakage into the furnace.
12. The furnace was visually inspected to ensure that the oil was self igniting and that a flame was still present in the furnace. The change in temperature inside the furnace also indicated the existence of a flame.

13. The fuel flow rate was set as per the calculated value to achieve 20.2 kW of heat of combustion. The primary air flow rate was increased from 5 l/min and kept constant at 10 l/min at all equivalence ratios for all the experiments, irrespective of fuel type. The secondary air flow was adjusted in order to achieve stoichiometric combustion ($\phi = 1$) of the liquid fuel.
14. The fuel was burned for around 30 to 45 minutes at stoichiometric conditions to allow the temperature inside the combustion chamber to stabilize. Once the temperature inside was stabilized, the first reading for the exhaust gas composition at stoichiometric conditions was recorded. The second reading at the same equivalence ratio was taken after 5 minutes.
15. In the case of emulsion combustion, the emulsions were stirred inside the fuel tank after every 5 minutes to ensure that the methanol and oil do not separate out.
16. After collecting data at stoichiometric conditions, the secondary air flow was adjusted to get the other equivalence ratios. The fuel flow and primary air flow rate remained the same.
17. At each equivalence ratio, it was necessary to wait for approximately 10 minutes in order to let the temperatures and oxygen output levels to stabilize. Once the combustion process was stable, the readings for flue gas composition were taken in the same way as done in stoichiometric case.
18. After all the readings were taken; the furnace was shut down by switching off the fuel pump. The furnace exhaust vents were opened all the way and the secondary air flow was set to 100 l/min (LPM).

19. The exhaust water cooling spray and the primary air were switched off after the temperatures recorded by thermocouple read less than 200 °C. The furnace was allowed to cool down to the ambient temperature.

5.6 Emulsion Preparation

The emulsions used in this project were made from 100% natural canola oil of Wesson brand, 99.99 % concentrated methanol purchased from EMD biosciences, Span 80 and Tween 80 surfactants from Sigma-Aldrich, USA. As discussed before, two emulsions of the following concentrations were made:

1. 89 – 9 Emulsion; having 9% methanol mixed in 89% canola oil with 2% (w/w) surfactant (75% Span 80 + 25% Tween 80) in it.
2. 85-12.5 Emulsion; having 12.5 % methanol mixed in 85% canola oil with 2.5% surfactant (75% Span 80 + 25% Tween 80) (w/w).

It is a common practice to use a mixture of a hydrophilic and a hydrophobic surfactants in order to get a more stable emulsion. Morais et. al. [32] used multiple Span and Tween surfactant mixtures to find out the best combination for stabilizing canola oil-in-water emulsion. The authors [32] suggest that total amount of surfactant should be added such that the HLB number of the surfactant mixture is equal to the HLB number of the parent liquid forming the emulsion. Canola oil was the parent liquid and methanol was the dispersed liquid for the emulsions used in this project. The required HLB number of canola oil is 7.0 [33]. HLB number of Span 80 and Tween 80 is 4.3 and 15.0, respectively. Mollet. et. al. [10] have defined the formula to determine the amount of a

surfactant (A) that must be mixed with some other surfactant (B) to achieve an HLB value of X, as

$$(\%)\mathrm{A} = \frac{[100 * (\mathrm{X} - \mathrm{HLB_B})]}{(\mathrm{HLB_A} - \mathrm{HLB_B})} \quad (3)$$

$$(\%)\mathrm{B} = 100 - (\%)\,\mathrm{A} \quad (4)$$

By using the above two equations, it was decided to add 25% Tween 80 and 75% Span 80 (w/w) to the emulsions. 89-9 emulsion and 85-12.5emulsions were made in batches of 1 liter. The procedure followed for making 89-9 emulsion is described in the following steps:

1. 865.8 grams (900 ml) of oil was taken in a glass beaker.
2. Total quantity of surfactant mixture added was equal to 2% of the weight of a 1000 ml blend, consisting of 865.8 grams (900 ml) oil and 80 grams (100 ml) methanol. Of this 2%, 75% was Span 80 and 25% was Tween 80 on a weight basis.
3. The oil and the surfactant mixture were blended using a mechanical blender for 2 minutes. This was done to distribute the surfactants uniformly in the oil.
4. 80 grams (100 ml) of methanol was then added to the beaker already containing oil and surfactants.
5. The oil, methanol and the surfactant mixture was blended for 20 minutes using a blender. A total of 4.5 liters of emulsion was made. Figure 25 shows the blending process for the 89-9 emulsion.

Figure 25: Mechanical blender being used to mix the oil, methanol and surfactants

6. After the blending process was completed, some amount of emulsion was collected in graduated vials to keep a track of the stability period. Figure 26 shows the 89-9 emulsion after 20 minutes of blending.

Figure 26: 89-9 emulsion after 20 minutes of blending

7. Stability of emulsions: To keep a track of the stability of the emulsion, the emulsion was visually inspected after every one hour until a separation was seen.

Figure 27 shows the 89-9 emulsion after 7 hours. Note that the methanol has separated out. The whitish-yellow color of the liquid sitting at the bottom indicates that there is still some methanol emulsified in the canola oil.

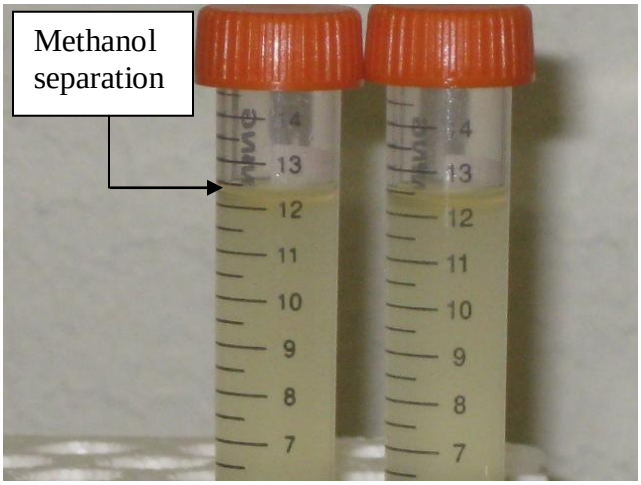

Figure 27: 89-9 emulsion after 7 hours

Same procedure was followed to make 85-12.5 emulsion. 120 grams (150 ml) of methanol was added to 817.7 grams (850 ml) of canola oil. The total quantity of the surfactant was 2.5 % (w/w) of this 1000 ml mixture of methanol and oil. The blending time was 30 minutes. Figures 28 and 29 show the 85-12.5 emulsion.

Figure 28: 85-12.5 emulsion just after preparation

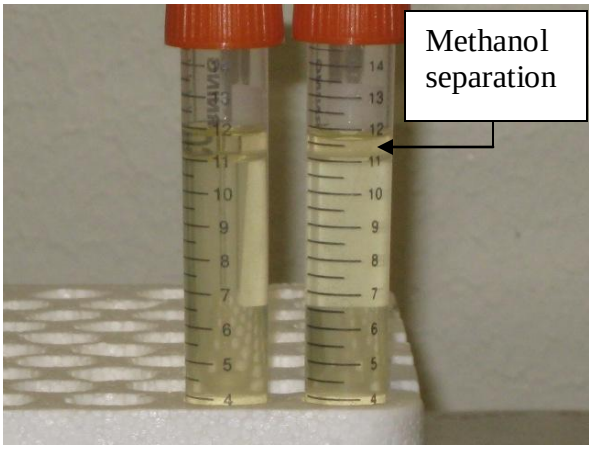

Figure 29: 85-12.5 emulsion after 4 hours

5.6.1 Viscosity of Emulsions

The viscosity of emulsions was measured by using a rotating type viscometer purchased from Brookfield Engineering Laboratories, Inc., USA. The viscometer measured the amount of torque required to rotate a spindle immersed in the fluid. The Brookfield viscometer model used in this project had a maximum torque rating of 0.06737 milli-Newton-m and a specified accuracy of ± 1%. The measured torque values were converted into dynamic viscosity (cP) by internal electronics and displayed on the display screen. The instrument was provided with an UL Adapter for taking viscosity measurements. Figure 30 shows the viscometer used in this project.

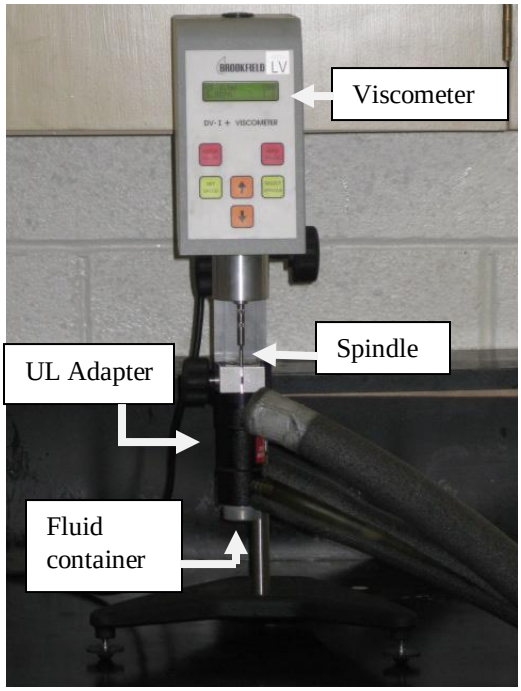

Figure 30: Brookfield Viscometer

The viscosity of canola oil, 89-9 emulsion and 85-12.5 emulsion was measured at a temperature of 25° C. A chiller, purchased from Thermo Scientific Inc., was used to control the temperature of the fluid sample during viscosity measurements. The chiller used a mixture of methanol and deionized water as the temperature controlling fluid. This methanol-water mixture flowed in a closed-loop between the UL Adapter of the viscometer and the chiller and maintained the temperature of the sample at a constant value. The chiller was switched on approximately 30 minutes before viscosity measurements in order to bring its internal temperature to 25 C.

The procedure followed for measuring the viscosity is explained below,

1. The viscometer was switched on and allowed to auto zero for 1 minute.
2. After auto zeroing was complete, the spindle was attached to the viscometer.
3. Fluid sample was filled in a cylindrical container and the container was attached to the UL Adapter.
4. After fixing the container in the UL Adapter, it took approximately 10 minutes for the fluid sample to reach a temperature of 25° C.
5. The spindle speed was set to a value such that, the percentage torque measured by the viscometer was as close as possible to 100%. This ensured maximum accuracy in the reading from the instrument.
6. It took around 10 minutes for the percentage torque value to stabilize.
7. The viscosity reading was taken once a stabilized state was reached.

6. RESULTS AND DISCUSSIONS

This section discusses the fuel properties for pure canola oil, 89-9 emulsion [9% methanol- in- 89% canola oil emulsion with 2% surfactant (w/w)] and 85-12.5 emulsion [12.5% methanol- in - 85% canola oil emulsion with 2.5% surfactant (w/w)]. In addition, the results of the combustion experiments of all the three fuel blends are presented in detail. NO_x, unburned hydrocarbons (UHC's), and CO emissions were recorded for all the fuels. Data for CO_2 production and excess O_2 in the exhaust was also collected. An approximation of the combustion efficiency at different combustion conditions was done through burned fraction calculations presented in the later part of this section. Details of the sauter mean diameter and combustion chamber temperature during all the experiments are presented in the end.

All the experiments were conducted for a constant heat output of 72,750 kJ/hr (69,000 BTU/hr). All the fuels were tested at equivalence ratios (ϕ) of 0.83, 0.91, 1.0, 1.05 and 1.11 and at swirl angles of 60° (SN = 1.4) and 51° (SN =1.0). Primary air for all the experiments was maintained constant at 10 l/min. Different equivalence ratios were achieved by regulating only the secondary air supply while keeping the primary air flow constant. The equivalence ratio (ϕ) was calculated by the following equation.

$$\phi = \left[\frac{\left(\frac{\text{Fuel}}{\text{Air}}\right)_{\text{Provided}}}{\left(\frac{\text{Fuel}}{\text{Air}}\right)_{\text{Stoichiometric}}} \right] \quad (5)$$

6.1 Fuel Properties

Following paragraphs provide the details of chemical formula, HHV, density and viscosity of the fuels studied in this project.

6.1.1 Ultimate Analysis and Chemical Formula of Fuels

100 % natural canola oil of Wesson brand was purchased from a grocery store in College Station, Texas. Ultimate Analysis of pure canola oil was done to find its elemental composition. Bomb Calorimeter test was also conducted to find the higher heating value (HHV) of the oil on an as received basis. Table 4 presents the results of the Ultimate analysis test.

Table 4: Ultimate Analysis of pure canola oil

Element	**% weight**
Carbon	80.22
Hydrogen	10.9
Oxygen	8.62
Nitrogen	0.14
Sulfur	0.004
water	0.115
Ash	0.001
$HHV_{as\ received}$ (kJ/kg)	40173.3

After knowing the elemental composition of canola oil, the chemical formula of the oil was found as shown in Table 5.

Table 5: Chemical formula of canola oil

Element	Weight (g) per 100 g of canola oil	Number of moles per 100 g of canola oil	Chemical formula of canola oil
C	80.22	6.685	$C_{6.685}H_{10.9}O_{0.54}N_{0.01}S_{0.0001}$
H	10.9	10.9	
O	8.62	0.53875	**Empirical Formula of canola oil**
N	0.14	0.01	
S	0.004	0.000125	$CH_{1.6305}O_{0.0806}N_{0.0015}S_{0.00002}$

Normalizing to 1 mole of carbon, empirical formula of pure canola oil was determined to be $CH_{1.6305}O_{0.0806}N_{0.0015}S_{0.00002}$ which had a molecular weight of 14.94 g/ mol C.

6.1.2 Chemical Formula of the Canola Oil-Methanol Emulsions

The chemical formula for the 89-9 emulsion [9% methanol-in-89% canola oil emulsion with 2% surfactant (w/w)] was calculated by considering the percentage mass of each component in 100 g of the blend. The calculations are shown in Table 6.

Table 6: Mass percent composition of 89-9 emulsion

Component	Chemical formula	% Mass
Canola oil	$C_{6.685}H_{10.9}O_{0.54}N_{0.01}S_{0.0001}$	89.82
Methanol	CH_3OH	8.21
Span 80	$C_{24}H_{44}O_6$	1.47
Tween 80	$C_{64}H_{124}O_{26}$	0.5

Once the percentage mass of each component in the emulsion was known then, the percentage contribution of each component to each element was calculated as shown in Table 7.

Table 7: Chemical formula of 89-9 emulsion

	Moles of C	**Moles of H**	**Moles of O**	**Moles of N**	**Moles of S**	**Chemical formula of 89-9 emulsion**
Canola oil	6.004	9.790	0.4839	0.0089	0.0001	$C_{6.7589}H_{11.3852}O_{0.784}N_{0.0089}S_{0.0001}$
Methanol	0.0821	0.3284	0.0821	_	_	
Span 80	0.3528	0.6468	0.0882	_	_	
Tween 80	0.32	0.62	0.13	_	_	**Empirical formula of 89-9 emulsion**
Total moles	6.7589	11.385	0.7842	0.0089	0.0001	$CH_{1.687}O_{0.1143}N_{0.0013}S_{0.00001}$

Normalizing to 1 mole of carbon atom, the empirical formula of the 89-9 emulsion was determined to be $CH_{1.687}O_{0.1143}N_{0.0013}S_{0.00001}$ which had a molecular weight 15.55 g/ mol C.

The chemical formula for the 85-12.5 emulsion [12.5% methanol-in-85% canola oil emulsion with 2.5% surfactant (w/w)] was calculated by the same method and is shown in Tables 8 and 9.

Table 8: Mass percent composition of 85-12.5 emulsion

Component	**Chemical formula**	**% Mass**
Canola oil	$C_{6.685}H_{10.9}O_{0.54}N_{0.01}S_{0.0001}$	85.08
Methanol	CH_3OH	12.48
Span 80	$C_{24}H_{44}O_6$	1.826
Tween 80	$C_{64}H_{124}O_{26}$	0.61

Table 9: Chemical formula of 85-12.5 emulsion

	Moles of C	**Moles of H**	**Moles of O**	**Moles of N**	**Moles of S**	**Chemical formula of 85-12.5 emulsion**
Canola oil	5.687	9.27	0.4584	0.0085	0.0001	$C_{6.6482}H_{11.329}O_{0.8513}N_{0.0085}S_{0.0001}$
Methanol	0.1284	0.4992	0.1248	_	_	
Span 80	0.4464	0.8034	0.1095	_	_	
Tween 80	0.39	0.7564	0.1586	_	_	**Empirical formula of 85-12.5 emulsion**
Total moles	6.6482	11.329	0.8513	0.0085	0.0001	$CH_{1.704}O_{0.128}N_{0.0012}S_{0.00001}$

Normalizing to 1 mole of carbon atom, the empirical formula of the 85-12.5 emulsion was determined to be $CH_{1.704}O_{0.128}N_{0.0012}S_{0.00001}$ with a molecular weight of 15.77 g/ mol C.

6.1.3 Viscosity and Stability of Emulsions

The viscosity of all the fuels was measured at 25° C using a rotational type viscometer. The stability period of each emulsion was estimated by visual inspecting it every 1 hour and checking for the separation of methanol and oil. The stability time and viscosity values for canola oil and its emulsions have been listed in Table 10. The change in viscosity of pure canola oil due to the addition of methanol and surfactants was calculated using the following formula,

$$(\%)\text{Reduction in Viscosity} = \left[\frac{\text{Viscosity}_{\text{canola oil}} - \text{Visocity}_{\text{emulsion}}}{\text{Viscosity}_{\text{canola oil}}}\right] * 100 \quad (6)$$

Table 10: Viscosity and stability of the fuels

Fuel Type	**Viscosity (cP) at 25 °C**	**Stability (hours)**	**% Reduction in Viscosity**
Canola Oil	55	-	-
89-9 Emulsion	38.8	7 hrs.	29.45
85-12.5 Emulsion	41.2	4 hrs.	25.09

From Table 10, it is seen that the 89-9 emulsion was stable for longer time as compared to 85-12.5 emulsion. This was due to the relatively less amount of methanol mixed in 89-9 emulsion. Table 10 also depicts that the percentage reduction in viscosity was more for 89-9 emulsion as compared to 85-12.5 emulsion. This was because of the higher amount of surfactants added to the 85-12.5 emulsion.

High viscosity of canola oil was attributed to its 94.4% to 99.1% triglycerides content [31]. Triglycerides are esters of one molecule of glycerol and three molecules of fatty acid. The most common fatty acids constituting canola oil were the straight chain unsaturated fatty acids containing 18 carbon atoms. These include stearic acid (about 1% saturated fatty acid), oleic acid (about 60 % monounsaturated fatty acid with a single double bond) and linoleic and linolenic acids (about 20% and 13% respectively; polyunsaturated fatty acid having two or three double bonds) [9]. The long hydrocarbon chains of the constituent fatty acids of canola oil are held together by London Dispersion Forces (type of Van der Waals force) [9] . Dispersion forces are attraction forces between instantaneous dipole and induced dipole. The magnitude of these forces increases, with an increase in the molecular weight and surface area of the molecule. The fatty acids in canola oil had a large surface area due to 18 carbon atoms in a single hydrocarbon chain. Larger surface area led to multiple dispersion forces between the different hydrocarbon chains and imparted high viscosity to canola oil.

The emulsions had a slightly higher molecular weight than canola oil. This was due to the high molecular weight of surfactants added to the emulsion. The contribution of surfactants to the elemental composition of emulsions can be seen in Tables 7 and 9. Surfactants were added to canola oil for reducing the surface tension of canola oil and interfacial tension between oil and methanol. It can be suggested that the emulsions had lower viscosity due to two reasons; decreased surface tension and the addition of methanol which led to a reduction in the dispersion forces between fatty acids.

6.2 Experimental Parameters

Equivalence ratio, fuel type and swirl number were the three main parameters whose effects were studied on the emission levels of pure canola oil, 89-9 emulsion and 85-12.5 emulsion. The details of different fuel blends and swirl number equation used, has been provided in sections 6.1 and 2.6 respectively. This section shows the calculations of the air and fuel flow rates in order to get a constant heat output of 72,750 kJ/hr from all the fuels at equivalence ratios 0.83, 091, 1.0, 1.05, 1.11.

6.2.1 Fuel Feed Rate

Based on the heating value of the fuels, the fuel volumetric flow rate was calculated by the following equation to achieve 72,750 kJ/hr of heat of combustion.

$$\dot{V}\left(\frac{ml}{min}\right) = \frac{\left[72750\left(\frac{kJ}{hr}\right) * 1000\left(\frac{g}{kg}\right)\right]}{\left[HHV\left(\frac{kJ}{kg}\right) * \rho_{fuel}\left(\frac{g}{ml}\right) * 60\left(\frac{min}{hr}\right)\right]} \quad (7)$$

Table 11 lists the heating values of pure canola oil, methanol and the surfactants used in this project.

Table 11: Higher heating value of canola oil, methanol and surfactants

Liquid	Higher Heating Value (kJ/kg)
Canola Oil	40,173.3
Methanol	20,022.6
Span 80	35,411.3
Tween 80	29,754.0

Higher heating value of the emulsions was estimated using the following equation under the assumption that no chemical reactions took place during mixing,

$$\mathrm{HHV_{emulsion}}\left(\frac{\mathrm{kJ}}{\mathrm{kg}}\right) = \left(\mathrm{m_{f,canola\ oil}} * \mathrm{HHV_{canola}}\right) + \left(\mathrm{m_{f,methanol}} * \mathrm{HHV_{methanol}}\right) + \left(\mathrm{m_{f,Span\ 80}} * \mathrm{HHV_{Span80}}\right) + \left(\mathrm{m_{f,Twen\ 80}} * \mathrm{HHV_{Tween\ 80}}\right) \quad (8)$$

where,

m_f = mass fraction of substance in the emulsion

Based on the above calculations, the volumetric fuel flow rate for canola oil, 89-9 emulsion and 85-12.5 emulsion was calculated to be 31.37 ml/ min (0.5 Gal/hr), 35.3 ml/min (0.56 Gal/hr) and 36.6 ml/min (0.58 Gal/hr), respectively. Table 12 summarizes the empirical formula, higher heating value and density of the fuels.

Table 12: Empirical formula, HHV and density of all three fuels

Fuel Type	**Chemical Empirical Formula**	**Molecular weight (g/mol C)**	**HHV (kJ/kg) as received**	**Density (g/ml)**
Pure Canola Oil	$CH_{1.6305}O_{0.0806}N_{0.0015}S_{0.00002}$	14.94	40173.3	0.9622
89-9 Emulsion	$CH_{1.687}O_{0.1143}N_{0.0013}S_{0.00001}$	15.55	38396.2	0.8983
85-12.5 Emulsion	$CH_{1.704}O_{0.128}N_{0.0012}S_{0.00001}$	15.77	37506	0.8815

From the Table 12 it is seen that the HHV of 89-9 and 85-12.5 emulsion was less than the HHV of pure canola oil by 4.4% and 6.6%, respectively. This effect can be attributed to the lower heat of combustion of methanol. The HHV of surfactants is higher than that of methanol; but, since the surfactants were added to the emulsions in small amounts, their contribution to the HHV of the emulsions was quite less. The density of the fuels was measured by a simple method. 50 ml of each fuel was taken in a graduated cylinder and the mass was measured on a weigh scale. Density was calculated by taking a ratio of the mass of 50 ml fuel to its volume. Density of the emulsions was slightly lower than canola oil due to the addition of methanol.

6.2.2 Air Flow Rate Calculations

After calculating fuel feed rate, the corresponding air flow rate was calculated. Stoichiometric air flow (l/min) needed for the complete combustion of pure canola oil (volumetric flow rate of canola oil = 31.55 ml/min) is shown below. Equation 9 represents the stoichiometric (balanced) combustion reaction equation of pure canola oil.

$$CH_{1.6305}O_{0.0806}N_{0.0015}S_{0.00002} + a*(O_2 + 3.76N_2) \rightarrow CO_2 + b*(H_2O) + c*N_2 + d*SO_2 \quad (9)$$

After balancing the stoichiometric combustion equation on both sides of the equation (8), the value of stoichiometric coefficients are as shown in Table 13.

Table 13: Stoichiometric coefficients for complete combustion of pure canola oil

Stoichiometric coefficient	Value
a	1.3673
b	0.81525
c	5.141
d	0.00002

Note that Equation 8 represents the combustion of 14.94 g of pure canola oil (molecular weight of pure canola oil on the basis of the empirical formula is 14.94 g/mol-Carbon). As a result, the amount of air needed ($m_{air,total}$) for the complete combustion of 14.94g of canola oil was,

$m_{air,total}$ = a * 4.76 moles of air

= 1.3673 * 4.76 moles of air

= 6.5084 moles of air

= 6.5084 moles * ($Air_{molecular\ weight}$)

= 6.5084 moles * 28.97 g/mole of air

= 188.5 grams of air

Therefore, the amount of air needed ($Air_{per\ gram\ of\ oil}$) by each gram of oil was,

$Air_{per\ gram\ of\ oil}$ = 188.5 g of air /14.94 g of canola oil

$Air_{per\ gram\ of\ oil}$ = 12.62 g of air/g of oil

Therefore, air to fuel ratio during stoichiometric combustion of pure canola oil was,

$(Air/Fuel)_{stoichiometric}$ = 12.62

The volumetric flow rate ($\dot{V}$) of pure canola oil during combustion was,

$\dot{V} = 31.55$ ml/min

Therefore, mass flow rate of canola oil during combustion was,

$\dot{m} = \dot{V} * \rho_{\text{canola oil}}$

= 0.917 g/ml * 31.55 ml/min

= 29 g/min of canola oil

Thus the mass flow rate of air required per minute was,

$\dot{m}_{air}$ = 29 g/min of canola oil * 12.62 g of air/g of oil

= 366 g of air / minute

The density of air at standard temperature and pressure is 1.2 g/l, so the total volumetric air flow rate at stoichiometric condition was,

$$\dot{V}_{\text{air,total}} = \frac{366_{\text{g of air per min}}}{1.2_{\text{g/l}}}$$

= 305 l/min of air

From the above calculations, it is seen that 305 l/min of total air flow was needed for stoichiometric combustion of 31.55 ml/min of pure canola oil. The air flow required at other equivalence ratios was found by dividing the stoichiometric air flow rate with the specific equivalence ratio.

Similar calculations were done for 89-9 emulsion and 85-12.5 emulsion using Engineering Equation Solver (EES). Tables 14 summarizes the flow rates of fuel and air at all the equivalence ratios. Note that, primary air flow rate during the combustion of all the fuels was held constant at 10 l/min.

Table 14: Fuel and air flow rates for the combustion experiments

Fuel Type	Equi-valence Ratio	Fuel Flow Rate (ml/min)	Total Air Required (l/min)	Primary Air Required[1] (l/min)	Secondary Air Required[2] (l/min)	A:F ratio
Pure Canola Oil	0.83	31.54	366	10	356.00	15.14
	0.91	31.54	335.5	10	325.50	13.88
	1	31.54	305	10	295.00	12.62
	1.05	31.54	289.75	10	279.75	11.99
	1.11	31.54	274.5	10	264.50	11.36
89-9 Emulsion	0.83	35.3	404	10	394.00	14.5
	0.91	35.3	371	10	361.00	13.3
	1	35.3	337	10	327.00	12.09
	1.05	35.3	320	10	310.00	11.48
	1.11	35.3	303	10	293.00	10.88
85-12.5 Emulsion	0.83	36.6	393	10	383.00	14.29
	0.91	36.6	360.25	10	350.25	13.1
	1	36.6	327.5	10	317.50	11.91
	1.05	36.6	311	10	301.00	11.31
	1.11	36.6	295	10	285.00	10.72

Note: (1) Air supplied to the nozzle for atomization of liquid fuel
(2) Air that passes through the swirler

6.3 Emissions

The emission results from the combustion experiments were obtained by using an exhaust gas analyzer. Emission data for NO, NO_2, NO_x (NO_x = NO + NO_2), CO, unburned hydrocarbons (UHC's) and CO_2 were collected at different equivalence ratios. The following paragraphs and figures provide the emission results obtained during the experiments.

6.3.1 NO_x Emissions

Since all the fuels considered in this study were basically nitrogen free, we can say that the NO_x formation was mainly due to the presence of air borne nitrogen. Two common mechanisms of NO_x production are Thermal NO_x and Prompt NO_x. Thermal NO_x mechanism is very temperature dependent and is more dominant at temperatures beyond 1600° C (1900 K). High temperatures are needed to break the triple bond between two nitrogen atoms and consequent oxidation reaction leading to NO_x formation. During prompt NO_x mechanism, the reaction between the hydrocarbon groups and molecular nitrogen in the air leads to rapid NO_x formation in the flame front. This mechanism is independent of temperature and residence time inside the furnace [34].

Table 15 lists the values of NO_x emissions recorded during the combustion experiments of pure canola oil, 89-9 emulsion and 85-12.5 emulsion at 60° and 51° swirl angles.

Table 15: Experimentally recorded NO_x emissions for all fuels at both swirl numbers.

Fuel Type/Swirl Number	Equi-valence Ratio	NO_x first reading (ppm)	NO_x second reading (ppm)	Average value of NO_x (ppm)	Standard deviation of NO_x (ppm)
Pure Canola Oil	0.83	117.5	120.5	119	2.1
	0.91	103.5	105.5	104.5	1.4
	1	83.2	83.4	83.3	0.1
60°	1.05	78.3	72.3	75.3	4.2
(SN = 1.4)	1.11	63.2	64.3	63.75	0.8
Pure Canola Oil	0.83	142.2	140.5	141.35	1.2
	0.91	115.7	120.8	118.25	3.6
	1	91.5	99.4	95.45	5.6
51°	1.05	78.5	79.8	79.15	0.9
(SN =1.0)	1.11	63.6	69.7	66.65	4.3
89-9 Emulsion	0.83	111.4	113.5	112.45	1.5
	0.91	94.4	96.4	95.4	1.4
	1	77.2	80.1	78.65	2.1
60°	1.05	53	59	56	4.2
(SN = 1.4)	1.11	44	41	42.5	2.1
89-9 Emulsion	0.83	117.1	119.4	118.25	1.6
	0.91	107.4	104.7	106.05	1.9
	1	89.6	86.1	87.85	2.5
51°	1.05	77.9	80	78.95	1.5
(SN = 1.0)	1.11	58.6	58.7	58.65	0.1
85-12.5 Emulsion	0.83	103.2	104.3	103.75	0.8
	0.91	86.1	93.1	89.6	4.9
	1	71	71	71	0.0
60°	1.05	32	39	35.5	4.9
(SN = 1.4)	1.11	16	21	18.5	3.5
85-12.5 Emulsion	0.83	108.5	105.5	107	2.1
	0.91	100.4	98.5	99.45	1.3
	1	71.3	74.4	72.85	2.2
51°	1.05	63	69	66	4.2
(SN=1.0)	1.11	48	47	47.5	0.7

Figures 31 and 32 show the NO_x production by all the fuels at swirl numbers of 1.4 and 1.0, respectively.

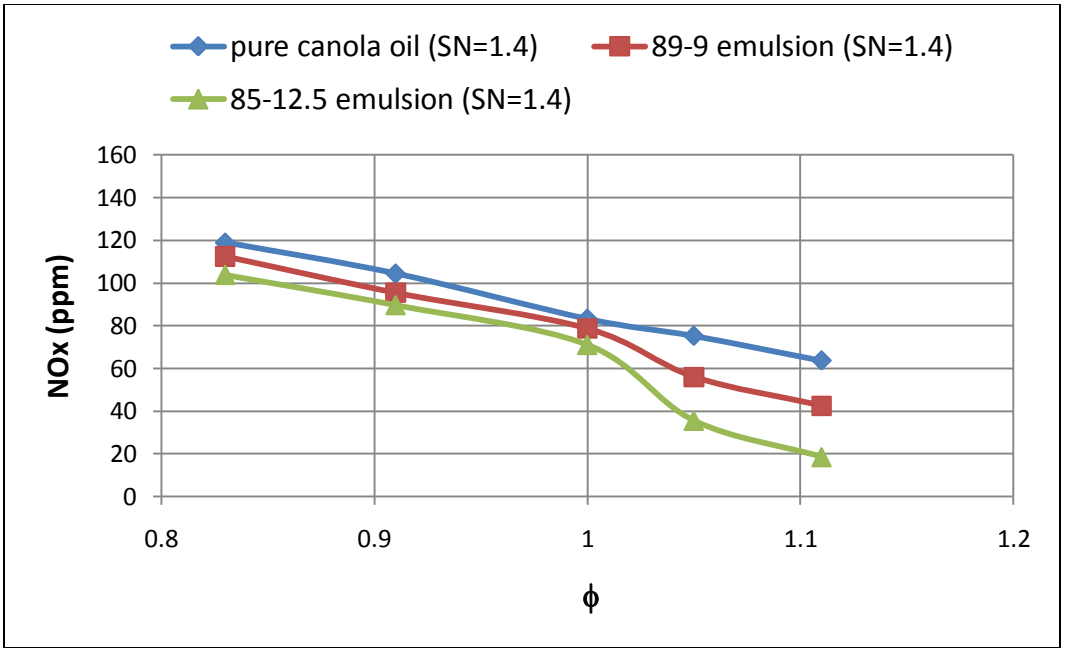

Figure 31: NO_x emissions from pure canola oil, 89-9 emulsion and 85-12.5 emulsion at SN = 1.4 for a constant heat output of 72,750 kJ/hr

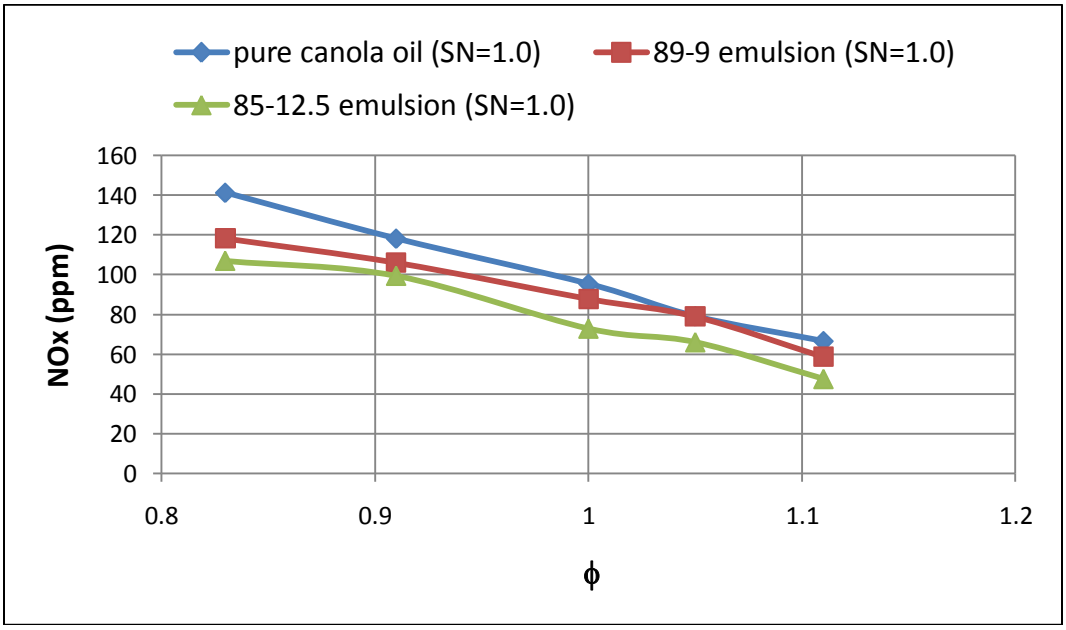

Figure 32: NO_x emissions from pure canola oil, 89-9 emulsion and 85-12.5 emulsion at SN = 1.0 for a constant heat output of 72,750 kJ/hr

- Effect of equivalence ratio on NO_x emissions

The maximum temperature recorded by the thermocouple (located 44.45 cm below the nozzle tip) nearest to the flame was about 1000° C for all the experiments. Considering the fact that "Thermal NO_x" is dominant at temperatures over 1600° C (1900 K), from the current experimental results, it can be hypothesized that the production of NO_x took place through the "Prompt Mechanism" [34]. Figures 31 and 32 show that more NO_x was produced at stoichiometric and lean conditions. It can be suggested that the presence of excess air in the furnace at lean conditions allowed more nitrogen to react with hydrocarbon groups which led to the formation of NO_x through the prompt mechanism. Daho et. al. [35] observed a decline in NO_x emissions for domestic fuel oil combustion when the equivalence ratio was increased from $\phi = 0.77$ to $\phi = 0.97$. Ishak et. al. [24] also recorded reduction in NO_x from diesel fuel with an increase in equivalence ratio from $\phi = 0.83$ to $\phi = 1.20$. The results shown in Figures 31 and 32 for vegetable oil blends are consistent with previous findings for other fuels.

However, the results shown in Figures 31 and 32 were not in total agreement with the classical literature which states that prompt NO_x formation should be more at fuel rich conditions due to higher unburned hydrocarbons present at those conditions. The discrepancy in the current result could be due to two reasons. Firstly, temperatures much higher than 1000° C might have been present in the flame zone leading to NO_x production not only by prompt route but also the "Thermal NO_x Mechanism". Second reason for lower NO_x at higher equivalence ratios might be due to the conversion of NO_x back to molecular nitrogen via "Reverse Prompt NOx Mechanism". The reverse

mechanism is dominant at fuel rich conditions and mainly involves the reaction of hydrogen cyanide (HCN) and ammonia (NH_3) with NO converting NOx back to N_2[36]. A comprehensive study involving the combustion equations should be undertaken to determine if the reverse prompt mechanism is favorable from the thermodynamic point of view for each equivalence ratio.

Habib et. al. [37] conducted natural gas combustion experiments in a 160 MW industrial boiler. The authors [37] recorded an increase in prompt NO_x formation with an increase in equivalence ratio, validating the concept mentioned in literature. Due to the discrepancy between the current results as shown in Figures 31 and 32 and the findings of Habib et. al. [37], a more detailed analysis is required to explain the influence of equivalence ratio on NO_x formation.

- Effect of swirl number on NO_x emissions

Figures 31 and 32 show that NO_x emission levels are inversely proportional to swirl number. Reduction in NOx emissions at higher swirl number can be attributed to a higher level of mixing between air and fuel during the combustion process. At higher swirl number, higher vorticity of the air passing downstream of the swirler enhanced the fuel-air mixing inside the combustion chamber resulting in a more complete combustion. Moreover, higher vorticity resulted in greater residence time of the fuel-air mixture allowing for a more complete and cleaner combustion. Ishak et. al. [24] found similar results with diesel fuel combustion in a liquid fuel burner system having a radial swirler. The authors [24] observed that at $\phi = 0.83$, NO_x emissions reduced by 10% when the

swirl angle was increased from 50° to 60°. Similar behavior can be seen in Figures 31 and 32 at $\phi = 0.83$. Mafra et al. [23] concluded that at lower swirl number, a fuel rich zone is developed inside the combustion chamber resulting in greater amounts of unburned hydrocarbons which promote greater NO_x emissions through the Prompt-NO_x Mechanism. Figures on page 89 and 90 show that the amount of unburnt hydrocarbons increased at lower swirl number. Table 16 depicts the reduction in NOx emissions as swirl number was increased from 1.0 to 1.4.

Table 16: Percentage reduction in NO_x due to increase in swirl number

Fuel Type	**Equi-valence ratio**	**NO_x ppm at 60 degree swirl angle (SN = 1.4)**	**NO_x ppm at 51 degree swirl angle (SN=1.0)**	**Percentage reduction in NO_x**
Pure canola oil	0.83	119	141.35	15.81
89-9 emulsion	0.83	112.45	118.25	4.90
85-12.5 emulsion	0.83	103.75	107	3.04

- Effect of fuel type on NO_x emissions

The effect of fuel type composition was also studied to determine its impact on NO_x formation. As seen in Figures 31 and 32, the 85-12.5 canola oil-methanol blend always resulted in lower emissions for equivalence ratio's of 0.83 to 1.11, and swirl numbers of 1.0 and 1.4.

There are two possible reasons for such an outcome. Since all the experiments were conducted for a constant heat output (72,750 kJ/hr) in the furnace, therefore, in the case of emulsions, the methanol and surfactant bound oxygen helped to lead an overall leaner combustion than expected. From Tables 5, 7, and 9, the amount of oxygen is 31.1% and 36.6% higher in 89-9 and 82.5-12.5 blends, respectively, than in pure canola oil on a molar basis. Similar results were also reported by Rakopoulos et. al. [38] during combustion of diesel and diesel-butanol blends in a direct injection diesel engine. Rakopoulos et. al [38] observed that NO_x emissions from the diesel-butanol blends were lower than that for diesel, with the reductions being higher with increased percentage of butanol in the blend. They attributed this effect to the overall leaner operation of the engine due to fuel bound oxygen, temperature lowering effect of butanol and its low cetane number causing longer ignition delays.

A possible hypothesis for lower NO_x emissions by the emulsions might also be due to the occurrence of micro-explosions. In the case of a methanol-in-canola oil emulsion droplet, methanol, having a higher vapor pressure is surrounded by canola oil with a relatively low vapor pressure. When such an emulsion droplet is subjected to high temperatures inside the furnace, the methanol reaches superheated conditions and vaporizes. The expansion of the methanol vapor helps to disperse the surrounding oil droplet into multiple, finer, secondary droplets which enhances the mixing of air and fuel leading to more efficient combustion. The 85-12.5 emulsion had more methanol emulsified in it as compared to 89-9 emulsion. The higher percentage of methanol might have contributed to more number of micro-explosions per unit volume of pure canola oil

in the 85-12.5 emulsion ultimately leading to least emissions of all the fuels. The effect of microexplosion in fuel blends in being currently studied by another graduate student under the supervision of Prof. Alvarado.

6.3.1.1 NO_x Emissions Corrected for 3% Oxygen in the Exhaust

If the amount of NO_x produced during combustion process is held constant, then one can easily reduce the NO_x ppm in the exhaust by supplying excess air to the furnace. Therefore, in order to prevent this, the amount of NO is normalized by the amount of O_2 provided to the combustion chamber [34]. The mole fraction of NO is corrected at a standard oxygen mole fraction which is 3% for utilities [34]. The equation for the correction as presented in Annamalai et. al. [34] is,

$$\frac{X_{NO,std}}{X_{NO}} = \left[\frac{(X_{O2,a} - X_{O2,std})}{X_{O2,a} - X_{O2}}\right] \quad (10)$$

where,

$X_{NO,std}$ = corrected NO mole fraction at standard oxygen mole fraction (ppm corrected to 3% O_2)

X_{NO} = uncorrected NO mole fraction (ppm)

$X_{O2,\,a}$ = ambient air mole fraction = 0.21

$X_{O2,std}$ = standard oxygen mole fraction = 0.03 or corrected to 3% O_2

X_{O2} = measured oxygen mole fraction in the exhaust gas stream

Table 17 lists the NO_x emissions corrected to 3% O_2 in the exhaust. Note that NO_x emissions increased at very lean conditions after correction because the actual emissions were recorded at more than 3% O_2 at these conditions. However, for all other

equivalence ratios, the NO_x emissions decreased because there was less than 3% O_2 in the exhaust prior to applying the correction factor.

Table 17: NO_x emissions from all fuels corrected to 3% oxygen in the exhaust

Fuel Type/Swirl Number	Equivalence Ratio	Experimentally recorded NOx (ppm)	NOx mole fraction corrected to 3% oxygen in exhaust (ppm)
Pure Canola Oil 60° (SN=1.4)	0.83	119	124.53
	0.91	104.5	103.35
	1	83.3	78.50
	1.05	75.3	68.80
	1.11	63.75	59.15
Pure Canola Oil 51° (SN=1.0)	0.83	141.35	154.20
	0.91	118.25	123.75
	1	95.45	93.38
	1.05	79.15	76.60
	1.11	66.65	63.14
89-9 Emulsion 60° (SN=1.4)	0.83	112.45	115.66
	0.91	95.4	93.33
	1	78.65	73.35
	1.05	56	50.40
	1.11	42.5	38.64
89-9 Emulsion 51° (SN=1.0)	0.83	118.25	127.46
	0.91	106.05	109.08
	1	87.85	85.48
	1.05	78.95	75.19
	1.11	58.65	54.98
85-12.5 Emulsion 60° (SN=1.4)	0.83	103.75	105.51
	0.91	89.6	86.25
	1	71	66.56
	1.05	35.5	31.32
	1.11	18.5	16.40
85-12.5 Emulsion 51° (SN=1.0)	0.83	107	113.29
	0.91	99.45	101.14
	1	72.85	69.38
	1.05	66	62.20
	1.11	47.5	43.18

Figures 33 and 34 show the NO_x emission for all the fuels corrected to 3% O_2.

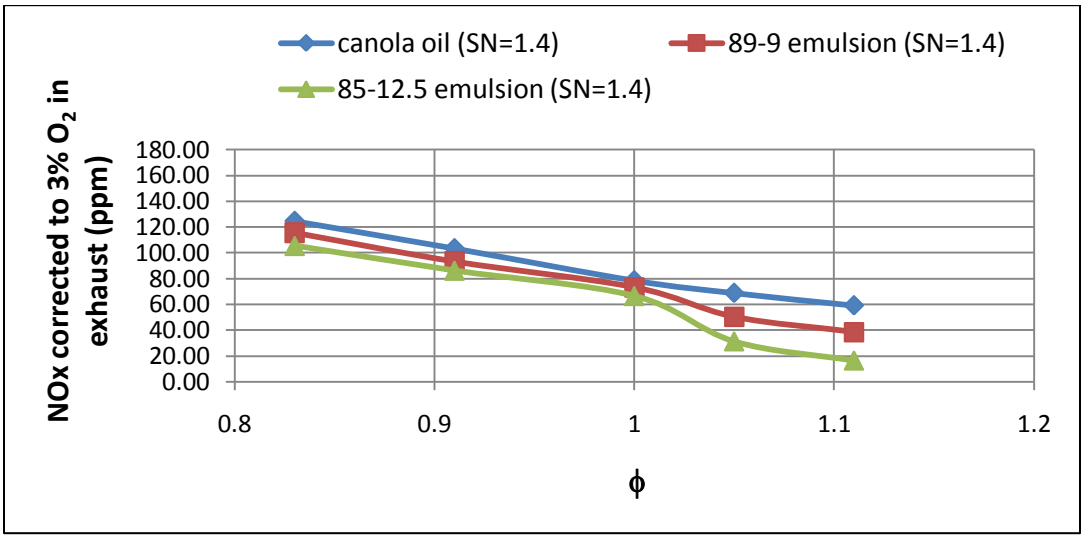

Figure 33: NO_x emissions (corrected to 3% oxygen) from canola oil, 89-9 emulsions and 85-12.5 emulsion at SN = 1.4 for a constant heat output of 72,750 kJ/hr

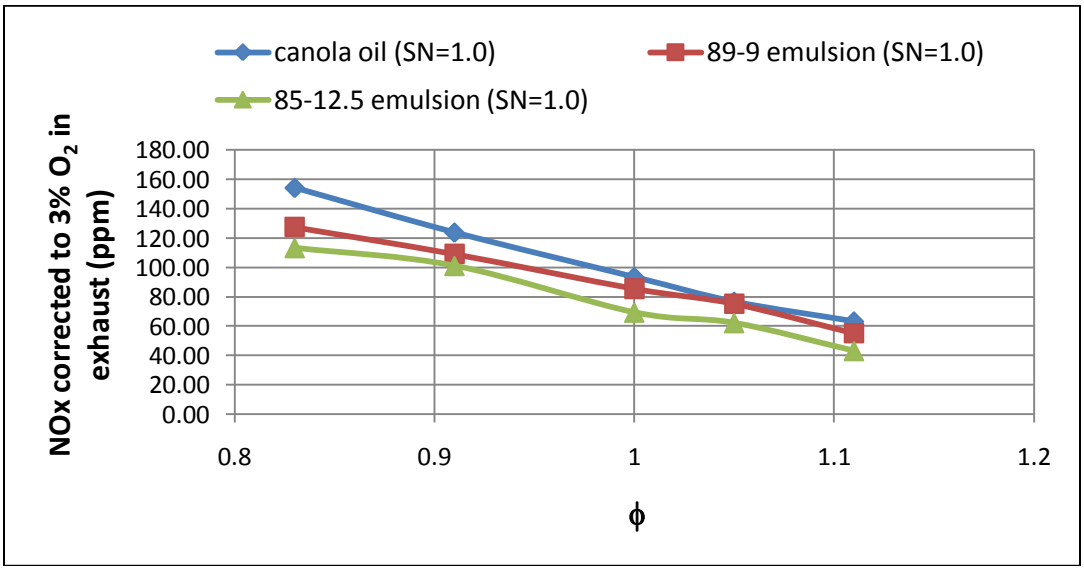

Figure 34: NO_x emissions (corrected to 3% oxygen) from canola oil, 89-9 emulsions and 85-12.5 emulsion at SN = 1.0 for a constant heat output of 72,750 kJ/hr

6.3.1.2 NO_x Emissions in Terms of Heat Input (g/GJ)

Reporting NO_x emissions on a heat basis is another method to prevent emission dilution. The following equation was used to convert NO_x mole fraction to grams per gigajoule. The equation is based on the assumption that all carbon reacts to form CO and CO_2 only as presented in Annamalai et. al. [34].

$$NO\ \left(\frac{g}{GJ}\right) = \frac{c * X_{NO} * M_k * 1000\ \left(\frac{g}{kg}\right)}{M_F * HHV_F * (X_{CO} + X_{CO2})} \quad (11)$$

where,

c = number of carbon atoms in the fuels empirical formula $C_cH_hO_oN_nS_s$

X_{NO} = NO_x dry mole fraction

M_k = M_{NO2} = NO_2 molecular weight (kg/kmol)

M_F = molecular weight of the fuel

HHV_F = higher heating value of the fuel (GJ/kg) on a DAF basis

X_{CO} = CO mole fraction (dry)

X_{CO2} = CO_2 mole fraction (dry)

The U.S. Environmental Protection Agency (EPA) stipulates that for reporting NO emission, M_k for NO should be that of NO_2 (M_{NO2} = 46.01 kg/kmol) because NO is eventually converted into NO_2 in the atmosphere [34]. Table 18 shows the NO_x in g/GJ unit.

Table 18: NO_x (g/GJ) emissions for all the fuels at both swirl numbers

Fuel Type/Swirl Number	ϕ	NO_X mole fraction (*10^-6)	Average CO mole fraction (*10^-6)	Average CO_2 mole fraction	HHV (KJ/Kg) as received	NO_X (g/kg of fuel as received)	NO_X (g/GJ)
Pure Canola Oil 60° (SN = 1.4)	0.83	119	3.5	0.13705	40173.3	2.67	66.48
	0.91	104.5	4.5	0.13745	40173.3	2.34	58.21
	1	83.3	3.5	0.1434	40173.3	1.79	44.48
	1.05	75.3	3129	0.1259	40173.3	1.80	44.69
	1.11	63.75	3768	0.11145	40173.3	1.70	42.37
89-9 emulsion 60° (SN = 1.4)	0.83	112.45	1.5	0.1259	38396.2	2.64	68.76
	0.91	95.4	4	0.1344	38396.2	2.10	54.64
	1	78.65	3	0.14245	38396.2	1.63	42.50
	1.05	56	2238	0.1354	38396.2	1.20	31.32
	1.11	42.5	2457	0.1256	38396.2	0.98	25.55
85-12.5 emulsion 60° (SN = 1.4)	0.83	103.75	0	0.1416	37506	2.14	56.94
	0.91	89.6	1	0.14865	37506	1.76	46.84
	1	71	2.5	0.15605	37506	1.33	35.36
	1.05	35.5	1244.5	0.13485	37506	0.76	20.27
	1.11	18.5	1834.5	0.1327	37506	0.40	10.69
Pure Canola Oil 51° (SN = 1.0)	0.83	141.35	3	0.03	40173.3	4.31	107.16
	0.91	118.25	4.5	0.045	40173.3	3.28	81.53
	1	95.45	10.5	0.105	40173.3	2.33	57.93
	1.05	79.15	3538.5	35.385	40173.3	2.02	50.30
	1.11	66.65	4166.5	41.665	40173.3	1.87	46.60
89-9 emulsion 51° (SN = 1.0)	0.83	118.25	2	0.1269	38396.2	2.76	71.73
	0.91	106.05	3	0.12835	38396.2	2.44	63.60
	1	87.85	3	0.12925	38396.2	2.01	52.32
	1.05	78.95	2383.5	0.11355	38396.2	2.01	52.42
	1.11	58.65	2818	0.1044	38396.2	1.62	42.11
85-12.5 emulsion 51° (SN = 1.0)	0.83	107	0.5	0.1278	37506	2.44	65.06
	0.91	99.45	2.5	0.13315	37506	2.18	58.04
	1	72.85	4	0.1437	37506	1.48	39.40
	1.05	66	1443.5	0.12795	37506	1.49	39.64
	1.11	47.5	2032.5	0.12415	37506	1.10	29.25

Figures 35 and 36 show the NO_x (g/GJ) emissions for all the fuels at both swirl numbers.

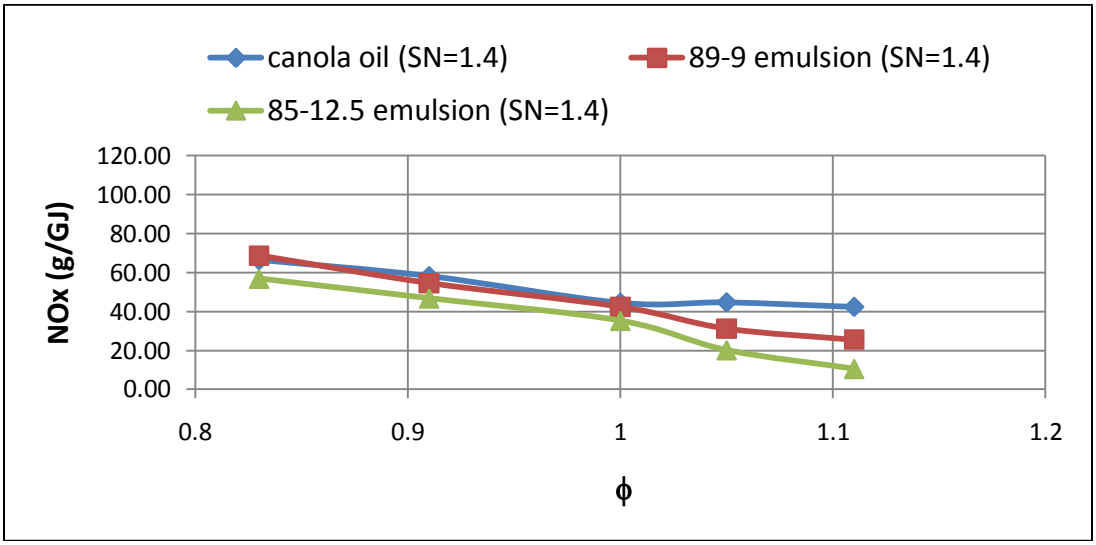

Figure 35: NO_x (g/GJ) emissions for pure canola oil, 89-9 emulsion and 85-12.5 emulsion at SN = 1.4 for a constant heat output of 72,750 kJ/hr

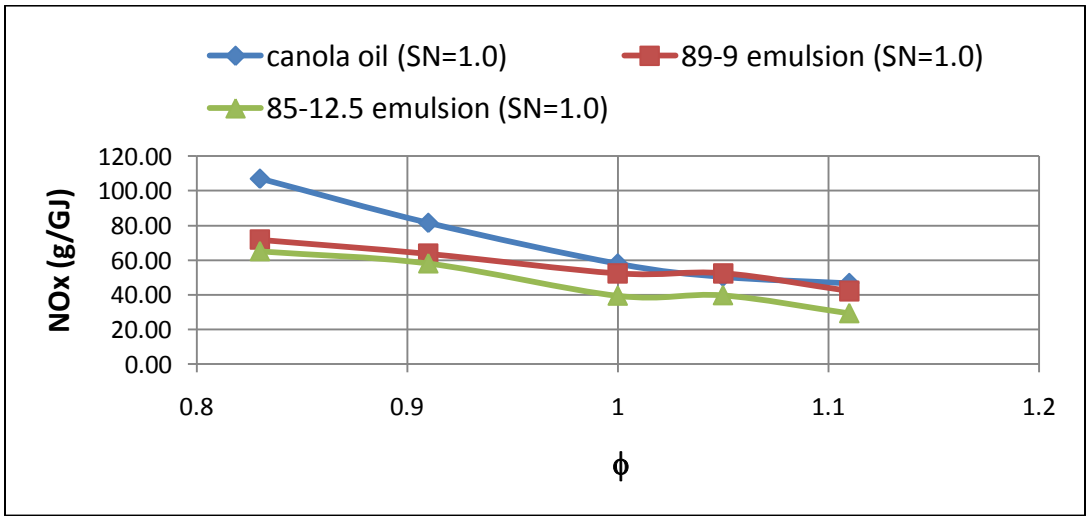

Figure 36: NO_x (g/GJ) emissions for pure canola oil, 89-9 emulsion and 85-12.5 emulsion at SN = 1.0 for a constant heat output of 72,750 kJ/hr

Both Figures 35- 36 show that the emulsions produced lower NO_x (g/GJ) emissions as compared to pure canola oil. Equation 10 takes into account the mole fractions of CO and CO_2 from the fuel. The CO production at lean conditions by all the fuels for SN = 1.4 and 1.0 is almost close to zero ppm (see Figures 41 - 42); but, since the CO_2 produced by pure canola oil is minimum at SN = 1.0 (see Figure 40), a sharp increase in NOx (g/GJ) emissions is seen for canola oil at $\phi > 1$ in Figure 36.

6.3.2 Unburned Hydrocarbon (UHC) Emissions

Unburned hydrocarbons are produced as a result of partial oxidation and in-complete combustion. Table 19 lists the values of unburnt hydrocarbons recorded during the combustion experiments of pure canola oil, 89-9 emulsion and 85-12.5 emulsion at 60 ° and 51 ° swirl angles.

Table 19: Unburned hydrocarbon emission for all fuels at both swirl numbers

Fuel Type/Swirl Number	Equi-valence ratio	UHC first reading (ppm)	UHC second reading (ppm)	Average value of UHC (ppm)	Standard deviation of UHC (ppm)
Pure Canola Oil 60° (SN = 1.4)	0.83	111	113	112	1.41
	0.91	158	159	158.5	0.71
	1	184	184	184	0.00
	1.05	270	265	267.5	3.54
	1.11	303	307	305	2.83
Pure Canola Oil 51° (SN = 1.0)	0.83	193	199	196	4.24
	0.91	211	213	212	1.41
	1	295	285	290	7.07
	1.05	300	303	301.5	2.12
	1.11	377	382	379.5	3.54
89-9 Emulsion 60° (SN = 1.4)	0.83	12	16	14	2.83
	0.91	21	20	20.5	0.71
	1	52	50	51	1.41
	1.05	90	96	93	4.24
	1.11	129	125	127	2.83
89-9 Emulsion 51° (SN = 1.0)	0.83	63	60	61.5	2.12
	0.91	80	84	82	2.83
	1	96	99	97.5	2.12
	1.05	197	195	196	1.41
	1.11	249	250	249.5	0.71
85-12.5 emulsion 60° (SN = 1.4)	0.83	0	0	0	0.00
	0.91	0	0	0	0.00
	1	0	0	0	0.00
	1.05	60	61	60.5	0.71
	1.11	141	139	140	1.41
85-12.5 Emulsion 51° (SN = 1.0)	0.83	0	0	0	0.00
	0.91	0	0	0	0.00
	1	0	0	0	0.00
	1.05	120	123	121.5	2.12
	1.11	178	171	174.5	4.95

- Effect of equivalence ratio on UHC emission

Figures 37 and 38 show that the amount of unburned hydrocarbons produced by all the fuels increased as the equivalence ratio was increased from $\phi = 0.83$ to $\phi = 1.11$. This was due to the fact that excess air inside the furnace at $\phi < 1.0$ aided in better and complete combustion and deficit air at $\phi > 1.0$ led to incomplete oxidation of the elemental components of the fuel producing higher unburned hydrocarbon groups.

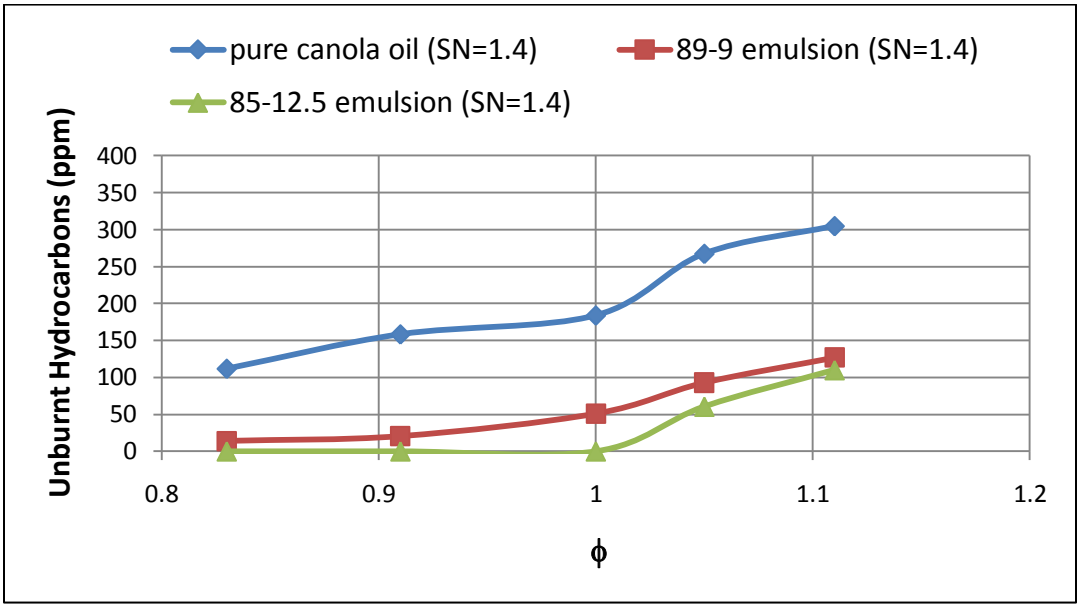

Figure 37: Unburned hydrocarbon emissions from pure canola oil, 89-9 emulsion and 85-12.5 emulsion at SN = 1.4 for a constant heat output of 72,750 kJ/hr

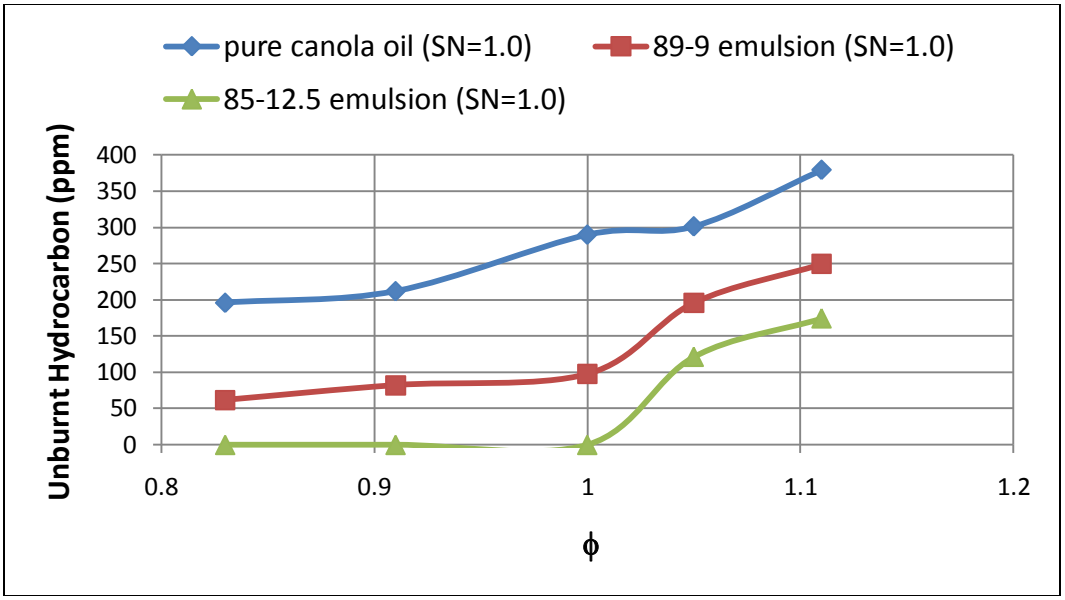

Figure 38: Unburned hydrocarbon emissions from pure canola oil, 89-9 emulsion and 85-12.5 emulsion at SN = 1.0 for a constant heat output of 72,750 kJ/hr

- Effect of swirl number on UHC emission

Figures 37 and 38 show that the swirl number was inversely related to UHC emission levels. All the fuels showed a reduction in UHC emissions when the swirl number was increased from SN =1.0 to SN = 1.4. This effect can be attributed to the enhanced fuel-air mixing at 60 ° vane angle helping in a better combustion process. The higher vorticity imparted to the secondary air at higher blade angles, increased the residence time and level of mixing of the air-fuel mixture leading to reduced UHC emissions. Table 20 depicts the percentage reduction in UHC when the swirl number was increased from 1.0 to 1.4.

Table 20: Percentage reduction in unburned hydrocarbon due to increase in swirl number

Fuel Type	Equivalence ratio	Average value of UHC (ppm) at 60 ° swirl angle	Average value of UHC (ppm) at 51 ° swirl angle	Percentage reduction in UHC emission
Pure canola oil	0.83	112	196	42.9
89-9 Emulsion	0.83	14	61.5	77.2
85-12.5 Emulsion	0.83	0	0	0.0

- Effect of fuel type on UHC emission

From Figures 37 and 38, it is seen that the emulsions produced lesser UHC emissions than pure canola oil at all combustion conditions and both swirl angles. There were no UHC emissions from 85-12.5 emulsion at stoichiometric and lean conditions. The reason for this result can be explained by the findings of Rakopolous et. al.[38]. The methanol and surfactant bound oxygen in the case of emulsions was found to help prevent the formation of local fuel rich zones inside the furnace. Moreover, a leaner combustion process helped reduce the UHC emissions from the emulsions.

6.3.3 Carbon Dioxide and Carbon Monoxide Emissions

Table 21 lists the values of CO_2 emissions recorded during the combustion experiments of pure canola oil, 89-9 emulsion and 85-12.5 emulsion at 60° and 51° swirl angles.

Table 21: CO_2 emissions from all the fuels at both swirl numbers

Fuel Type / Swirl Number	Equi-valence ratio	CO_2 first reading (%)	CO_2 second reading (%)	Average value of CO_2 (%)	Standard deviation of CO_2 (%)
Pure Canola Oil	0.83	13.75	13.66	13.705	0.06
	0.91	13.64	13.85	13.745	0.15
	1	14.25	14.43	14.34	0.13
60°	1.05	12.52	12.66	12.59	0.10
(SN = 1.4)	1.11	11.08	11.21	11.145	0.09
Pure Canola Oil	0.83	10.06	10.14	10.1	0.06
	0.91	11.16	11.05	11.105	0.08
	1	12.63	12.6	12.615	0.02
51°	1.05	11.76	11.63	11.695	0.09
(SN = 1.0)	1.11	10.41	10.66	10.535	0.18
89-9 Emulsion	0.83	12.65	12.53	12.59	0.08
	0.91	13.29	13.59	13.44	0.21
	1	14.14	14.35	14.245	0.15
60°	1.05	13.43	13.65	13.54	0.16
(SN = 1.4)	1.11	12.86	12.26	12.56	0.42
89-9 Emulsion	0.83	12.74	12.64	12.69	0.07
	0.91	12.82	12.85	12.835	0.02
	1	12.88	12.97	12.925	0.06
51°	1.05	11.32	11.39	11.355	0.05
(SN = 1.0)	1.11	10.47	10.41	10.44	0.04
85-12.5 Emulsion	0.83	14.17	14.15	14.16	0.01
	0.91	14.88	14.85	14.865	0.02
	1	15.52	15.69	15.605	0.12
60 °	1.05	13.58	13.39	13.485	0.13
(SN = 1.4)	1.11	13.31	13.23	13.27	0.06
85-12.5 Emulsion	0.83	12.85	12.71	12.78	0.10
	0.91	13.44	13.19	13.315	0.18
	1	14.31	14.43	14.37	0.08
51°	1.05	12.93	12.66	12.795	0.19
(SN = 1.0)	1.11	12.39	12.44	12.415	0.04

Table 22 lists the values of CO emissions recorded during the combustion experiments of pure canola oil, 89-9 and 85-12.5 emulsions at 60° and 51° swirl angles.

Table 22: CO emissions from all the fuels at both swirl numbers

Fuel Type/Swirl Number	Equi-valence ratio	CO first reading (ppm)	CO second reading (ppm)	Average value of CO (ppm)	Standard deviation of CO (ppm)
Pure Canola Oil	0.83	3	4	3.5	0.71
	0.91	5	4	4.5	0.71
	1	3	4	3.5	0.71
60° (SN = 1.4)	1.05	3126	3132	3129	4.24
	1.11	3767	3769	3768	1.41
Pure Canola Oil	0.83	3	3	3	0.00
	0.91	4	5	4.5	0.71
	1	10	11	10.5	0.71
51° (SN = 1.0)	1.05	3539	3538	3538.5	0.71
	1.11	4164	4169	4166.5	3.54
89-9 Emulsion	0.83	2	1	1.5	0.71
	0.91	3	5	4	1.41
	1	3	3	3	0.00
60° (SN = 1.4)	1.05	2235	2241	2238	4.24
	1.11	2454	2460	2457	4.24
89-9 Emulsion	0.83	1	3	2	1.41
	0.91	1	5	3	2.83
	1	2	4	3	1.41
51° (SN = 1.0)	1.05	2382	2385	2383.5	2.12
	1.11	2819	2817	2818	1.41
85-12.5 Emulsion	0.83	0	0	0	0.00
	0.91	1	1	1	0.00
	1	2	3	2.5	0.71
60° (SN = 1.4)	1.05	1242	1247	1244.5	3.54
	1.11	1835	1834	1834.5	0.71
85-12.5 Emulsion	0.83	0	1	0.5	0.71
	0.91	3	2	2.5	0.71
	1	4	4	4	0.00
51° (SN = 1.0)	1.05	1444	1443	1443.5	0.71
	1.11	2030	2035	2032.5	3.54

- Effect of equivalence ratio on CO_2 and CO formation

Figures 39 and 40 show that the peak of CO_2 formation for all the fuels was at the stoichiometric condition. On the lean side ($\phi<1$), the excess amount of air, diluted the

carbon dioxide inside the furnace. When the fuels were burned at rich conditions (ϕ>1), the lack of sufficient amount of oxygen prevented the complete oxidation of carbon to carbon dioxide. Note that the CO_2 values for pure canola oil and 89-9 emulsion at stoichiometric conditions overlap in both Figures 39 and 40. This was because both the fuels burned by almost the same amount at this condition (see burnt fraction plots on page 102).

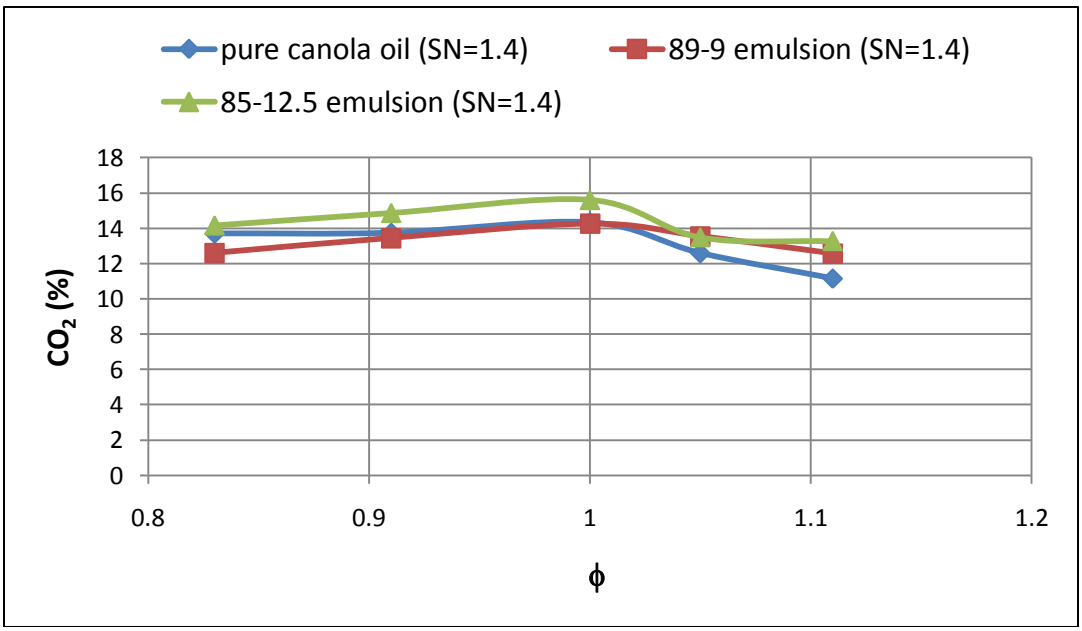

Figure 39: CO_2 emissions from pure canola oil, 89-9 emulsion and 85-12.5 emulsion at SN = 1.4 for a constant heat output of 72,750 kJ/hr

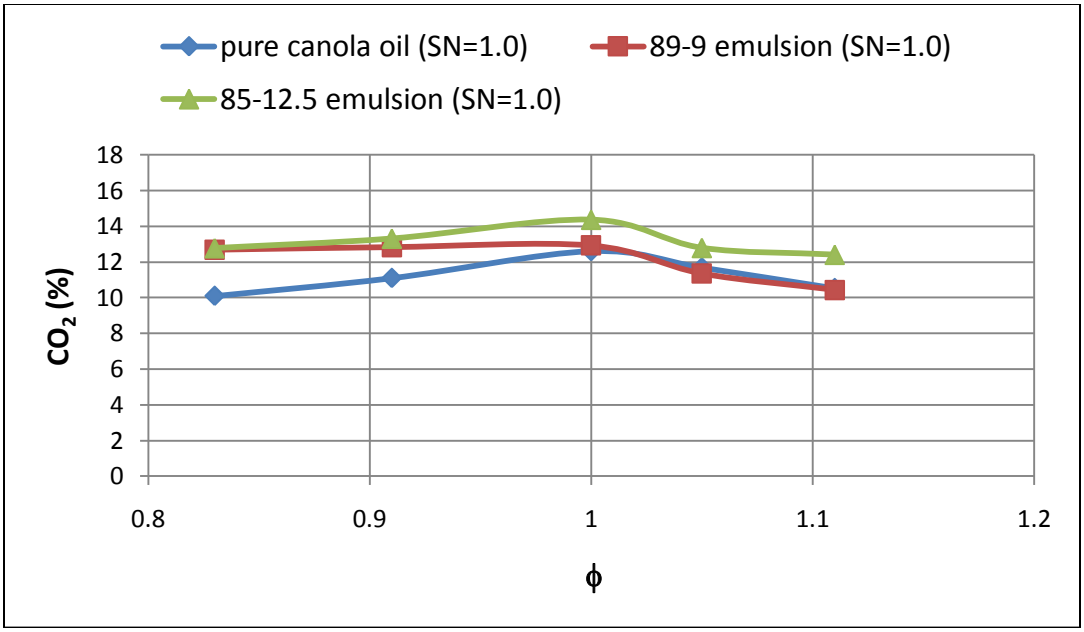

Figure 40: CO_2 emissions from pure canola oil, 89-9 emulsion and 85-12.5 emulsion at SN = 1.0 for a constant heat output of 72,750 kJ/hr

The carbon monoxide emission results are presented in Figures 41 and 42. The CO production of all the fuels was almost close to zero when burned at lean and stoichiometric conditions. These results are in agreement with those obtained by Hoon Kiat Ng. et. al. [39] during the combustion of No.2 diesel and blends of diesel and palm oil methyl ester (POME) in a non-pressurized water cooled combustor. Hoon Kiat Ng. et. al. [39] recorded minimum CO emissions at $\phi = 0.8$ for both, diesel and POME. On the fuel rich side, the CO values increased rapidly indicating incomplete oxidation.

Even during the richer combustion ($\phi>1$), it was seen that the emulsions produced lesser CO as compared to pure canola oil. 85-12.5 emulsion produced the least CO emissions of all the fuels. This was due to the presence of methanol and surfactant bound oxygen which resulted in a relatively leaner combustion of the emulsion. Rakopolous et.

al. [38] also suggested that the fuel bound oxygen in the diesel-butanol blends helps prevent the formation of local fuel rich zones inside the diesel engine which resulted in reduced CO emission. The results shown in Figures 41 and 42 for vegetable oil blends are consistent with previous findings for other fuels.

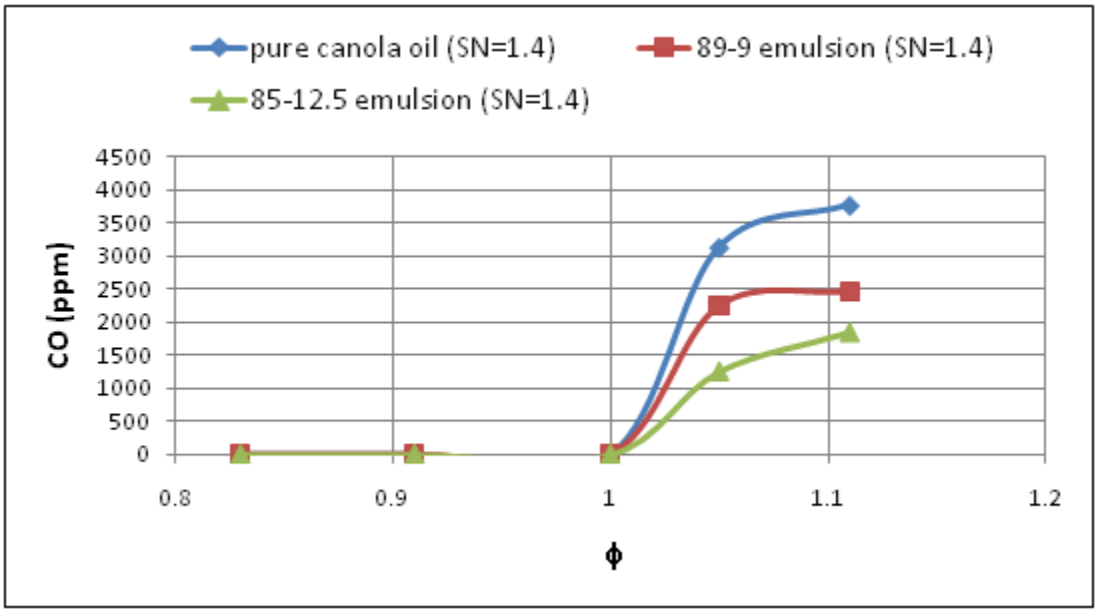

Figure 41: CO emissions from pure canola oil, 89-9 emulsion and 85-12.5 emulsion at SN = 1.4 for a constant heat output of 72,750 kJ/hr

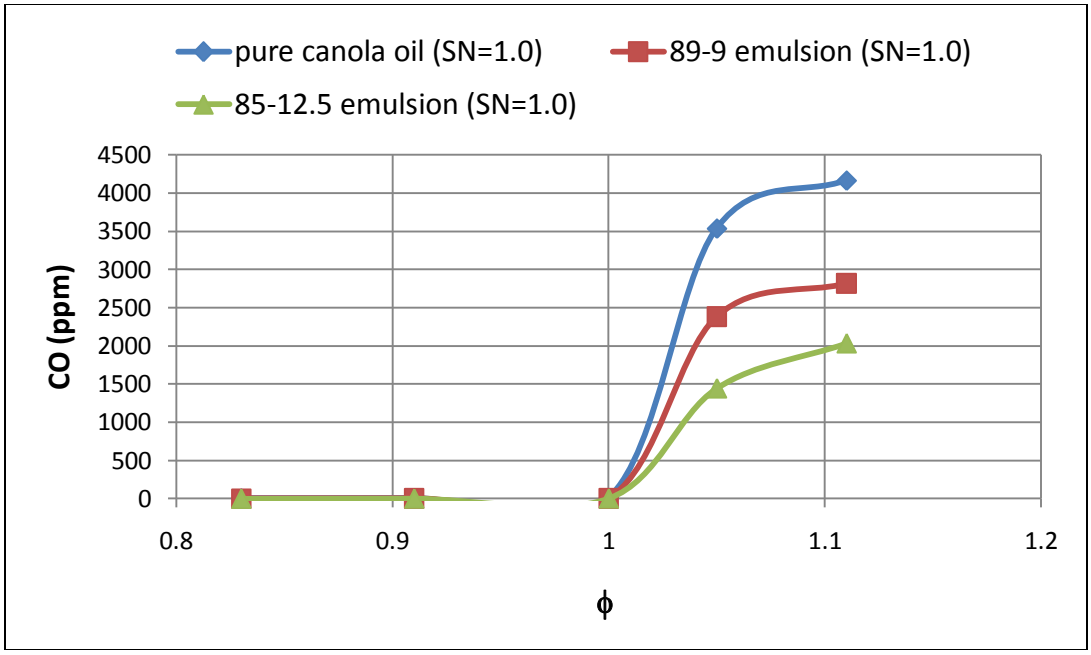

Figure 42: CO emissions from pure canola oil, 89-9 emulsion and 85-12.5 emulsion at SN = 1.0 for a constant heat output of 72,750 kJ/hr

- Effect of swirl number on CO_2 and CO emissions

Figures 39 and 40 show that the CO_2 production by all the fuels is proportional to the swirl number. Comparing the performance of each fuel at ϕ = 0.83, it is seen that the CO_2 production for all the fuels increased when the swirl number was increased from 1.0 to 1.4. This result was as expected because the amount of unburned hydrocarbons emissions decreased at higher swirl number. The secondary air was imparted higher vorticity at blade angle of 60 ° as compared to that at 51 °. Due to the higher amount of turbulence, the fuel and air were mixed much better and the residence time of this mixture was also increased. These two effects together gave higher CO_2 production from all the fuels at SN= 1.4. Table 23 lists the % CO_2 increment when the swirl number was

increased from 1.0 to 1.4. Note that the CO_2 formation from 89-9 emulsion is almost the same at both swirl angles.

Table 23: Percentage increase in CO_2 due to increase in swirl number

Fuel type	**Equi-valence Ratio**	**Experimentally recorded CO_2 (%) at SN = 1.4**	**Experimentally recorded CO_2 (%) at SN = 1.0**	**Percentage increase in CO_2**
Pure canola oil	0.83	13.705	10.100	26.3
89-9 Emulsion	0.83	12.590	12.690	-0.8
85-12.5 Emulsion	0.83	14.160	12.780	9.8

Calculations for CO reduction due to increase in swirl angle when $\phi > 1$, have not been done as it is not a common practice to burn heavy fuel oil at fuel rich conditions.

- Effect of fuel type on CO_2 and CO emissions

Figures 39 and 40, show that both the emulsions produced more CO_2 than pure canola oil at fuel lean combustion conditions. The same trend was seen during fuel rich combustion except a few coinciding points representing similar CO_2 values.

As mentioned afore, the presence of methanol and surfactant bound oxygen in case of emulsions helped them to undergo efficient combustion which resulted in more CO_2. Same explanation can be attributed for the lesser CO production by the emulsions when $\phi>1$, as seen in Figures 41 and 42.

6.3.4 Burned Fraction (BF)

Burned fraction (BF) is a term used to determine the fraction of fuel that underwent complete combustion. Thien [40] approximated the burned fraction of a fuel through the following equation,

$$BF = \frac{1}{\phi} * \left[1 - \frac{X_{O2}}{X_{O2,A}}\right] \quad (12)$$

where,

ϕ = measured equivalence ratio from air and fuel flow rates,

X_{O2} = mole fraction of oxygen in the exhaust gas (dry basis)

$X_{O2,A}$ = mole fraction of oxygen in the ambient air (dry basis)

Table 24 lists the BF values of all the fuels at swirl angles of 60° and 51°.

Table 24: Burned fraction values for all the fuels at both swirl numbers

Fuel Type/ Swirl Number	Equi-valence ratio	Excess O_2 in Exhaust (mole fraction)	O_2 mole fraction in ambient	Measured Equivalence Ratio	Burned Fraction
Pure Canola Oil	0.83	0.038	0.21	0.83	0.98
	0.91	0.028	0.21	0.91	0.96
	1	0.019	0.21	1.00	0.91
60°	1.05	0.013	0.21	1.04	0.90
(SN = 1.4)	1.11	0.016	0.21	1.10	0.84
89-9 Emulsion	0.83	0.035	0.21	0.84	1.00
	0.91	0.026	0.21	0.91	0.96
	1	0.017	0.21	1.00	0.92
60°	1.05	0.01	0.21	1.06	0.90
(SN = 1.4)	1.11	0.012	0.21	1.12	0.84
85-12.5 Emulsion	0.83	0.033	0.21	0.83	1.01
	0.91	0.023	0.21	0.90	0.98
	1	0.018	0.21	1.00	0.91
60°	1.05	0.006	0.21	1.05	0.92
(SN = 1.4)	1.11	0.007	0.21	1.11	0.87
Pure canola Oil	0.83	0.045	0.21	0.83	0.94
	0.91	0.038	0.21	0.91	0.90
	1	0.026	0.21	1.00	0.88
51°	1.05	0.024	0.21	1.05	0.84
(SN = 1.0)	1.11	0.02	0.21	1.11	0.81
89-9 Emulsion	0.83	0.043	0.21	0.83	0.96
	0.91	0.035	0.21	0.91	0.92
	1	0.025	0.21	1.00	0.88
51°	1.05	0.021	0.21	1.05	0.86
(SN = 1.0)	1.11	0.018	0.21	1.11	0.82
89-9 Emulsion	0.83	0.04	0.21	0.82	0.98
	0.91	0.033	0.21	0.90	0.94
	1	0.021	0.21	1.00	0.90
51°	1.05	0.019	0.21	1.04	0.88
(SN = 1.0)	1.11	0.012	0.21	1.10	0.86

Note that, BF value is more than 1 at some of the lean combustion conditions. These values represent the limitations of equation 11 and experimental uncertainty.

- Effect of equivalence ratio on burned fraction

The effect of equivalence ratio on the burned fraction of all the three fuels is shown in Figures 43 and 44. The general trend in Figures 43 and 44 depicts that the burned fraction for all the fuels was maximum at ϕ = 0.83. As the equivalence ratio was increased from ϕ = 0.83 to ϕ = 1.11, a gradual decrease in the BF values was observed. Availability of extra air in the combustion chamber at lean conditions, helped the fuel to better mix with air and allowed greater amount of fuel to undergo combustion. Exactly opposite phenomenon was observed at fuel rich conditions due to the lack of sufficient amount of air in the furnace. In Figure 43, it is seen that burned fraction for 85-12.5 emulsion deviates from the general trend at ϕ = 1. As seen in figure on page 89, 85-12.5 emulsion produced little unburned hydrocarbon amount when ϕ was between 0.83 and 1.0. This contributed to its almost optimal burned fraction as seen in Figure 43 at ϕ =1.0. Moreover, the level of mixing brought about by SN=1.4 also contributed to an optimal burned fraction at ϕ = 1.0.

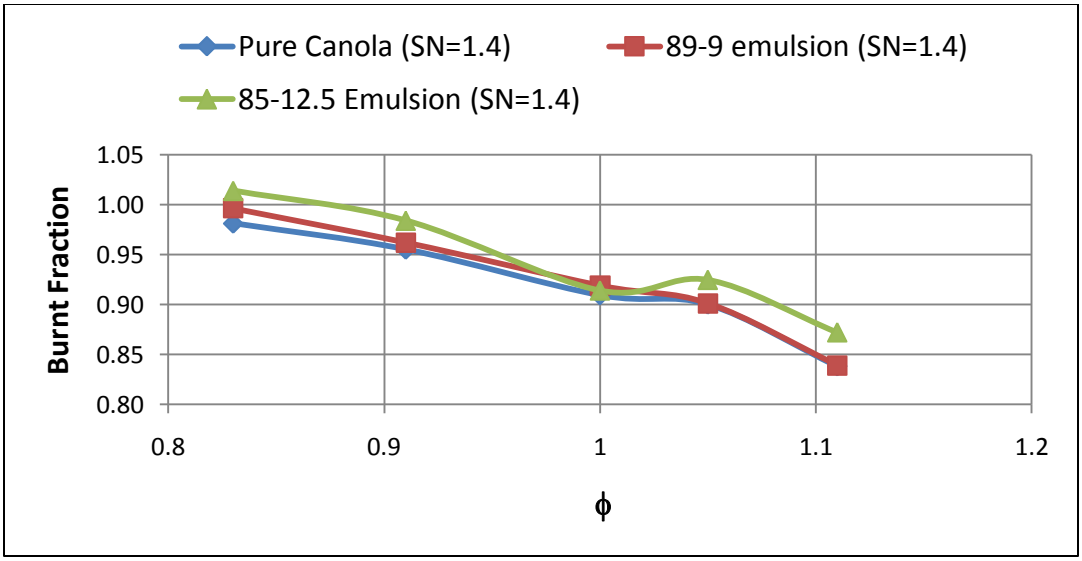

Figure 43: Burned fraction values for pure canola oil, 89-9 emulsion and 85-12.5 emulsion at SN = 1.4 for a constant heat output of 72,750 kJ/hr

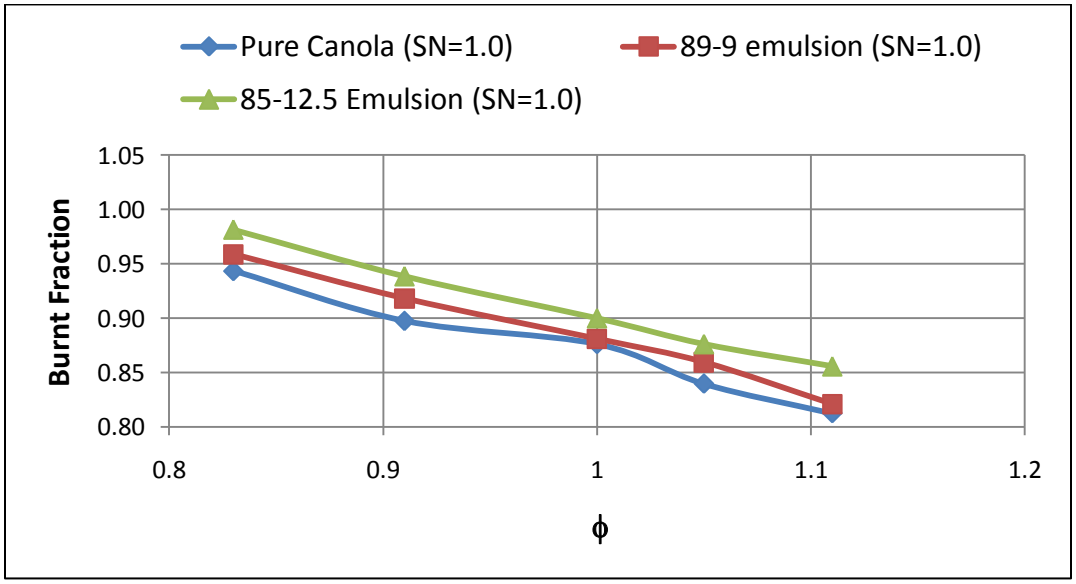

Figure 44: Burned fraction values for pure canola oil, 89-9 emulsion and 85-12.5 emulsion at SN = 1.0 for a constant heat output of 72,750 kJ/hr

- Effect of swirl number on burned fraction

From Figures 43-44, it is seen that the swirl number definitely influenced the fuel burned fraction. All the fuels showed higher values of burned fraction when the swirl number was increased from SN = 1.0 to SN = 1.40. The result for such an outcome is the increased vorticity in the air at SN = 1.4 which helped in the formation of better quality fuel-air mixture and undergo efficient combustion. Table 25 shows the percentage increase in BF due to change of swirl number from 1.0 to 1.4.

Another hypothesis that can be suggested for higher BF at SN = 1.4 is the formation of a stronger internal recirculation zone (IRZ). An IRZ is produced during combustion at high swirl numbers (usually SN > 0.6) [22]. The adverse pressure gradient in the core of the vortex leads to the reversal of flow along combustion chamber axis. Due to this, the IRZ contains a mixture of chemically active combustion products which act as a storage of heat facilitating easy burning of the newly sprayed fuel.

Table 25: Percentage increase in burned fraction due to increase in swirl number

Fuel type	**Equivalence ratio**	**Burned fraction values at SN = 1.4**	**Burned fraction values at SN = 1.0**	**Percentage increased in BF**
Pure canola oil	0.83	0.98	0.94	3.9
89-9 emulsion	0.83	1.00	0.96	3.8
85-12.5 emulsion	0.83	1.01	0.98	3.2

- Effect of fuel type on burned fraction

Figures 43 and 44 show that, the emulsions burned in higher amounts than pure canola oil at both the swirl numbers and at all equivalence ratios. There are two possible hypothesizes for this result. First hypothesize for this result could be related to the high viscosity of pure canola oil compared to its emulsions. Since the canola oil had higher viscosity, it could be suggested that the nozzle produced relatively bigger canola oil droplets due to the strong cohesive forces (i.e. greater surface tension) between the canola oil molecules. Bigger droplets reduced canola oil's ability to easily mix with air and form ignitable mixture, thus leading to lower burned fraction of canola oil. Similar results were observed by Pascal et al. [41] during the combustion of palm oil in an internal combustion engine. Pascal et al. [41] observed that the higher viscosity of palm oil compared to diesel fuel decreased the palm oils ability to form ignitable blends which led to higher unburned hydrocarbon emissions from palm oil. The results shown in Figures 43 and 44 for canola oil are in agreement with the previous findings for palm oil.

Another hypothesis for higher BF of emulsions is the occurrence of micro-explosions. The secondary atomization of canola oil droplet caused due to the rapid expansion of methanol vapors within it, could have produced very fine droplets of oil. The finer droplets could evaporate much faster leading to efficient combustion.

6.4 Furnace Temperature

For all the experiments, the furnace was preheated to a temperature of about 800°C - 815°C (as shown by 1st thermocouple) by burning natural gas. The 1st thermocouple was at a distance of 44.45 cm (17.5 in) below the nozzle tip. Thermocouple recorded the temperature after every 20 seconds. The following figures show the furnace temperatures recorded by the 1st thermocouple during liquid fuel combustion only. Note that the small dip at the beginning of the curve denotes the time when natural gas flow was gradually reduced and liquid fuel flow was increased to get a constant heat output of 72,750 kJ/hr. In all the experiments, the fuel was first burned at stoichiometric condition, then fuel lean and after that at fuel rich conditions. Whenever the equivalence ratio was changed by adjusting the secondary air flow, the furnace temperature usually took about 10 minutes to stabilize. At each equivalence ratio, the emission data was collected twice.

Figures 45-47 show the temperature plots obtained during the combustion experiments at swirl angle of 60° (SN=1.4).

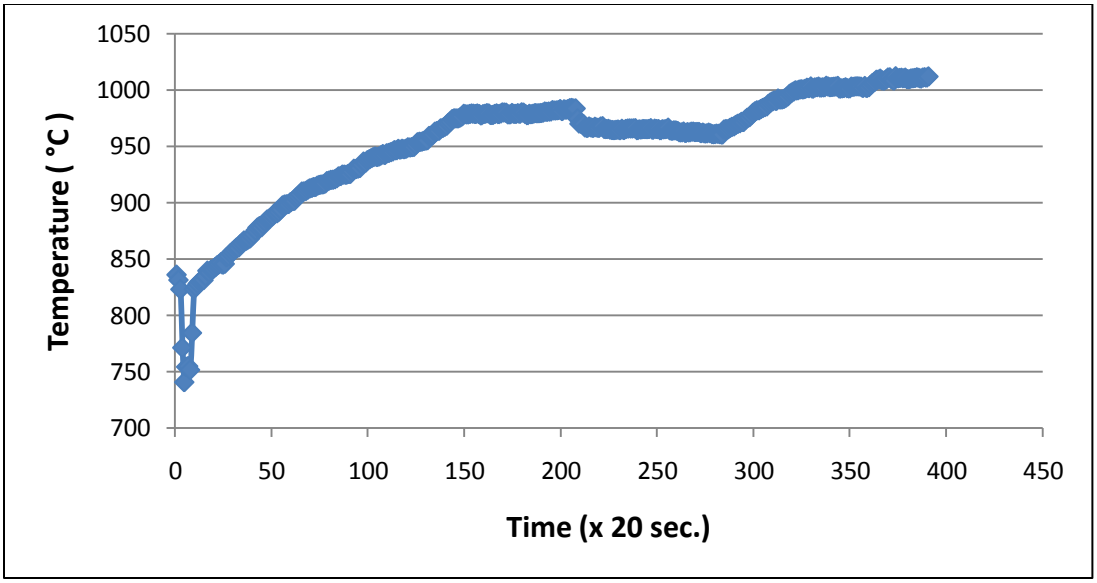

Figure 45: Furnace temperature (as shown by 1st thermocouple) during canola oil combustion (SN = 1.4)

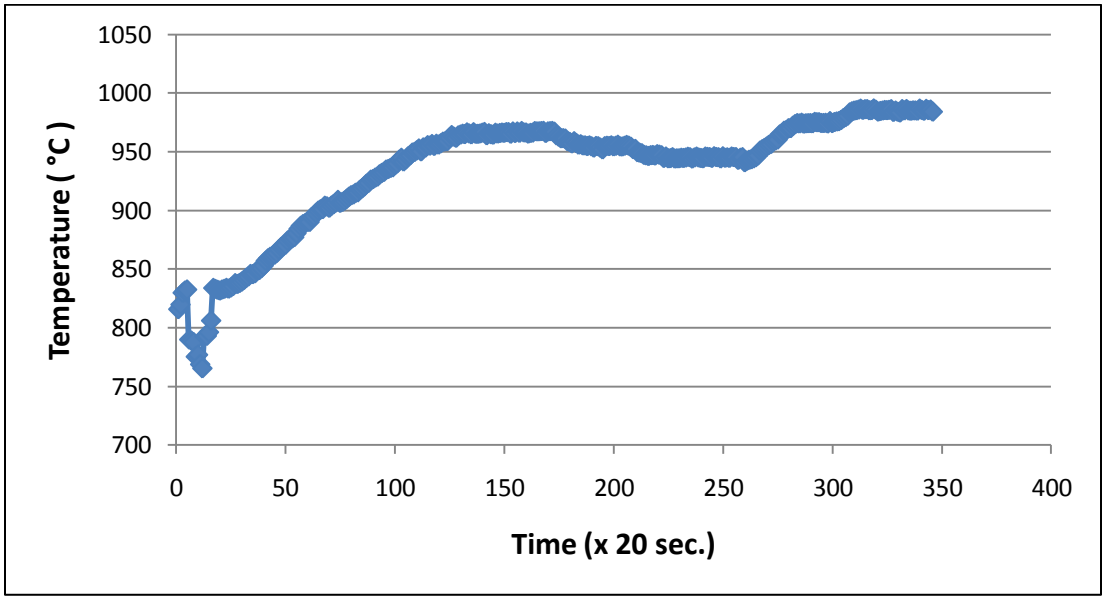

Figure 46: Furnace temperature (as shown by 1st thermocouple) during combustion of 89-9 emulsion (SN = 1.4)

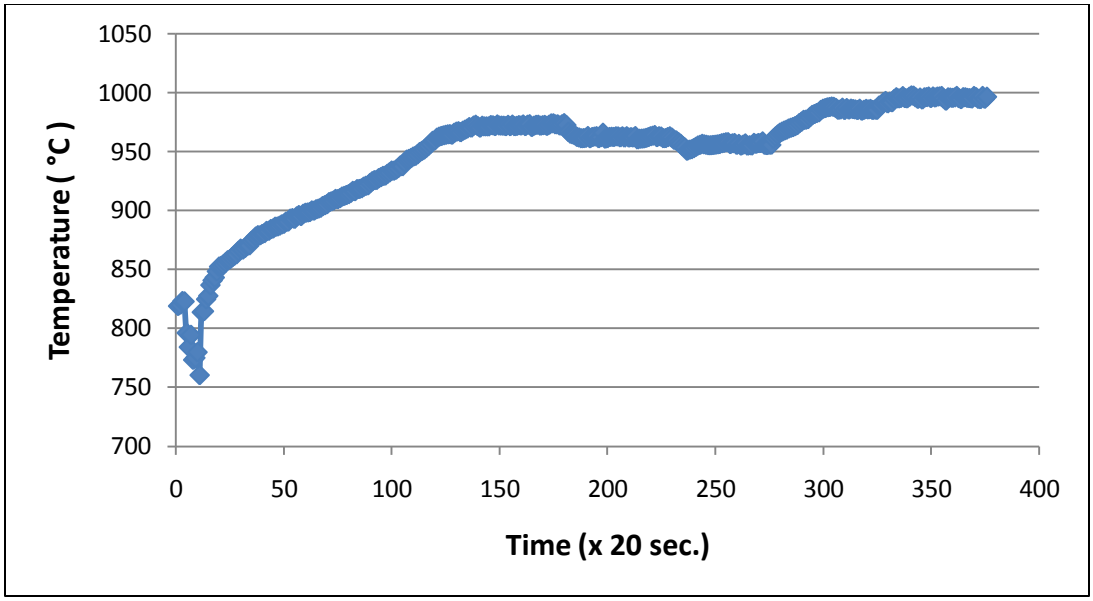

Figure 47: Furnace temperature (as shown by 1st thermocouple) during 85-12.5 emulsion combustion (SN = 1.4)

Similar temperature plots were also obtained during the combustion of canola oil, 89-9 emulsion and 85-12.5 emulsion at 51° swirl angle (SN = 1.0), as shown by Figures 48-50.

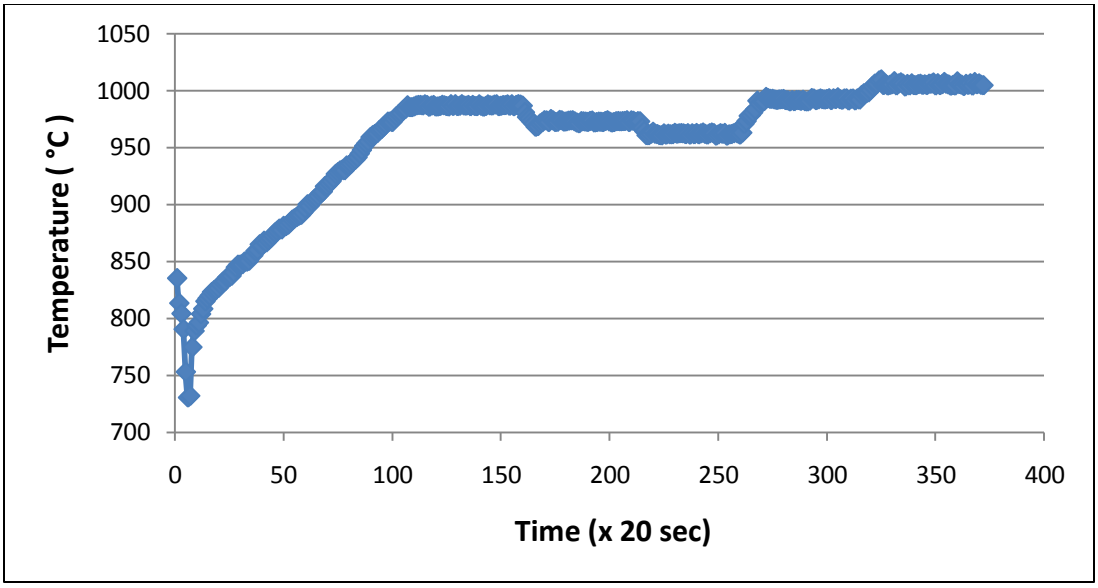

Figure 48: Furnace temperature (as shown by 1st thermocouple) during canola oil combustion (SN = 1.0)

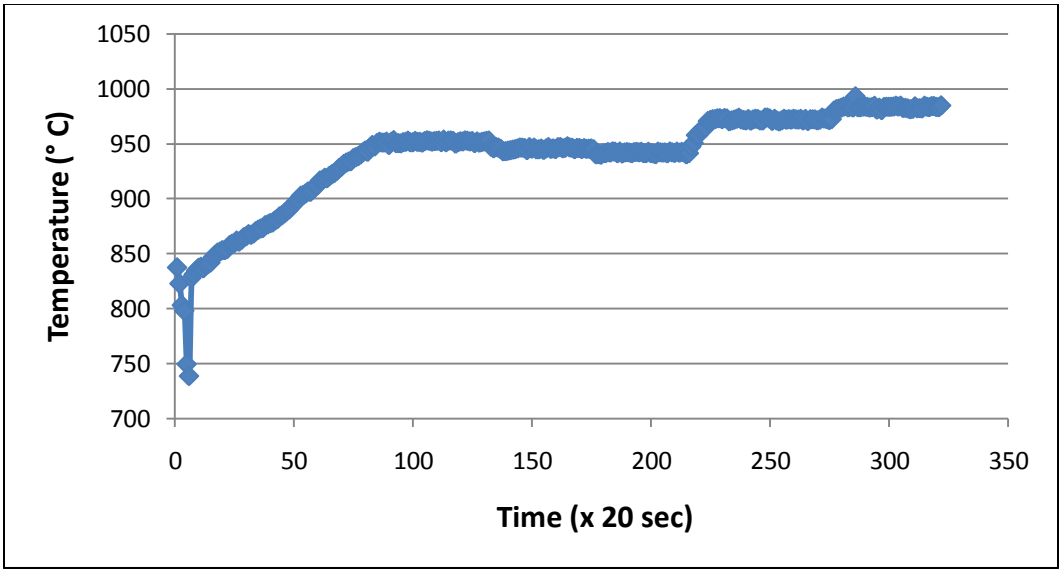

Figure 49: Furnace temperature (as shown by 1st thermocouple) during 89-9 emulsion combustion (SN = 1.0)

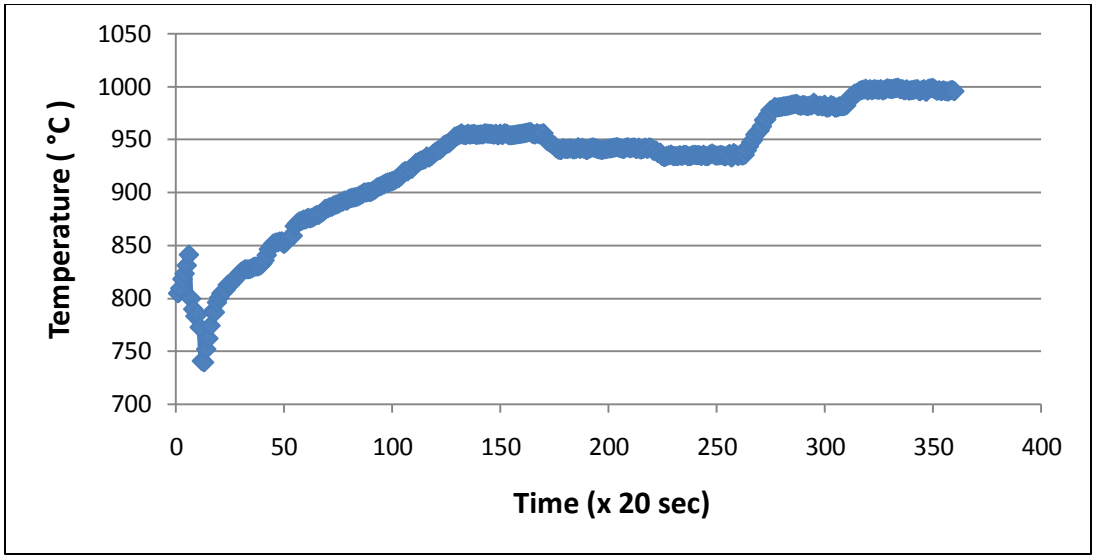

Figure 50: Furnace temperature (as shown by 1st thermocouple) during 85-12.5 emulsion combustion (SN = 1.0)

Table 26 lists the average temperatures at which the emission data for each equivalence ratio were recorded.

Table 26: Experimental temperature (as shown by 1st thermocouple) at which emissions were collected

Fuel Type/Swirl Number	Equivalence Ratio	Temperature at which emissions were recorded experimentally (°C)	$T_\phi - T_{\phi=1.0}$	Average NOx emissions (ppm)
Pure Canola Oil	0.83	960	-18	119
	0.91	965	-13	104.5
	1	978	0	83.3
60° (SN = 1.4)	1.05	1002	24	75.3
	1.11	1010	32	63.75
89-9 emulsion	0.83	955	-17	112.45
	0.91	961	-11	95.4
	1	972	0	78.65
60° (SN = 1.4)	1.05	984	12	56
	1.11	997	25	42.5
85-12.5 emulsion	0.83	945	-22	103.75
	0.91	955	-12	89.6
	1	967	0	71
60° (SN = 1.4)	1.05	975	8	35.5
	1.11	984	17	18.5
Pure Canola Oil	0.83	961	-25	141.35
	0.91	972	-14	118.25
	1	986	0	95.45
51° (SN = 1.0)	1.05	992	6	79.15
	1.11	1005	19	66.65
89-9 emulsion	0.83	942	-9	118.25
	0.91	945	-6	106.05
	1	951	0	87.85
51° (SN = 1.0)	1.05	972	21	78.95
	1.11	983	32	58.65
85-12.5 emulsion	0.83	935	-19	107
	0.91	941	-13	99.45
	1	954	0	72.85
51° (SN = 1.0)	1.05	982	28	66
	1.11	996	42	47.5

From Table 26, it is seen that furnace temperature decreased at fuel lean conditions and increased during fuel rich combustion. However, for each fuel, the temperature difference between fuel rich and stoichiometric condition, and, fuel lean and stoichiometric condition was not more than ± 30° C, indicating that the furnace operated at a relatively steady state.

Table 26 also shows a weak correlation between Thermal NO_x emission level and the furnace temperature. It is seen that as the temperature decreased ($\phi<1$), the NO_x ppm increased for all the fuels. However, it should be noted that the temperatures listed in Table 26 were measured at 44.45 cm below the nozzle tip and not inside the flame zone. Experimental flame temperatures for each fuel could help better understand the contribution of thermal NO_x to the total nitrogen oxide formation inside the furnace.

6.4.1 Adiabatic Flame Temperature (AFT)

Adiabatic flame temperature calculation for each fuel at different equivalence ratios was done using Engineering Equation Solver. Table 27 lists the AFT for all the fuels. Note that, the adiabatic flame temperature of all three fuels at a particular equivalence ratio was almost in a similar range. However, there was a big difference (almost 1000° C) between temperatures recorded experimentally and the AFT. This was due to the ideal combustion conditions assumed for adiabatic flame temperature calculations. However, precautionary measures should be taken in the future to make sure that such a temperature difference is not caused due to heat losses from the furnace. Figure 51 shows the adiabatic flame temperature variation with equivalence ratio.

Table 27: Adiabatic Flame Temperature of all the fuels

Equivalence Ratio	Adiabatic flame temp for Pure canola oil (°C)	Adiabatic flame temp for 89-9 emulsion (°C)	Adiabatic flame temp for 85-12.5 emulsion (°C)
0.83	1863	1886	1893
0.91	1987	2010	2018
1	2129	2154	2162
1.05	2209	2234	2242
1.11	2297	2321	2328

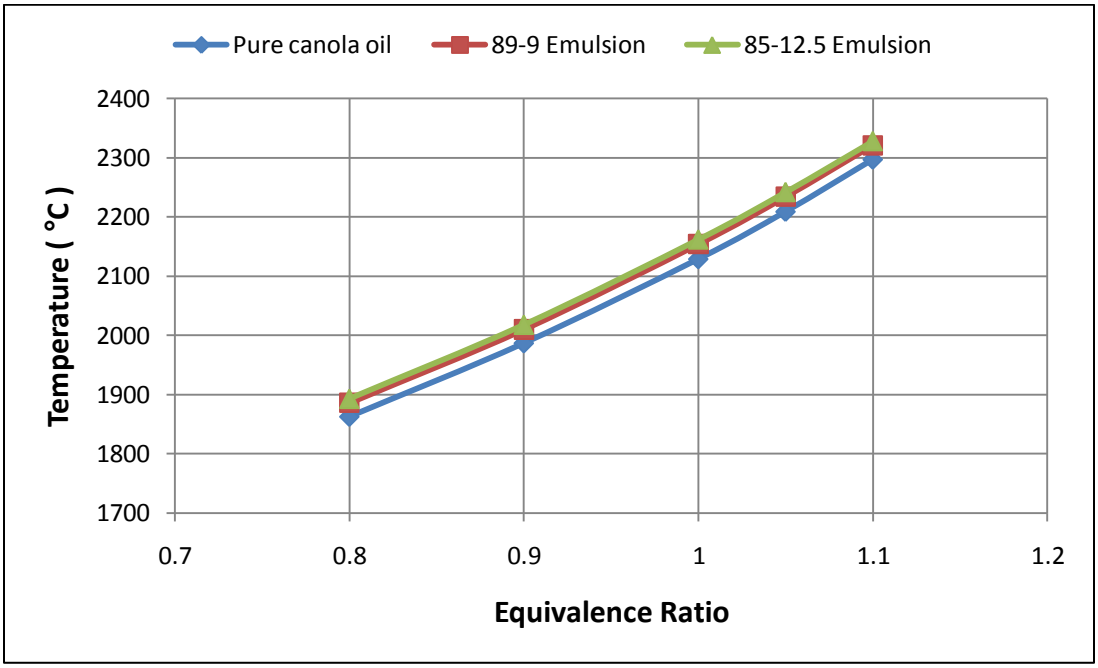

Figure 51: Adiabatic flame temperatures of canola oil, 89-9 and 85-12.5 emulsions

6.5 Droplet Size Measurement

A spray contains droplets with a range of sizes. In order to get some knowledge of the droplet size distribution, a mean or average diameter calculation can be helpful especially in applications like combustion where there is continuous heat and mass transfer between dispersed liquid and surrounding oxidizer. The most important diameter for combustion applications is Sauter mean diameter. Sauter mean diameter (SMD) is defined as the diameter of that drop whose volume to surface ratio value is the same as the arithmetic mean of volume to surface values on the total number of drops belonging to the sample spray under examination[42].

Nozzles have different design and construction and so various correlations for SMD have been proposed for each type of design. For twin fluid atomizers, the correlation proposed by Nukiyama and Tanasawa [43] is used most often. The following equation proposed by Nukiyama et. al. [43] was used to calculate the Sauter mean diameter of droplets of canola and its corresponding emulsions in this project.

$$d_0 = \left(\frac{0.585}{U_R}\right) * \left(\frac{\sigma}{\rho_L}\right)^{0.5} + 1.415 * 10^6 * \left(\frac{\mu_L}{\sqrt{\sigma * \rho_L}}\right)^{0.45} \left(\frac{Q_L}{Q_G}\right)^{1.5} \quad (13)$$

where,

d_0 is the Sauter mean diameter (μm)

U_R is the relative velocity of air to the velocity of the liquid

σ is the surface tension of liquid (kg/s^2)

ρ_L is the density of liquid (kg/m^3)

μ_L is the viscosity of liquid (kg/ms)

Q_L is the volumetric flow rate of the liquid

Q_G is the volumetric flow rate of the gas

The surface tension of canola oil has been taken from the work published by Shu et. al. [44]. The surface tension of the emulsions was estimated by considering the mass fraction of canola oil and methanol in the blend. Since, Span 80 and Tween 80 were added in very small amounts to the emulsions, their contribution to the surface tension was not taken into account.

$$\sigma_{emulsion} = \left(m_{f,canola\ oil} * \sigma_{canola\ oil}\right) + \left(m_{f,methanol} * \sigma_{methanol}\right) \quad (14)$$

where,

σ is the surface tension

m_f is the mass fraction of substance in the blend

Table 28 lists the experimental parameters used to calculate the SMD of fuel droplets. Press et. al. [45] studied the atomization of water-in-mineral oil emulsions. The authors [45] found that the values of SMD increased with increase in emulsion viscosity and the amount of oil in the blends. From Table 28, it is seen that even though the emulsions have lesser oil content and lesser viscosity than pure canola oil, still they had slightly higher SMD values. This might be due to the higher volumetric flow rates of emulsions. Also, accurate measurements of the surface tension of both emulsions might help in getting a more accurate SMD value of emulsion droplets.

Table 28: SMD values for droplets of canola oil and its emulsions

Fuel Type	**σ (Kg/s^2)**	**ρ_L (Kg/m^3)**	**Q_L (m^3/s)**	**Q_G (m^3/s)**	**Nozzle orifice area (m^2)**	**V_L (m/s)**	**V_G (m/s)**	**U_R**	**μ_L (Kg/ms)**	**SMD (μm)**
Canola Oil	0.0278	962	5.26E-07	0.000167	1.96E-07	2.68	852	318	0.055	32.4
89-9 Emulsion	0.0264	890	5.88E-07	0.000167	1.96E-07	3.00	852	284	0.0388	33.7
85-12.5 Emulsion	0.026	880	6.10E-07	0.000167	1.96E-07	3.11	852	274	0.0388	35.8

7. CONCLUSIONS

The 30 kW furnace facility at Coal and Biomass Energy Laboratory (CBEL) at Texas A&M University was successfully modified and given the capability to combust liquid fuels. Through this research project, an attempt was made to understand the influence of equivalence ratio, swirl number and fuel type on the combustion efficiency and emissions produced during the combustion of pure canola oil, 89-9 emulsion [9% methanol-in-89% canola oil with 2% surfactant (w/w)] and 85-12.5 emulsion [12.5% methanol-in-85% canola oil with 2.5% surfactant (w/w)]. The major conclusions of this research work are explained below.

7.1 Viscosity, Stability and Higher Heating Value - Conclusions

From the viscosity, stability and higher heating value (HHV) data, it can be said that,

- The viscosity of emulsions was influenced by the amount of methanol and surfactant added to the blend. Since 85-12.5 emulsion had higher percentage of surfactant, it had a slightly greater viscosity than 89-9 emulsion. Overall, addition of methanol to canola oil, led to reduced viscosity of the blends.
- Stability of the emulsions was inversely related to the amount of methanol added to the blend. The 89-9 emulsion was stable for three hours more than 85-12.5 emulsion.
- The heating value of emulsions was also inversely related to the amount of methanol present in the blend. The HHV of 89-9 emulsion and 85-12.5 emulsion

was less than HHV of pure canola oil by 4.4% and 6.6% respectively. The reduction was due to the low heat of combustion of methanol.

7.2 Swirl Number - Conclusions

The positioning of swirler blades at 60° and 51° (with respect to vertical axis) gave swirl numbers of 1.4 and 1.0, respectively. The higher vorticity imparted to the secondary air at higher swirl numbers helped the fuel and air to mix in a better manner and undergo an efficient combustion process.

For all three fuels:

- Lesser amounts of oxygen (in the exhaust) and unburned hydrocarbons were recorded at SN = 1.4 than at SN = 1.0.
- Higher amount of carbon dioxide (CO_2) was produced at SN = 1.4 as compared to SN = 1.0. This indicated more complete combustion of all fuels at higher swirl numbers.
- NO_x emission levels were the most affected by swirl number. NO_x from all three fuels was minimum at swirl number of 1.4 (swirl angle = 60°).

7.3 Fuel Type - Conclusions

The experimental results showed that fuel type had a major effect on the combustion products. In the case of emulsions, emission levels were inversely related to the percentage of methanol added to the blend. Higher the methanol content in the blend, lower the emissions.

- The CO_2 production was lowest in case of canola oil combustion.
- The amount of oxygen (in the exhaust), NO_x, UHC, and CO emissions from pure canola oil was always higher as compared to emissions from both the emulsions at both swirl numbers.
- 85-12.5 emulsion produced the lowest NO_x, unburned hydrocarbons and CO emissions at swirl number of 1.4. Highest CO_2 production was also seen for this emulsion. This result can be attributed to an overall leaner and more complete combustion of the fuel due to methanol and surfactant bound oxygen.

7.4 Burned Fraction - Conclusions

Burned fraction (BF) of the fuels was used as a measure of combustion efficiency. Burned fraction was affected by equivalence ratio, swirl number and fuel type:

- Burned fraction of all the fuels was maximum at $\phi = 0.83$. This was due to the extra air present in the combustion chamber that aided in a more complete combustion. Higher BF was achieved at SN = 1.4 than SN = 1.0.
- The emulsions always burned in higher amounts as compared to pure canola oil at both the swirl angles. Higher BF values of emulsions showed that the elemental composition of a fuel had a major effect on its combustion characteristics. In the case of emulsions, the presence of oxygen in methanol and the surfactants helped to lead an overall leaner combustion and reduce emissions.

8. FUTURE WORK

This study was instrumental in identifying combustion characteristics of pure canola oil and its emulsions with methanol. Considering that the furnace at Coal and Biomass Energy Laboratory at TAMU is now equipped with liquid fuel injection system, this facility should be used to understand combustion phenomena of emulsified fuels in greater depths. The following recommendations should be considered for further work in near future:

1. Blends having higher percentage of methanol should be investigated to determine their effects on emission levels.
2. Influence of swirl numbers greater than 1.4, on the combustion process should be studied as well.
3. A new refractory having a quarl should be used and emission results of new experiments should be compared with the current results.
4. Other bio-oils like corn oil, waste vegetable oil, algae-derived SVO, jatropa oil, and liquids (rich in hydrocarbons) obtained as a by-product of gasification can be emulsified with low grade alcohols. The combustion characteristic of these fuels can help promote the use of emulsified fuel technology even more.

REFERENCES

[1] http://www.eia.doe.gov/cneaf/electricity/epa/figes1.html, (16 Mar. 2011).

[2] P.O.Gomez, Development of a low NOx burner system for coal fired power plants using coal and biomass, Master's Thesis, Mechanical Engineering Department, Texas A&M University, College Station, 2008.

[3] http://lifestyle.iloveindia.com/lounge/common-uses-for-glycerin-2704.html, (16 Mar. 2011).

[4] Y. Ali, M.A. Hanna, Alternative diesel fuels from vegetable oils, Bioresource Technology 50 (1994) 153-163.

[5] G. Knothe, R.O. Dunn, M.O. Bagby, The use of vegetable oils and their derivatives as alternative diesel fuels, American Chemical Society (1997) 172-208.

[6] D. Chang, J. Van Gerpen, I. Lee, L. Johnson, E. Hammond, S. Marley, Fuel properties and emissions of soybean oil esters as diesel fuel, Journal of the American Oil Chemists' Society 73 (1996) 1549-1555.

[7] J. Krahl, A. Munack, M. Bahadir, L. Schumacher, N. Elser, Survey about biodiesel exhaust emissions and their environmental effects, American Society of Agricultural Engineers (1996) 136-148.

[8] T. Houlihan, The triple crown, Power Engineering 44 (2009).

[9] F. Shahidi, Canola and Rapeseed, Van Nostrand Reinhold, New York, 1990.

[10] H. Mollet, A. Grubenmann, Formulation Technology: Emulsions, Suspensions, Solid Forms, Wiley-VCH, Germany, 2001.

[11] S. Jafari, Y. He, B. Bhandari, Optimization of nano-emulsions production by microfluidization, European Food Research and Technology 225 (2007) 733-741.

[12] P. Becher, Encyclopedia of Emulsion Technology Vol. 1 Basic Theory, Marcel Dekker Inc, New York, 1983.

[13] R. Strayer, J. Blake, W. Craig, Canola and high erucic rapeseed oil as substitutes for diesel fuel: Preliminary tests, Journal of the American Oil Chemists' Society 60 (1983) 1587-1592.

[14] M. Ziejewski, H. Goettler, G.L. Pratt, Comparative analysis of the long-term performance of a diesel engine on vegetable oil based alternate fuels, Society of Automotive Engineers (1986) Paper No. 860301.

[15] Y. Yoshimoto, M. Onodera, H. Tamaki, Performance and emission characteristics of diesel engines fueled by vegetable oils, Society of Automotive Engineers (2001) Paper No. 2001-01-1807

[16] Y. Yoshimoto, M. Onodera, Performance of a diesel engine fueled by rapeseed oil blended with oxygenated organic compounds, Society of Automotive Engineers (2002) Paper No. 2002-01-2854

[17] A. Kerihuel, M. Senthil Kumar, J. Bellettre, M. Tazerout, Ethanol animal fat emulsions as a diesel engine fuel - Part 1: Formulations and influential parameters, Fuel 85 (2006) 2640-2645.

[18] M.S. Kumar, A. Kerihuel, J. Bellettre, M. Tazerout, Ethanol animal fat emulsions as a diesel engine fuel - Part 2: Engine test analysis, Fuel 85 (2006) 2646-2652.

[19] G. Vaitilingom, C. Perilhon, A. Liennard, M. Gandon, Development of rape seed oil burners for drying and heating, Industrial Crops and Products 7 (1998) 273-279.

[20] S.P.Krumdieck, J.W.Daily, Evaluating the feasibility of biomass pyrolysis oil for spray combustion applications, Combustion Science and Technology 134 (1998) 351-365.

[21] R. Chellini, Fuel/water emulsion: A low NOx alternative to water or steam injection, 1990.

[22] J. M. Beer, N.A. Chigier, Combustion Aerodynamics, John Wiley and Sons Inc, New York, 1972.

[23] M.R. Mafra, F.L. Fassani, E.F. Zanoelo, W.A. Bizzo, Influence of swirl number and fuel equivalence ratio on NO emission in an experimental LPG-fired chamber, Applied Thermal Engineering 30 (2010) 928-934.

[24] M. S. A. Ishak, M.N.M. Jaafar, The effect of swirl number on reducing emissions from liquid fuel burner system, Journal Mechanical 19 (2005) 48-56.

[25] R. Villasenor, R. Escalera, A highly radiative combustion chamber for heavy fuel oil combustion, International Journal of Heat and Mass Transfer 41 (1998) 3087-3097.

[26] T. Kadota, H. Yamasaki, Recent advances in the combustion of water fuel emulsion, Progress in Energy and Combustion Science 28 (2002) 385-404.

[27] Y. Kitamura, Q. Huang, Y. Oka, T. Takahashi, Flashing of superheated water-in-oil emulsions, Journal of Chemical Engineering of Japan 23 (1990) 711 - 715.

[28] L. Ferrante, M. Miccio, F. Miccio, R. Solimene, Fluidized bed combustion of liquid biofuels: Application of integrated diagnostics for micro-explosions characterization, Energy & Fuels 22 (2008) 4213-4222.

[29] http://www.microfluidicscorp.com/images/stories/pdf/m-110y.pdf, (16 Mar. 2011)

[30] R. Pal, Effect of droplet size on the rheology of emulsions, AIChE Journal 42 (1996) 3181-3190.

[31] http://www.canolacouncil.org/uploads/Chemical1-6.pdf, (16 Mar. 2011).

[32] J.M. de Morais, O.D. Henrique dos Santos, T. Delicato, R. Azzini Goncalves, P. Alves da Rocha-Filho, Physicochemical characterization of canola oil/water nano-emulsions obtained by determination of required HLB number and emulsion phase inversion methods, Journal of Dispersion Science and Technology 27 (2006) 109-115.

[33] http://www.theherbarie.com/files/resource-center/formulating/Required_HLB_for_Oils_and_Lipids.pdf, (16 Mar. 2011).

[34] K. Annamalai, I.K. Puri, Combustion Science and Engineering, CRC Press, Florida, 2007.

[35] T. Daho, G. Vaitilingom, O. Sanogo, Optimization of the combustion of blends of domestic fuel oil and cottonseed oil in a non-modified domestic boiler, Fuel 88 (2009) 1261-1268.

[36] K.K. Kuo, Principles of Combustion, 2 ed., John Wiley and Sons, Inc., 2005.

[37] M.A. Habib, M. Elshafei, M. Dajani, Influence of combustion parameters on NOx production in an industrial boiler, Computers & Fluids 37 (2008) 12-23.

[38] D.C. Rakopoulos, C.D. Rakopoulos, E.G. Giakoumis, A.M. Dimaratos, D.C. Kyritsis, Effects of butanol-diesel fuel blends on the performance and emissions of a high-speed DI diesel engine, Energy Conversion and Management 51 (2010) 1989-1997.

[39] H.K. Ng, S. Gan, Combustion performance and exhaust emissions from the non-pressurised combustion of palm oil biodiesel blends, Applied Thermal Engineering 30 (2010) 2476-2484.

[40] B. Thien, Cofiring with coal: feedlot biomass blends, Ph.D. Thesis, Mechanical Engineering Department, Texas A&M University, College Station, TX, 2002.

[41] P. Ndayishimiye, M. Tazerout, Use of palm oil-based biofuel in the internal combustion engines: Performance and emissions characteristics, Energy 36 (2011) 1790-1796.

[42] N.A. Chigier, The atomization and burning of liquid fuel sprays, Progress in Energy and Combustion Science 2 (1976) 97-114.

[43] S. Nukiyama, Y. Tanasawa, Experiments on the atomization of liquids in an airstream, The Japan Society of Mechanical Engineer 5 (1939) 68-75.

[44] Q. Shu, J. Wang, B. Peng, D. Wang, G. Wang, Predicting the surface tension of biodiesel fuels by a mixture topological index method, at 313 K, Fuel 87 (2008) 3586-3590.

[45] L. Broniarz-Press, M. Ochowiak, J. Rozanski, S. Woziwodzki, The atomization of water-oil emulsions, Experimental Thermal and Fluid Science 33 (2009) 955-962.

[46] T.M. Kegel, Basic Measurement Uncertainty, 71st International School of Hydrocarbon Measurement, Oklahoma City, OK April 9-11 (1996) 1-7.

[47] B. Lawrence, Cofiring of coal and dairy biomass in a 100,000 BTU/hr furnace, Master's Thesis, Mechanical Engineering Department, Texas A&M University, College Station, 2007.

APPENDIX A

UNCERTAINTY ANALYSIS

The uncertainty analysis done in this project follows the example of Kegel [46]. Table A.1 lists all the instruments used in the project and their uncertainty parameters taken from the instructor's manual provided for each instrument. The formula for calculating the total instrument uncertainty has been taken from [47] and is shown below.

$$U_{total} = \sqrt{\left(U_{accuracy}{}^2\right) + \left(U_{resolution}{}^2\right)} \quad (15)$$

where,

U_{total} is the total uncertainty in the instrument

$U_{accuracy}$ is the uncertainty due to the accuracy of instrument

$U_{resolution}$ is the uncertainty due to the resolution of instrument

Table A.1: Instrument Uncertainty

Instrument	Accuracy	Unit	Resolution	Units	Total instrument uncertainty
Primary air flow meter	± 3	%	0.1	l/min	3.00
Secondary air flow meter	± 15	l/min	1	l/min	15.03
Fuel flow meter	± 1	%	0.1	gal/hr	1.00
Viscometer	± 1	%	0.1	cP	1.00
O_2 analyzer	0.1	%	0.1	%	varies
CO_2 analyzer	± 3	%	0.01	%	varies
CO analyzer	± 4	%	1	ppm	varies
NO_x analyzer	± 4	ppm	1	ppm	4.12
C_xH_y analyzer	± 100	ppm	1	ppm	10.00

Uncertainty in Equivalence Ratio (ϕ)

The equivalence ratio was calculated from the values measured by the air and fuel flow meters. Since the flow meters have a degree of inaccuracy, the equivalence ratio would also have uncertainty due to the same.

The formula for equivalence ratio (ϕ) is given as

$$\phi = \left[\frac{\left(\frac{\text{Fuel}}{\text{Air}}\right)_{\text{Provided}}}{\left(\frac{\text{Fuel}}{\text{Air}}\right)_{\text{Stoichiometric}}}\right] \tag{16}$$

Deleting the fuel terms as it is constant at all equivalence ratios, we get

$$\phi = \left[\frac{\text{Air}_{\text{stoichiometric}}}{\text{Air}_{\text{provided}}}\right] \tag{17}$$

Air supplied for the combustion process is a sum of primary and secondary air, so the above equation can be written as

$$\phi = \left[\frac{A_{p,st} + A_{s,st}}{A_{p,pr} + A_{s,pr}}\right] \tag{18}$$

where,

$A_{p,st}$ is the stoichiometric primary air

As,st is the stoichiometric secondary air

Ap, pr is the primary air provided

As,pr is the secondary air provided

To determine the uncertainty, the partial derivative of equivalence ratio with respect to each individual variable must be calculated,

$$\frac{\partial \phi}{\partial A_{p,st}} = \frac{1}{(A_{p,pr} + A_{s,pr})} \tag{19}$$

$$\frac{\partial \phi}{\partial A_{s,st}} = \frac{1}{(A_{p,pr} + A_{s,pr})} \tag{20}$$

$$\frac{\partial \phi}{\partial A_{p,st}} = - \frac{(A_{p,st} + A_{s,st})}{\left((A_{p,pr} + A_{s,pr})^2\right)} \quad (21)$$

$$\frac{\partial \phi}{\partial A_{s,st}} = - \frac{(A_{p,st} + A_{s,st})}{\left((A_{p,pr} + A_{s,pr})^2\right)} \quad (22)$$

By using the above equations, the uncertainty in the equivalence ratio for pure canola oil at stoichiometric condition and swirl number of 1.4 was calculated. The sample calculations are shown in Table A.2.

Table A.2: Complete uncertainty analysis in equivalence ratio for pure canola oil at stoichiometric condition and SN = 1.4

Input variable	Equivalence Ratio	Air Type	Value	$\delta\phi/\delta x_i$	x_i/ϕ	$s_{xi}=(\delta\phi/\delta x_i)*(x_i/\phi)$	u_{xi}	$s_{xi}*u_{xi}$	$(s_{xi}*u_{xi})^2$	Contribution
X_1	1	Primary Air,s	10.1	0.003310	10.1	0.03343	0.17228	0.00576	0.0000332	1.92
X_2	1	Secondary Air,s	292	0.003310	292	0.96657	0.02985	0.028856	0.0008327	48.08
X_3	1	Primary Air ,pr	10.1	0.003310	10.1	0.03343	0.17228	0.00576	0.0000332	1.92
X_4	1	Secondary Air, pr	292	0.003310	292	0.96657	0.02985	0.028856	0.0008327	48.08
								SUM	0.0017317	100.00
								Total (%)	4.16	

where,

S_{xi} = sensitivity coefficient

U_{xi} = standard uncertainty

(S_{xi}*U_{xi}) = combined standard uncertainty

Table A.3 lists the uncertainty in equivalence ratio for all the experiments. Note that for all the fuels, the equivalence ratio uncertainty is lowest at fuel lean conditions and it maximum at fuel rich combustion. This was because, at ϕ <1, higher amounts of secondary air was supplied to the furnace. Since the percentage accuracy of the flow meters is with regards to the full scale of the instrument, at higher flow rates, the instrument operated at higher accuracy.

Table A.3: Percentage uncertainty in equivalence for pure canola oil, 89-9 emulsion, 85-12.5 emulsion at both swirl numbers.

Fuel type/ Swirl number	Equivalence ratio	Uncertainty (%)	Average uncertainty (%)
Pure canola Oil 60° (SN = 1.4)	0.83	4.00	4.154
	0.91	4.00	
	1	4.16	
	1.05	4.22	
	1.11	4.39	
89-9 Emulsion 60° (SN = 1.4)	0.83	3.59	3.768
	0.91	3.61	
	1	3.73	
	1.05	3.86	
	1.11	4.05	
85-12.5 Emulsion 60° (SN = 1.4)	0.83	3.69	3.862
	0.91	3.70	
	1	3.86	
	1.05	3.96	
	1.11	4.10	
Pure canola Oil 51° (SN = 1.0)	0.83	3.96	4.162
	0.91	4.02	
	1	4.13	
	1.05	4.27	
	1.11	4.43	
89-9 Emulsion 51° (SN = 1.0)	0.83	3.57	3.756
	0.91	3.61	
	1	3.75	
	1.05	3.83	
	1.11	4.02	
89-9 Emulsion 51° (SN = 1.0)	0.83	3.66	3.836
	0.91	3.67	
	1	3.87	
	1.05	3.90	
	1.11	4.08	

VITA

Shreyas Mahesh Bhimani was born in Mumbai, India. He graduated with first class from Charotar Institute of Technology, Changa, Gujarat University, India, with a Bachelor of Mechanical Engineering degree in June 2007. He enrolled in Texas A&M University, College Station in Spring of 2008 and received his Master of Science in mechanical engineering in May 2011.

Mr. Bhimani can be contacted by email at shreyas.bhimani@gmail.com. He can be contacted in person at,

Texas A&M University

Department of Mechanical Engineering

3123 TAMU

College Station

TX 77843-3123

c/o Dr. Jorge Alvarado